REACTIONS OF CN RADICALS STUDIED BY KINETIC SPECTROPHOTOMETRY

by

Alan John Leitch, B.Sc.

A Thesis presented for the degree of
Doctor of Philosophy in the Faculty of Science
at the University of Edinburgh

1978

To

Alice and Arnold

Jones

DECLARATION

I hereby declare that this thesis has been composed by me, and that the work described in it is my own except where due acknowledgement is made. This thesis has not been submitted previously for any other degree.

ACKNOWLEDGEMENTS

I should like to express my appreciation to the Science Research Council for providing me with a grant, and also Shell Research Limited for their CASE award. My thanks go to Professor C. Kemball and the Chemistry Department for the use of laboratory and research facilities.

I am indebted to my supervisor Dr. R.J. Donovan for his help and encouragement throughout my period of study. To my supervisor at Thornton Research Centre, Dr. C. Morley, I express my thanks for his guidance during my time at Shell and his helpful discussions.

I should like also to thank the typing pool at British Gas Engineering Research Station, Maureen Holland and Marie Manson for typing this manuscript. The help received from Mr. J. Broom (glass blower) and Mr. H. MacKenzie (physical laboratory) is gratefully acknowledged.

In conclusion, I would like to thank everyone who gave me their support and encouragement during the writing of this thesis, and everyone not already mentioned above, who helped me during my research, especially Robin Strain.

ABSTRACT

The technique of time-resolved resonance absorption spectroscopy was used to monitor the decay of photolytically produced CN radicals. Care was taken to ensure that any vibrationally excited CN, produced in the primary photolytic process, was relaxed to the ground state. Thus rate constants given in this work apply strictly for the removal of $CN(X^2\Sigma, v''=0)$ radicals in the absence of feeding by vibrational relaxation of higher levels, in contrast to previous work where this was not taken into account.

For the first time, rate constants are reported for the reactions of CN radicals with the molecules H_2O, D_2O, HCl, DCl, CO_2, N_2O, OCS, CO and HCN. No isotope effects were observed for the deuterated species. Rate data for the reactions of $CN(X^2\Sigma, v''=0)$ with O_2, NO, H_2, CH_4 and C_2H_6 were also obtained and compared with previous data.

The data show that recombination of CN radicals in the presence of both NO and CO occurs by a mechanism analogous to that for catalysed recombination of halogen atoms. A small negative activation energy (-10 ± 4 kJ mol^{-1}), characteristic of such processes, was calculated for the NO case.

The reaction of CN $(X^2\Sigma, v''=1)$ with H_2 was also studied and compared with the $CN(v''=0)$ case. However, it was not possible to state categorically that rate enhancement occurred with vibrational excitation, as vibrational to rotational energy transfer may have been important. Hence, only an upper limit of 1.7 is given for the rate constant ratio, $k_{v''=1}/k_{v''=0}$.

A value of $\Delta H^o_{f_{295}}(CN) = 417.6\pm1.3$ kJ mol^{-1} was determined using the equilibrium constant for the reaction $CN + HCN \rightleftharpoons C_2N_2 + H$. This is in agreement with several recent results, reinforcing the need for a change in the currently accepted value.

Work on the study of CN radicals in flames at Thornton Research Centre (Shell Research Ltd.), using the technique of resonance fluorescence, led to several practical suggestions for improving this technique, especially the use of a tunable dye laser to excite the CN radicals.

CONTENTS

page

CHAPTER 1 : INTRODUCTION

General Introduction 1

Methods of Production of $CN(X^2\Sigma)$ Radicals 3

Reaction of $CN(X^2\Sigma, v''=0)$ with C_2N_2 5

Reactions of $CN(X^2\Sigma, v''=0)$ with O and O_2 8

Reactions of $CN(X^2\Sigma)$ with Fuel Molecules 12

Reactions of $CN(X^2\Sigma)$ with Nitrogen Compounds 18

Reactions of Vibrationally Excited $CN(X^2\Sigma)$ Radicals 20

Vibrational Energy Effects in Other Systems 24

The Study of $CN(B^2\Sigma)$ 27

This Work. 29

CHAPTER 2 : EXPERIMENTAL

General Introduction 31

Description of Apparatus 33

Description of Individual Components 33

1. CN Emission Lamp 33
2. Flash Lamp 38
3. Reaction Vessel 41
4. Monochromator and Optical System 42
5. Photomultiplier 43
6. Signal and Data Processing 50

Experimental Procedure 52

Production of CN Radicals 53

Gas Handling 54

Gas Purities 55

Experimental Uncertainties. 55

CHAPTER 3 : CN EMISSION AND ABSORPTION

Introduction 57

The $CN(B^2\Sigma-X^2\Sigma)$ Violet System 57

CN Emission Spectra 60

Vibrational Distributions 60

Rotational Distributions 63

Absorption by CN Radicals 65

The Beer-Lambert Law 66

Absolute CN Concentrations 71

Summary. 74

CHAPTER 4 : PRELIMINARY EXPERIMENTS

Introduction 75

CN Vibrational Distributions 76

Previous Work 76

This Work 78

Diffusion 79

Vibrational Relaxation of CN Radicals 83

Previous Work 84

Empirical Calculations 87

Recombination of CN Radicals 89

Reaction of CN with Cyanogen 90

Reaction of CN with Impurities 97

Reaction Products 98

Conclusions. 98

CHAPTER 5 : REACTIONS OF $CN(X^2\Sigma, v''=0)$ WITH SMALL MOLECULES CONTAINING O, N, C AND S ATOMS

Introduction 100

Results and Discussion 101

1. Reaction with O_2 101
2. Catalysed Recombination of CN Radicals 104
3. Reactions with CO_2, N_2O and OCS. 113

CHAPTER 6 : REACTIONS WITH H_2O, HCl AND HCN

Introduction 119

Results and Discussion 119

1. Reaction with H_2O and D_2O 119
2. Reaction with HCl and DCl 120
3. Reaction with HCN. 123

CHAPTER 7 : REACTIONS WITH H_2, CH_4 AND C_2H_6

Introduction 125

Results and Discussion 125

1. Reaction of $CN(X^2\Sigma, v''=0)$ with H_2 125
2. Reaction of $CN(X^2\Sigma, v''=0)$ with CH_4 128
3. Reaction of $CN(X^2\Sigma, v''=0)$ with C_2H_6 131
4. General Discussion 131

Conclusions. 134

CHAPTER 8 : REACTION OF $CN(X^2\Sigma, v''=1)$ WITH H_2

Introduction 135

Production of $CN(X^2\Sigma, v''=1)$ 136

Results 137

Reaction of $CN(X^2\Sigma, v''=1)$ with H_2 137

Reaction of $CN(X^2\Sigma, v''=0)$ with H_2 139

Discussion. 139

CHAPTER 9 : CN RADICALS IN FLAMES

Introduction 142

Flames 143

Flame Nitrogen Chemistry 145

Resonance Fluorescence 148

Experimental 149

Results and Discussion. 156

CHAPTER 10 : SUMMARY AND CONCLUSIONS

Résumé 161

Future Experiments and Improvements. 163

APPENDICES

Appendix I 164

Appendix II 167

Appendix III 172

Appendix IV 174

Appendix V 179

REFERENCES 180

LECTURES ATTENDED 188

CHAPTER 1

CHAPTER 1

INTRODUCTION

GENERAL INTRODUCTION

For many years, astronomers have observed cyanide radicals in their studies of space and the stars.[1] These radicals have been shown to exist in the heads of comets, in the sun and stars, and in interstellar space. A more recent interest in CN radicals however, arises from their importance in combustion reactions in hydrocarbon flames.

The mechanism of the thermal fixation of atmospheric nitrogen in flames has been investigated[2] and is reasonably well understood. However the fixation of fuel nitrogen and subsequent conversion to nitrogen oxides is less well understood . CN radicals are thought to be involved in some of the rate determining steps in the fixation of fuel nitrogen. An example of such a process, suggested by Appleton and Heywood[3] , is as follows.

$$CN + O \longrightarrow CO + N \qquad (1.01)$$

$$N + O_2 \longrightarrow NO + O \qquad (1.02)$$

Environmental considerations[4] make the production of NO_x (nitrogen oxides:- NO, NO_2, N_2O, N_2O_4 etc) undesirable. Both NO and NO_2 are poisonous and both are involved in the catalytic removal of O_3 in the stratosphere via the NO_x cycle[5]. This cycle, which is essentially the same as the ClO_x and HO_x cycles[5-8], is detailed below.

$$NO + O_3 \longrightarrow NO_2 + O_2 \qquad (1.03)$$

$$O + NO_2 \longrightarrow NO + O_2 \qquad (1.04)$$

$$NO_2 + h\nu \longrightarrow NO + O \qquad (1.05)$$

The molecules NO and NO_2 are also involved in the production of photochemical smog in the troposphere under conditions where the concentration of hydrocarbons is significant. Leighton[4] was the first to give a quantitative account of the mechanism of photochemical smog formation. Later Khan et al.[9] proposed the participation of singlet molecular oxygen, and computer modelling studies gave good agreement with actual conditions observed in smoggy atmoshperes. Basically, an oxidising atmosphere containing ozone and peroxyacylnitrates (PAN) is built up which causes damage to crops and trees, cracking in rubbers, reduced visibility, and eye irritation. The best known example is the smog produced over Los Angeles due to the high concentration of hydrocarbons and nitrogen oxides from automobile exhausts.

The overall fluctuations of ozone concentrations in the various layers of the atmosphere involve many interrelated competing elementary reactions[10]. These include reactions of both ground and excited electronic states.

Since kinetic data on CN radical reactions are somewhat scarce, the determination of more rate data for these reactions should aid the understanding of the processes occurring in flames, and allow more successful computer modelling of combustion processes to evolve.

In a hydrocarbon flame, the reaction of CN radicals with four major components of the flame should be considered namely:-

1) fuel e.g. H_2, CH_4, C_2H_6.

2) oxidising agent e.g. O_3, O_2, O.

3) nitrogen containing compounds e.g. N_2O, NO, NO_2.

4) combustion products e.g. CO_2, H_2O and HCN.

In this work, a selection of the above reactions was studied along with several related reactions.

There now follows a discussion of the methods used to prepare CN radicals and a summary of the kinetic data given in the literature for the reactions of CN radicals in their ground electronic state. The effects of vibrational excitation of $CN(X^2\Sigma)$ will also be discussed.

METHODS OF PRODUCTION OF $CN(X^2\Sigma)$ RADICALS

Several different methods have been used to produce CN radicals from a variety of parent molecules. White [11] produced $CN(X^2\Sigma)$ radicals via an R.F. oscillator which produced an electric discharge through cyanogen flowing continuously through an absorption cell. Haggart and Winkler [12] used the reaction of active nitrogen with cyanogen in a flow system to produce CN radicals.

The technique of flash photolysis was used by Paul and Dalby[13] to produce $CN(X^2\Sigma)$ radicals from cyanogen and cyanogen chloride. The photolysis of cyanogen is essentially more satisfactory since only CN radicals are produced, whereas ClCN photolysis gives rise to chlorine atoms, which could complicate the study of CN reactions.

Flash spectroscopy was used by Basco[14] and Basco et al.[15] in their study of the photolysis of RCN where R = CN, I, Cl. The production of CN radicals was monitored as a function of time and

as a function of RCN pressure. They found that the CN radicals produced were vibrationally excited.

In an attempt to determine the mechanism by which excitation was taking place, they used various filter solutions in the outer jacket of their double walled reaction vessel to blank out regions of the continuum produced by the photolysis flash. Considerations of the bond energies of R-CN precursors and the excess energy available to photolytically produced radicals, together with the importance of wavelengths in the region 360-440 nm for the production of vibrationally excited radicals (due to secondary excitation following absorption and re-emission in the $CN(B^2\Sigma-X^2\Sigma)$ system), led to the following mechanism being proposed.

$$RCN + h\nu \longrightarrow CN(X^2\Sigma, v'' = 0) + R \qquad (1.06)$$

$$CN(X^2\Sigma, v'' = 0) + h\nu \longrightarrow CN(B^2\Sigma, v' = 0,1,2,3...) \qquad (1.07)$$

$$CN(B^2\Sigma, v' = 0,1,2..) \longrightarrow CN(X^2\Sigma, v'' = 0,1,2,3...) + h\nu \qquad (1.08)$$

$$CN(B^2\Sigma, v' = 0,1,2..) + M \longrightarrow CN(X^2\Sigma, v'' = 0,1,2,3...) + M \qquad (1.09)$$

In their laser-induced fluorescence study of $CN(X^2\Sigma)$ radicals, produced by photolysis of cyanogen at 160nm, Cody et al.[15a] found evidence for the direct population of vibrational levels up to v''=4 in the primary photochemical step. About 95% of the total vibrational energy appeared initially in the v''=0 and v''=1 levels. For the photolysis of pure cyanogen (≤ 4 Nm^{-2}), the initial relative populations were $N^0_{v''=0} = 0.74\pm0.02$ and $N^0_{v''=1} = 0.26\pm0.02$, equivalent to a vibrational temperature of 2750 K.

Boden and Thrush[16] used a chemical reaction to produce $CN(X^2\Sigma)$ radicals in their capacity flow reactor. Titration of active nitrogen with NO gave oxygen atoms which were subsequently reacted with C_2N_2 to produce $CN(X^2\Sigma)$ radicals. The mechanism they proposed for this reaction, at the elevated temperature used, is as follows.

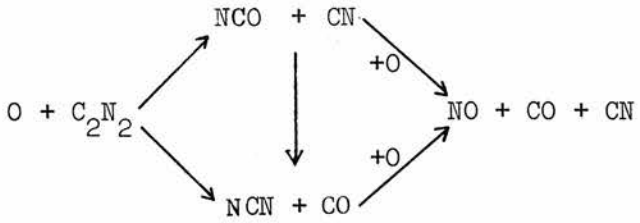

(1.10)

A 30 ns pulse from a 20 MeV Febetron was used by Bullock and Cooper[17-19] and Bullock et al.[20] in their technique of pulse radiolysis of cyanogen/argon mixtures to produce $CN(X^2\Sigma)$ radicals. This system suffers the disadvantage that the electron pulse may induce radiolysis of reactants or initiate secondary processes which could complicate the study of $CN(X^2\Sigma)$.

Wolfrum and coworkers[21-23] used the technique of flash photolysis to produce $CN(X^2\Sigma)$ radicals in several vibrational levels.

REACTIONS OF $CN(X^2\Sigma, v''=0)$ WITH C_2N_2

A knowledge of the reaction of CN radicals with cyanogen is of particular importance to the present work as cyanogen is used as the source of CN radicals. Paul and Dalby[13] were the first workers to determine a rate constant for the reaction

$$CN + C_2N_2 \xrightarrow{k_{11}} C_3N_3 \qquad (1.11)$$

where the product is stabilised by collisions with a third body.

By carrying out their experiments at different temperatures, they obtained the following Arrhenius expression for the rate constant k_{11}.

$$k_{11} = 1.21 \times 10^{-13} \exp(-8.8 \text{ kJ mol}^{-1}/RT) \text{ cm}^3 \text{ molecule}^{-1} \text{ s}^{-1} \qquad (1.12)$$

This gave a value of $k_{11} = 3.5 \times 10^{-15}$ cm^3 molecule^{-1} s^{-1} at 301 K.

They considered the possible importance of CN radical recombination (reaction 1.13) but dismissed this as being negligible since, even if the rate constant was large, the low concentrations of CN($X^2\Sigma$) present would make the contribution of reaction 1.13 to the overall decay of CN($X^2\Sigma$) unimportant.

$$CN + CN \xrightarrow{k_{13}} C_2N_2 \qquad (1.13)$$

Here again collisions with a third body are necessary to stabilise the product by removing the excess energy.

Concern was expressed that the reaction of CN with cyanogen would be in strong competition with the reaction of CN radicals with reactant molecules, and that the contribution to the overall decay of CN would be significant. In practice the reaction of CN with C_2N_2 is too slow for this to occur in most cases.

Paul and Dalby also considered the decay of CN radicals produced by the photolysis of ClCN, and obtained a rate constant of about 2.5×10^{-15} cm^3 molecule^{-1} s^{-1} at room temperature for the following reaction.

$$CN + ClCN \longrightarrow (CN)_2 + Cl \qquad (1.14)$$

The activation energy for this reaction was found to be the same as for reaction 1.11. They accept however that production of chlorine atoms from the photolysis of ClCN would complicate the kinetics of CN decay.

Boden and Thrush[16] obtained a value of 1.8×10^{-12} cm^3 molecule^{-1}s^{-1} for k_{11} at 687 K which is in fact two orders of magnitude greater than the value calculated from the Arrhenius expression of Paul and Dalby[13]. At temperatures around 300 K, reaction 1.11 is important, but for higher temperatures, Boden and Thrush proposed the following mechanism to explain the acceleration in rate observed for the reaction of CN with oxygen atoms at high partial pressures of cyanogen and in the absence of molecular oxygen.

$$CN + C_2N_2 \longrightarrow C_3N + N_2 \qquad (1.15)$$

$$O + C_3N \longrightarrow C_2N + CO \qquad (1.16)$$

$$O + C_2N \longrightarrow CN + CO \qquad (1.17)$$

Dunn et al.[24] estimated k_{11} to be $\sim 10^{-14}$ cm^3 molecule^{-1}s^{-1} (295 K) from the onset of polymer formation in their investigation of the reaction of hydrogen atoms with cyanogen. This is greater than the value obtained by Paul and Dalby[13], and it was suggested by Bullock and Cooper[18] that HCN impurity was the cause of this, whereas Boden and Thrush[16] suggested that temperature heterogeneity could be the explanation.

Bullock and Cooper[18] discussed the relative importance of reactions 1.11 and 1.18.

$$CN + CN + M \longrightarrow (CN)_2 + M \qquad (1.18)$$

They found the decay of $CN(X^2\Sigma)$ to be second order with respect to $[CN]$ initially, corresponding to reaction 1.18, but after about 200μs a good first order decay corresponding to reaction 1.11

dominated. At pressures of $C_2N_2 > 500\ Nm^{-2}$, the kinetics were entirely first order contrary to the data of Basco et al.[15] who observed second order decay at all pressures of C_2N_2. However, Basco et al. admit that their results could fit first order kinetics.

From an Arrhenius plot, Bullock and Cooper[18] obtained the following expression for k_{11}

$$\log_{10}k_{11} = -12.03 - (13.1\ kJmol^{-1}/2.3\ RT)cm^3molecule^{-1}s^{-1} \quad (1.19)$$

which has both A and E Arrhenius factors larger than those determined by Paul and Dalby[13]. The reaction must be sterically hindered however, since even this value of A is not particularly large. The value of k_{11} at 300 K was $4.9 \times 10^{-15} cm^3 molecule^{-1} s^{-1}$, essentially in agreement with the room temperature value of Paul and Dalby.

REACTION OF $CN(X^2\Sigma, v'' = 0)$ WITH O AND O_2

In combustion processes, where oxygen is present in large concentrations, it is of value to know how cyanide radicals react with both atomic and molecular oxygen. However, these reactions have only been studied at about 300 K. It is therefore necessary to determine Arrhenius parameters so that data can be extrapolated to flame temperatures ($\sim$ 3000 K) and incorporated into an overall model of the combustion process.

Paul and Dalby[13] obtained a value of $9.1 \times 10^{-12} cm^3 molecule^{-1} s^{-1}$ for the reaction of $CN(X^2\Sigma)$ with molecular oxygen at room temperature (reaction 1.20) assuming that chain processes were unimportant. No error limits were given due to the approximate nature of their determination.

$$CN + O_2 \xrightarrow{k_{20}} NCO + O \qquad (1.20)$$

A strong NCO absorption spectrum was observed shortly after the photolysis flash confirming this reaction product.

Basco[14] obtained a value of $7.6 \times 10^{-12} cm^3 molecule^{-1} s^{-1}$ for the rate constant for reaction 1.20 at room temperature. Although no error limits were given for this result, it is in good agreement with the value obtained by Paul and Dalby[13].

Basco calculated that the following reaction, resulting in the production of vibrationally excited NO in the presence of excess oxygen, could account for $\leqslant$ 15% of the net rate of removal of $CN(X^2\Sigma)$.

$$CN + O_2 \longrightarrow CO + NO_v \qquad (1.21)$$

However the following radical-atom reaction could also account for the production of vibrationally excited NO.

$$O + NCO \longrightarrow NO_v + CO \qquad (1.22)$$

The production of ozone was found to accompany the reaction of CN with molecular oxygen, and is in fact good evidence for the production of oxygen atoms, especially since one ozone molecule is produced for every CN radical removed. The molecules NCO and either N_2C_2O or NCO_2CN were observed as products.

Morrow and McGrath[25] also found evidence for the oxygen transfer process of reaction 1.20 followed by reaction 1.22 rather than the formation of NO and CO products via a four centre reaction involving CN and O_2. Boden and Thrush[16] also supported this mechanism since the A factor for a four centre reaction would have been lower than the value estimated from their data. The result they obtained for k_{20} was $(7.3 \pm 3.3) \times 10^{-12}$ cm^{3}molecule^{-1}s^{-1} at 687 K, in good agreement with previous room temperature values, implying a zero activation energy. This would not be the case for a four centre mechanism where two bonds of appreciable bond energy would have to be broken, resulting in a substantial activation energy.

Bullock and Cooper[18] observed both NCO and NCN absorptions in their pulse radiolysis study of $C_2N_2/O_2/Ar$ mixtures. The kinetics of the formation and decay of both NCO and NCN were thought to be complicated, involving radical-radical reactions, and were not studied. The rate of appearance of NCO was observed and will be discussed later along with a consideration of vibrationally excited CN. The value of k_{20} obtained was 1.11×10^{-11} cm^3 molecule^{-1}s^{-1} at 300 K and a slightly lower value at 377 K, implying a small negative activation energy.

The reaction of $CN(X^2\Sigma)$ with O_2 was also studied by Wolfrum and coworkers[21-23] who obtained the following Arrhenius expression.

$$k_{20}=(5.3\pm1.7)\times10^{-11}\exp(-4.2\pm1.4 \text{ kJmol}^{-1}/RT)\text{cm}^3\text{molecule}^{-1}\text{s}^{-1} \qquad (1.23)$$

This gives a value of 8.6×10^{-12} cm^{3}molecule^{-1}s^{-1} (298 K) in agreement with previous room temperature values. However, the

positive activation energy observed[23] conflicts with the small negative value obtained by Bullock and Cooper[18].

In their study of O + C_2N_2, Boden and Thrush[16] determined Arrhenius parameters for the following reaction of $O(^3P)$ with $CN(X^2\Sigma)$.

$$O + CN \xrightarrow{k_{24}} CO + N \qquad (1.24)$$

The expression they obtained was

$$k_{24}=1.05\times10^{-10}\exp(-10.0\ kJmol^{-1}/RT)cm^3molecule^{-1}s^{-1} \qquad (1.25)$$

which gives a value of $k_{24} = 1.8 \times 10^{-12} cm^3 molecule^{-1} s^{-1}$ at 298 K. This does not agree with the value of $(1.99 \pm 0.66) \times 10^{-11} cm^3 molecule^{-1} s^{-1}$ obtained by Wolfrum and coworkers[21-23] for k_{24} which was shown to be independent of temperature for $295 \leqslant T \leqslant 387$ K.

Schmatjko and Wolfrum[26] determined the product energy distribution of the O-atom reaction with CN. They found that the following two processes were taking place simultaneously.

$$CN + O(^3P) \longrightarrow CO_v + N(^2D) \qquad (1.24a)$$

$$\longrightarrow CO_v + N(^4S) \qquad (1.24b)$$

Reaction 1.24a accounted for about 85% of the products, most of the energy of the reaction going into the metastable nitrogen atom. Only the lowest vibrational levels of the CO molecule were occupied. The other 15% of the products were ground state nitrogen atoms and vibrationally excited CO_v $(6 \leqslant v \leqslant 9)$, with partial inversion of the populations.

REACTION OF CN($X^2\Sigma$) WITH FUEL MOLECULES

Another important consideration for the reactions of CN radicals in flames is their reaction with fuel molecules. The various combustable materials for which rate constants have been obtained include hydrogen, alkanes, alkenes and benzene.

Haggart and Winkler[12] studied the reaction of CN with molecular hydrogen but in no great detail. Paul and Dalby[13] identified HCN as a product of this reaction (reaction 1.26) by infra-red spectroscopy and gas chromatographic analysis.

$$CN + H_2 \xrightarrow{k_{26}} HCN + H \qquad (1.26)$$

Unfortunately, they did not have enough data to obtain a rate constant.

An upper limit of $k_{26} = 3.3 \times 10^{-13} cm^3 molecule^{-1} s^{-1}$ was determined by Boden and Thrush[16] at 687 K, corresponding to $k_{26} < 4.9 \times 10^{-14} cm^3 molecule^{-1} s^{-1}$ at 295 K using the value of 29 $kJmol^{-1}$, determined by Hartel and Polanyi[27], for the activation energy. The value of $k_{26} = 3 \times 10^{-14} cm^3 molecule^{-1} s^{-1}$ obtained by Iwai et al.[28] at room temperature is in agreement with the above upper limit.

Boden and Thrush[16] considered the elementary chain steps of the radicals formed in the thermal reaction of molecular hydrogen with cyanogen, which was studied by Robertson and Pease[29] at 900 K. Reaction 1.26 was given as an elementary step of this reaction. Boden and Thrush incorporated their limiting value for k_{26} into the overall kinetics of the $H_2 + C_2N_2$ chain reaction. In order to arrive at the same overall activation energy (301 $kJmol^{-1}$) and reaction rates as Robertson and Pease, Boden and Thrush

proposed a new value of $\Delta H^{o}_{f}(CN) = 418 \pm 12.5$ kJmol^{-1}, which is slightly lower than the previously accepted value.

Wolfrum and coworkers[22] obtained the following Arrhenius expression for the reaction of $CN(X^{2}\Sigma)$ with molecular hydrogen, under conditions where the hydrogen concentration was more than a factor of ten greater than the cyanogen concentration.

$$k_{26} = (10 \pm 3.3) \times 10^{-11} \exp(-22.2 \text{ kJmol}^{-1}/RT) \text{ cm}^{3}\text{molecule}^{-1}\text{s}^{-1} \quad (1.27)$$

This gives a value of 1.2×10^{-14} cm^{3}molecule^{-1}s^{-1} at 295 K which is well within the limit given by Boden and Thrush[16].

In the reactions of $CN(X^{2}\Sigma)$ radicals with alkenes, the radicals exhibit their electrophilic nature by undergoing addition reactions, which may be compared to similar reactions of $O(^{3}P)$ and halogen atoms.

Paul and Dalby[13] photolysed cyanogen/ethylene mixtures in an attempt to study the kinetics of the CN + C_2H_4 reaction. However, because the reaction was so rapid, they were only able to observe the decay of the CN ($B^{2}\Sigma - X^{2}\Sigma$) absorption signal for high partial pressures of C_2N_2 (3.33×10^{4} Nm^{-2}) and low partial pressures of C_2H_4 (1.33 Nm^{-2}). Under these conditions, the observed decay was attributed to excess CN radicals remaining after all the ethylene molecules had reacted. This meant that $[CN] \simeq [C_2H_4]$ and so their estimate of 2.3×10^{-9} cm^{3}molecule^{-1}s^{-1} for the bimolecular rate constant for the reaction of CN + C_2H_4 at room temperature is not reliable.

The reactions of $CN(X^{2}\Sigma)$ with several alkenes were studied by Bullock and Cooper[17] who found that the observed rate constants were close to the collision limit, implying that collision geometry was unimportant. The values of the bimolecular rate constants obtained are given in Table 1.01.

Table 1.01

Rate Constants for Reactions with Alkenes[17]

Reactant	Rate Constant /10^{-10} cm^3 $molecule^{-1}$ s^{-1}
Ethylene	1.8 ± 0.25
Propylene	2.7 ± 0.3
1,3-butadiene	4.3 ± 0.5
Benzene	2.8 + 0.25

The rate constants are found to increase with molecular size as would be expected from the collision number. Benzene however did not follow this trend. This electrophilic behaviour of CN radicals (addition to alkenes) was compared to the addition of $O(^3P)$ to alkenes, where the increase in rate constants was attributed to increased alkylation of the double bond giving a lower activation energy. The activation energy for CN addition to alkenes was assumed to be zero because of the high rate constants obtained.

The addition of CN to C_2H_4 was also compared to addition of chlorine atoms to C_2H_4 for which the rate constant (2.6×10^{-11} cm^3 $molecule^{-1}$ s^{-1}) was about a factor of ten less. Nevertheless, $CN(X^2\Sigma)$ radicals do undergo addition reactions with alkenes and this is an indication of the radical's pseudo halogen properties.

Hydrogen abstraction by $CN(X^2\Sigma)$ radicals from alkanes is a much slower process than the addition of $CN(X^2\Sigma)$ to alkenes.

Previous work includes the reactions of $CN(X^2\Sigma)$ with methane, ethane, and propane as well as a comparison of abstraction by CN radicals and abstraction by halogen atoms.

Boden and Thrush[16] gave an upper limit of 1.2×10^{-12} cm^3 $molecule^{-1}s^{-1}$ for the abstraction of hydrogen from methane by $CN(X^2\Sigma)$ at 687 K.

$$CN + CH_4 \longrightarrow HCN + CH_3 \qquad (1.28)$$

The above reaction was also studied by Bullock and Cooper[17,19] who obtained a value of $(7.40 \pm 0.17) \times 10^{-13}$ cm^3 $molecule^{-1}s^{-1}$ for the rate constant for the removal of CN(v" = 0) at 300 K. The following Arrhenius expression was derived from temperature dependence work.

$$k_{28}=2.14\times10^{-11}\exp(-8.3\pm0.8\ kJmol^{-1}/RT)\ cm^3\ molecule^{-1}s^{-1} \qquad (1.29)$$

This yields a value of 5×10^{-12} cm^3 $molecule^{-1}s^{-1}$ at 687 K which is greater than the upper limit given by Boden and Thrush[16] for this temperature.

Bullock and Cooper[19] also studied the reaction of $CN(X^2\Sigma, v" = 0)$ with CD_4 and found the rate constant to be about half the value for the corresponding CH_4 reaction, indicating the importance of a tunnelling effect.

Schacke et al.[22] determined the Arrhenius parameters for the reaction of CN with methane and obtained the following expression for k_{28}.

$$k_{28}=5.28\times10^{-11}\exp(-12.1\ kJmol^{-1}/RT)\ cm^3\ molecule^{-1}s^{-1} \qquad (1.30)$$

The activation energy is slightly greater than obtained by Bullock and Cooper[19], giving agreement with the upper limit suggested by Boden and Thrush[16]. The above expression for k_{28} gives a value of 4.1×10^{-13} cm^3 molecule^{-1} s^{-1} at 300 K.

For the reaction of CN($X^2\Sigma$) with ethane, Bullock and Cooper[19] obtained less accurate Arrhenius values than for their methane results. The A factor was 2.5×10^{-11} cm^3 molecule^{-1} s^{-1} (4.0×10^{-11}, upper limit) and the activation energy was given as zero (1.6 kJmol^{-1}, upper limit).

$$CN + C_2H_6 \xrightarrow{k_{31}} HCN + C_2H_5 \qquad (1.31)$$

The value of k_{31} at 300 K was given as $(2.41 \pm 0.17) \times 10^{-11}$ cm^3 molecule^{-1} s^{-1}, which is larger than the value of 1.33×10^{-11} cm^3 molecule^{-1} s^{-1} given by Schacke et al.[22].

Bullock and Cooper[17] compared the ratio of the rate constants k_{31}/k_{28} to the ratio obtained by Goy et al.[30] and found it to agree within their experimental uncertainties. However, the difference in activation energies for reactions 1.28 and 1.31 was given as 15.5 kJmol^{-1} by Goy et al. compared to 8.3 kJmol^{-1} given by Bullock and Cooper[19].

Paul and Dalby[13] gave an approximate rate constant of 6.6×10^{-11} cm^3 molecule^{-1} s^{-1} for the reaction of CN($X^2\Sigma$) with propane. The value, quoted by Bullock and Cooper[19], of $(5.3 \pm 0.8) \times 10^{-11}$ cm^3 molecule^{-1} s^{-1} is in good agreement. This reaction was considered to have zero activation energy.

Reports on the reactions of CN($X^2\Sigma$) with alkanes comment on the pseudo halogen nature of the CN radical in these reactions.

Boden and Thrush[16] pointed out that the abstraction reactions of CN were about 67 $kJmol^{-1}$ more exothermic than the corresponding Cl atom reactions.

$$CN + H_2 \longrightarrow HCN + H \quad , \quad \Delta H^{o}_{298} = -64.5\ kJmol^{-1} \qquad (1.26)$$

$$CN + CH_4 \longrightarrow HCN + CH_3 \quad , \quad \Delta H^{o}_{298} = -61.9\ kJmol^{-1} \qquad (1.28)$$

$$CN + C_2H_6 \longrightarrow HCN + C_2H_5 \quad , \quad \Delta H^{o}_{298} = -88.2\ kJmol^{-1} \qquad (1.31)$$

$$Cl + H_2 \longrightarrow HCl + H \quad , \quad \Delta H^{o}_{298} = +4.7\ kJmol^{-1} \qquad (1.32)$$

$$Cl + CH_4 \longrightarrow HCl + CH_3 \quad , \quad \Delta H^{o}_{298} = +7.3\ kJmol^{-1} \qquad (1.33)$$

$$Cl + C_2H_6 \longrightarrow HCl + C_2H_5 \quad , \quad \Delta H^{o}_{298} = -19.0\ kJmol^{-1} \qquad (1.34)$$

However, reaction 1.26 was found to be about eight times slower than reaction 1.32. Similarly, reaction 1.28 ($< 1.2 \times 10^{-12} cm^3\ molecule^{-1} s^{-1}$) was slower than reaction 1.33 ($2.5 \times 10^{-12} cm^3\ molecule^{-1} s^{-1}$, given by Fettis and Knox[31]). Goy et al.[30] showed that the difference in activation energy between reactions 1.28 and 1.31 was 15.5 $kJmol^{-1}$ while the corresponding difference for Cl atoms (between reactions 1.33 and 1.34) was only 11.7 $kJmol^{-1}$. Boden and Thrush[16] concluded therefore that CN abstraction reactions had slightly higher activation energies than the Cl atom reactions.

From comparisons with halogen abstraction reactions, Bullock and Cooper[19] concluded that $CN(X^2\Sigma)$ radicals had activation energies for abstraction from alkanes which are less than the values for the corresponding Cl atom reactions. The A factors of the CN reactions were found to be a factor of ten less than the collisional value, and it was suggested that the orientation of the diatomic CN radical could account for most of the steric factor.

Schacke et al.[22] obtained a value of 1.33×10^{-11} cm^3 $molecule^{-1}s^{-1}$ for the rate constant of reaction 1.31 ($CN + C_2H_6$) but did not determine the activation energy. If the activation energy is assumed to be zero, then three values for the difference in activation energy, ΔE_A, of reactions 1.28 and 1.31 emerge. These are 15.5, 12.1, and 8.3 $kJmol^{-1}$ from the work of Goy et al.[30], Wolfrum and coworkers[22], and Bullock and Cooper[19] respectively.

It would appear that the value of ΔE_A from the steady state photolysis studies of Goy et al. is too high. Fettis and Knox[31] give the values 16 and 4.3 $kJmol^{-1}$ respectively for reactions 1.33 and 1.34. Hence, it would appear that the activation energies for the abstraction reactions of CN ($X^2\Sigma$) with alkanes are slightly less than for the corresponding Cl atom reactions.

REACTIONS OF CN($X^2\Sigma$) WITH NITROGEN COMPOUNDS

The reaction of CN ($X^2\Sigma$) with NO was studied extensively by Basco and Norrish[32] who also observed vibrational effects which will be discussed later. They observed a continuous ultra-violet absorption spectrum, of a molecular product, which was similar to that observed for NOCl and NOBr. This suggested NOCN, nitrosyl cyanide, as the product, first postulated by Norrish and Smith[33] some years before. The existence and structure of NOCN are now well established[34-36].

Basco and Norrish[32] successively flashed the same reaction mixtures and produced vibrationally excited NO from the photolysis of NOCN. The relative populations of the CN ($X^2\Sigma$) vibrational levels did not alter appreciably on addition of NO implying that chemical reaction was much faster than vibrational relaxation.

Two methods were used to determine the rate constant for the

reaction of CN with NO. The first was to monitor the decay of CN radicals, and the second was to determine the pressure of NO present at different delay times, when the CN concentrations were equal. Both methods gave good agreement and the average bimolecular rate constant obtained (reaction 1.35) was 2.0×10^{-12} cm^3 $molecule^{-1}s^{-1}$ corresponding to 3.3×10^{-31} cm^6 $molecule^{-2}s^{-1}$ with N_2 as third body.

$$CN + NO + (M) \xrightarrow{k_{35}} NOCN + (M) \qquad (1.35)$$

Boden and Thrush[16] obtained a value of $(5.0 \pm 3.3) \times 10^{-13}$ cm^3 $molecule^{-1}s^{-1}$ for k_{35} at 687 K. They discussed the possibility of O atom transfer from NO to CN but dismissed it since the reaction was endothermic. They suggest that their value of k_{35} corresponds to the following four centre reaction proposed by Rentzepis and Sugden[37].

$$CN + NO \longrightarrow CO + N_2 \qquad (1.36)$$

Boden and Thrush[16] considered that the association of NO and CN at their high temperature (687 K) would be much slower than their results indicated and so reaction 1.36 seems likely. An upper limit for k_{35}, given by Schacke et al.[21], was $<1.7 \times 10^{-12}$ cm^3 $molecule^{-1}s^{-1}$ at 298 K which is nearly equal to the value of Basco and Norrish[32]. Hence the reaction of CN with NO appears to take place by two different mechanisms depending on the temperature at which the reaction takes place.

The reaction of CN ($X^2\Sigma$) radicals with ammonia (reaction 1.37) was studied by Boden and Thrush[16] who obtained a value of $(8.8 \pm 3.0) \times 10^{-12}$ cm^3 $molecule^{-1}s^{-1}$ for the bimolecular rate constant.

$$CN + NH_3 \longrightarrow HCN + NH_2 \qquad (1.37)$$

Bullock et al.[20] monitored the decay of CN ($X^2\Sigma$) in the presence of

NH_3 and obtained a rate constant of 2.1×10^{-11} cm^3 $molecule^{-1}s^{-1}$ for the removal of CN (v" = 0) at 300 K and 1.8×10^{-11} cm^3 $molecule^{-1}s^{-1}$ at 375 K.

The small negative activation energy calculated, <2.1 $kJmol^{-1}$, gave agreement with the high temperature value of Boden and Thrush.[16]

REACTIONS OF VIBRATIONALLY EXCITED CN ($X^2\Sigma$) RADICALS

Basco and Norrish[32], in their study of the reaction of CN ($X^2\Sigma$) with NO found evidence for both chemical reaction and vibrational energy transfer. They discovered that vibrationally excited nitric oxide, NO_v, was produced in their flash photolysis system both with and without a nitric oxide filter for the flash. This meant that excitation was partly due to other species present in the mixture. The two most likely mechanisms were

a) energy transfer from vibrationally excited CN_v to NO (v = 0) and

b) the photolysis of NOCN to give NO_v.

The latter explanation is reasonable since photolysis of NOBr and NOCl is known to produce NO_v with appreciable population of excited levels.

Using the technique of pulse radiolysis, Bullock and Cooper[18] monitored the reactions of vibrationally excited CN radicals. For the reaction of CN with cyanogen, the rate constant determined for the removal of CN (v" = 0) at 377 K was larger at lower cyanogen pressures. A plot of observed rate coefficient against cyanogen pressure was linear at 300 K but curved at 377 K. The above observations may be explained if, at higher cyanogen pressures and elevated temperatures, vibrational relaxation to CN ($X^2\Sigma$, v" = 0) occurs more efficiently.

The expected efficiency of near resonant vibration to vibration energy transfer from CN_v to HCN impurity was given as the explanation of the high value of the rate constant obtained by Dunn et al.[24] for the removal of CN_v in their system (ν_{CN} = 2042.4 cm^{-1}, ν_{HCN} = 2041.2 cm^{-1}).

For the reaction of CN ($X^2\Sigma$) with molecular oxygen, Bullock and Cooper[18] observed that the rate constant increased with the vibrational energy of the CN radical as shown in table 1.02. A study of the rate of formation of the NCO product gave a rate constant of (1.98 $\pm$ 0.13) x 10^{-11} cm^3 $molecule^{-1}s^{-1}$ which is greater than the value for the disappearance of CN (v" = 0) which is evidence for an enhanced rate of reaction for vibrationally excited CN.

Table 1.02

Rate constants for reaction with Oxygen[18]

Molecule and Band (v', v")	Rate constant/10^{-11} cm^3 $molecule^{-1}s^{-1}$	
	303 K	375 K
CN (0, 0) removal	1.12 $\pm$ 0.02	1.05 $\pm$ 0.04
(1, 1)	1.26 $\pm$ 0.03	
(2, 2)	1.53 $\pm$ 0.04	
(3, 3)	1.63 $\pm$ 0.05	
(4, 4)	1.94 $\pm$ 0.58	1.79 $\pm$ 0.05
NCO appearance		
(0, 0, 0)	1.98 $\pm$ 0.13	1.84 $\pm$ 0.10

Since the energy mismatch for efficient transfer of vibrational energy from CN to O_2 was large, Bullock and

Cooper[18] attributed the increments in rate constants as v" increased to increasing rate of reaction. The transition complex NC-O-O with a weak O-O bond was proposed, and it was suggested that the vibrational energy of the CN would aid the breaking of the O-O bond to give NCO and oxygen atoms.

Schacke et al.[21] however observed the opposite trend to that given in table 1.02 for the same reaction. They found the rate constant at 298 K to decrease monotonically from 1.05×10^{-11} for CN ($X^2\Sigma$, v" = 0) to 2.64×10^{-12} cm^3 $molecule^{-1}s^{-1}$ for CN ($X^2\Sigma$, v" = 7).

The discrepancy between these two sets of results remains to be resolved. The differences in rate constants observed for the vibrational levels studied by both Bullock and Cooper[18] and Schacke et al.[21] were small and of the order of the experimental uncertainty. The relative importance of vibrational effects could differ under the markedly different conditions used for the two sets of experiments, and this could account for the inconsistent results.

Schacke et al.[21] also studied the effect of vibrational energy of CN ($X^2\Sigma$) on its reaction with atomic oxygen. The rate constants at 298 K for CN ($X^2\Sigma$, $0 \leqslant v" \leqslant 6$) were the same and equal to 2.10×10^{-11} cm^3 $molecule^{-1}s^{-1}$, but for CN ($X^2\Sigma$, v" = 7) the value was 1.05×10^{-10} cm^3 $molecule^{-1}s^{-1}$. This may be explained by the effective use of the vibrational energy of level v" = 7 in overcoming the endothermicity of the following reaction.

$$O + CN_v \longrightarrow NO + C \quad , \quad \Delta H^o_o = +139 \text{ kJmol}^{-1} \qquad (1.38)$$

For the reaction of CN ($X^2\Sigma$) with ethylene, Bullock and Cooper[17] found the differences in rate constant for removal of

CN (v" = 0) and CN (v" = 4) to be of the order of the random error in their technique. They had expected the removal of CN (v" = 4) to have a substantially greater rate constant if vibrational relaxation was important or if vibrational energy contributed to rate enhancement. Neither effect therefore appears to be important for this very fast reaction.

The same arguments were given by Bullock and Cooper[17,19] for the reactions of CN with methane and ethane. For the methane experiments however, curvature in the Arrhenius plot indicated that vibrational relaxation of CN (v"> 0) to CN (v" = 0) caused the removal of CN (v" = 0) to be slower than expected. Again for the methane experiments the rate constant for removal of CN (v" = 0) increased less with increasing temperature than for CN (v" = 4), and this is attributable to the vibrational relaxation of v" = 1 - 4.

If the internal energy of CN ($X^2\Sigma$) was helping to overcome the activation energy of the abstraction reaction with methane, the effect of vibrational energy would be less pronounced at higher temperatures and not more pronounced as was found.

Bullock and Cooper[19] also studied the reaction of vibrationally excited CN radicals with CD_4. They found that the ratio of the rate constants for removal of CN (v" = 4) and CN (v" = 0), $k_{v" = 4}/k_{v" = 0}$, was greater for reaction with CD_4 than for reaction with CH_4. This was attributed to enhanced relaxation processes in the CD_4 case, as the probability of vibrational energy transfer to CD_4 is greater than for transfer to CH_4 (V + T $\rightarrow$ V process).

The reaction of CN ($X^2\Sigma$) with ammonia was studied by Bullock et al.[20] and the rate constants for the removal of CN ($X^2\Sigma$) increased with increasing v", as shown in table 1.03.

Table 1.03

Rate constants for reaction with ammonia[20]

Molecule and band (v', v")	T/K	Rate constant /10^{-11} cm^3 $molecule^{-1}$ s^{-1}
CN (0, 0) removal	300	2.09
CN (2, 2) removal	300	2.49
CN (4, 4) removal	300	3.77
NH_2 (0, 0, 0) appearance	300	1.91
CN (0, 0) removal	375	1.79
CN (4, 4) removal	375	2.32

However, it was not possible to distinguish between enhanced reactivity and vibrational relaxation as the mechanism for the increased rate of removal for the higher vibrational levels.

Cottrell and Matheson[38] suggested that excess energy from vibration to vibration energy transfer processes was more easily incorporated into rotational degrees of freedom by molecules such as NH_3 and CH_4, which have low movements of inertia and high peripheral speeds of rotation. If the observed increments in rate constant in table 1.03 were due entirely to vibrational relaxation, ammonia is more than fifty times more efficient than methane as a relaxing molecule. Bullock et al.[20] indicated that polar interactions could be important in the reaction of CN with ammonia.

VIBRATIONAL ENERGY EFFECTS IN OTHER SYSTEMS

As far back as 1889, Arrhenius[39] investigated the temperature dependence of reaction rates for systems with activation energy

barriers. Only in recent years however, with the advent of energy selection techniques using chemical and dye lasers, has the role of specific internal excitation been investigated for systems with energy barriers.

For some exothermic reactions of atoms with simple diatomic molecules, the products have been shown to be vibrationally excited. This phenomenon was first observed by Polanyi[40] in the reaction of potassium atoms with molecular bromine. The KBr product was so highly vibrationally excited that subsequent collision with a potassium atom resulted in electronic excitation of the atom.

Parker and Pimental[41] observed product vibrational excitation in the following reactions.

$$F + H_2 \xrightarrow{k_v} HF_v + H \qquad (1.39)$$

$$F + D_2 \xrightarrow{k_v} DF_v + D \qquad (1.40)$$

These reactions have also been studied by Polanyi and Woodall[42] and Berry[43].

HF and DF were produced in levels v = 0 - 3 and v = 0 - 4 respectively. The ratio of the rate constants for the production of vibrationally excited products, k_v/k_{v-1}, was greater than unity, increasing with v to a maximum at v = 2 for HF and v = 3 for DF and then decreasing again at higher v. Parker and Pimentel[44] observed similar results for the reaction of $F + CHCl_3$.

Detailed energy balancing considerations (c.f. Principle of Microscopic Reversibility) suggested that vibrational excitation could give rate enhancement for the reverse of reactions 1.39 and 1.40.

In general, rate enhancement would be expected to occur with vibrational excitation of a reactant in an endothermic or thermoneutral reaction.

Bauer et al.[45] observed that H_2-D_2 metathesis took place with high probability only when energy is localised in vibrational modes. Jaffe and Anderson[46] obtained extremely small reaction cross sections for the reaction of HI with DI (reaction 1.41) with translational energies up to 2.5 times the activation energy for the reaction.

$$HI + DI \longrightarrow HD + I_2 \qquad (1.41)$$

They suggested that specific rotational or vibrational excitation of the reactants might be required to give an appreciable reaction probability.

In a molecular beam experiment, Odiorne et al.[47] observed a rate enhancement of about two orders of magnitude for HCl (v = 1) compared to HCl (v = 0) in the following reaction.

$$K + HCl_v \longrightarrow KCl + H \qquad (1.42)$$

Sims et al.[48] observed similar large increases in rate constant with vibrational excitation for the reaction of Cl and Br atoms with H_2, which was in agreement with trajectory calculations.

Both Kurylo et al.[49] and Gordon and Lin[50] observed rate enhancement following vibrational excitation of ozone in its reaction with nitric oxide. Potter et al.[51] studied the reaction of OH with O_3, with OH in levels up to v = 9, and again rate enhancement with vibrational excitation was observed, as was the case also for the reaction of $O + HCl_v$ studied by Karney et al.[52]

The above are only a few examples of the ever increasing studies of the effects of vibrational excitation on reaction rates.

It should however be pointed out that rate enhancements are observed primarily for endothermic or thermoneutral reactions, and that the magnitude of enhancement decreases with increasing exothermicity to an extent where vibrational excitation becomes unimportant.

THE STUDY OF CN ($B^2\Sigma$)

The study of the production of CN ($B^2\Sigma$) radicals in active nitrogen flames has been undertaken by several groups of workers. The main contributors to this work were Bayes[53], Thrush and coworkers[54-59], Broida and coworkers[60-62], and Provencher and Kenney[63,64].

Electronically excited CN radicals were found to be produced by reaction of active nitrogen with carbonaceous materials such as hydrocarbons, halogenated hydrocarbons and cyanogen derivatives. Several mechanisms were proposed for the production of CN ($B^2\Sigma$) and it is thought that the P_1' distribution arises from cyanogen derivatives, the P_2' from halogenated hydrocarbons and the P_3' distributions occurs under blue flame conditions, where P_1', P_2' and P_3' are three different vibrational energy distributions.

The fluorescent lifetime of the $B^2\Sigma$ state of CN was determined by Jackson[65] and Luk and Bersohn[66] to be 49 and 60 ns respectively. West and Berry[67] observed both electronic and vibrational laser emission from CN radicals produced by photodissociative and predissociative fragmentation of cyanide containing molecules e.g. HCN, ClCN, C_2N_2 etc.

Chamberlain and Simons[68] have used their new technique of polarised photofluorescence excitation spectroscopy to study the vacuum ultraviolet photodissociation of HCN and BrCN. They found that both HCN and BrCN were produced initially in non-linear

excited electronic states of symmetry A', which rapidly predissociated to give CN ($B^2\Sigma$). The CN ($B^2\Sigma$) radicals then fluoresced and from the polarisation of the fluorescence signal, the predissociative lifetime of excited BrCN was determined to be 0.6 ps.

Reactions of ground state CN ($X^2\Sigma$) radicals have been shown to be similar to those of halogen atoms. Bersohn[69] discussed how the electron affinity of CN ($B^2\Sigma$) (5.75 eV) is much greater than that of the fluorine atom. Hence CN ($B^2\Sigma$) may be termed a superhalogen. This superhalogen nature is borne out in the following example given by Bersohn.

The cross section for the quenching of CN ($B^2\Sigma$) by Xe was found to be anomalously high compared to quenching be He and Ar. This may be explained in terms of the production of a quasi-stable species, XCN^*, similar to the molecule XeF^* for which ample experimental evidence exists.[70,71]

Table 1.04 clearly shows the relative reactivities of the different electronic states of the cyanide radical. The rate constants for fluorine atom reactions are also given to illustrate the superhalogen nature of CN ($B^2\Sigma$).

Table 1.04

Rate constants for CN and F atom reactions

Reactant	Rate constant/cm^3 $molecule^{-1}$ s^{-1}			Reference
	H_2	CH_4	O_2	
CN ($B^2\Sigma$)	4.5×10^{-11}	10.5×10^{-11}	151×10^{-12}	66
F	4.4×10^{-12}	5.4×10^{-12}		31
CN ($X^2\Sigma$)	3×10^{-14}	$\leqslant 1.1 \times 10^{-12}$	7.3×10^{-12}	16,62

THIS WORK

The aim of this work was to determine new rate constants for CN ($X^2\Sigma$, v" = 0) reactions, and to determine more accurate values for previously measured rate constants. In particular, in this work care was taken to eliminate feeding of CN ($X^2\Sigma$, v" = 0) from higher vibrational levels and to obtain rate constants which apply strictly for the removal of CN ($X^2\Sigma$, v" = 0) in the absence of vibrational relaxation processes.

In previous work, little attempt has been made to separate the two processes of vibrational relaxation and reaction, and so contributions from vibrational relaxation could be incorporated in the previously determined rate constants.

Of interest are the reactions of CN ($X^2\Sigma$, v" = 0) with molecules present in combustion processes, which include fuel molecules, oxidant, nitrogen containing molecules and combustion products. It was also of interest to determine the effect of vibrational excitation of CN ($X^2\Sigma$) radicals on the reaction with H_2 which had not been previously studied.

In this kinetic spectrophotometric study of CN radicals, a novel combination of two techniques, previously used on separate systems, was employed for the first time in the study of CN radical reactions.

Firstly, a high intensity CN lamp which emitted the CN ($B^2\Sigma$— $X^2\Sigma$) violet system was used as a monitoring source for CN ($X^2\Sigma$) radicals produced in the reaction vessel. This gave a signal to noise ratio superior to that obtained in previous work. A similar lamp was used by Boden and Thrush[16] who developed it from their studies of CN ($B^2\Sigma$) radicals in their active nitrogen flow system.

Secondly, a flash lamp which was co-axial to the reaction vessel was used (c.f. Wolfrum and coworkers[21-23]), giving more efficient photolysis of reactants than a conventional parallel flash lamp. This also enhances sensitivity since a lower concentration of parent molecules is needed to produce the desired CN concentration.

Although this combination of techniques was novel for studying CN radical reactions, it has been used previously by Morley and Smith[72] in their study of OH radicals.

CHAPTER 2

CHAPTER 2

EXPERIMENTAL

GENERAL INTRODUCTION

The experimental arrangement used in this study of the reactions of CN radicals was a development of the original flash photolysis technique used by Porter[73]. The apparatus for flash photolysis consists of three essential parts which are a photolysis flash lamp, a reaction vessel, and a method of detection of transient species produced by the photolysis flash.

The photolysis lamp is usually a cylindrical quartz tube, with an electrode at either end, filled with inert gas and connected to a capacitor, a charging unit and a switching device to discharge the flash. The lamp is designed to produce a short, high intensity light pulse and is usually parallel to and of similar length to the reaction vessel, which is typically a cylindrical quartz tube with windows at either end. A reflector is sometimes used to enclose the lamp and reaction vessel and so focus more light into the reaction zone.

Two methods of detection of transient species are commonly used with different advantages for different types of work. These two methods are called flash spectroscopy and kinetic spectrophotometry, and are described by Porter and West.[74]

Flash spectrosocopy involves the use of a spectroflash lamp to monitor the absorptions of transient species photographically with a spectrograph. This spectroflash lamp should have a short duration flash (shorter than the photolysis flash) and should give a clean continuum emission over as wide a spectral range as possible. A delay unit is used so that the spectroflash may be

triggered at any desired time interval after the photolysis flash.

Using this technique, any absorptions which occur over a wide range of wavelengths may be detected in a single experiment at a given delay time. To determine kinetic data from this method, several photographs at different delay times must be obtained.

In the technique of kinetic spectrophotometry[74], the light from, for example, a tungsten lamp (continuum source) is focussed through the reaction vessel onto the slit of a monochromator which is used to select a single wavelength. A photoelectric detector is set to measure the light intensity leaving the monochromator and the signal, triggered by the photolysis flash, is stored in a fast recorder e.g. a storage oscilloscope. In essence, a single wavelength is observed over a chosen time interval.

When flash spectroscopy is used for kinetic studies, several photographs at different delay times must be obtained. The absorptions must then be analysed on a densitometer and corrections made for the sensitivity of the photographic emulsion. Hence for kinetic work, kinetic spectrophotometry is more accurate and an absorption-time profile for a transient species may be obtained directly from a single experiment.

However, flash spectroscopy is useful for preliminary work on new systems where the actual transient species, their lifetimes and their absorption wavelengths have not previously been determined. This method may also be used to monitor very fast decays with half lives less than the duration of the photolysis flash.

Measurement of very fast rates is extremely difficult using kinetic spectrophotometry since scattered light from the photolysis flash tends to swamp the absorption; Boxall and Simons[75] have however

described a method for overcoming this problem by employing a dual beam technique.

Since the absorption wavelengths of CN radicals are well known[76] and the half lives of the radicals are very much greater than the duration of the photolysis flash, the technique of kinetic spectrophotometry was used in this kinetic study. A brief description of the apparatus used is given, followed by a more detailed account of the individual components.

DESCRIPTION OF APPARATUS

The general experimental arrangement may be seen in fig. 2.01. A CN emission lamp was used instead of a tungsten continuum lamp for the monitoring source. Emission from this lamp passed through the reaction vessel and entered the monochromator which was set to select the desired wavelength, and the light from the exit slit was detected by a photomultiplier. The signal from the photomultiplier was then fed to a transient recorder with facilities for visual display and digital output.

The CN radicals were produced by flash photolysis of cyanogen/helium mixtures, the main primary product of photolysis being CN radicals.

DESCRIPTION OF INDIVIDUAL COMPONENTS

1. CN Emission Lamp

Resonance absorption of the CN ($B^2\Sigma$ — $X^2\Sigma$) system was used to monitor the decay of ground state CN ($X^2\Sigma$). The CN lamp used in this work gave strong CN ($B^2\Sigma$ — $X^2\Sigma$) emission. A diagram of the emission lamp and flow system is given in fig. 2.02. Basically the lamp is similar to that used by Morley and Smith[72].

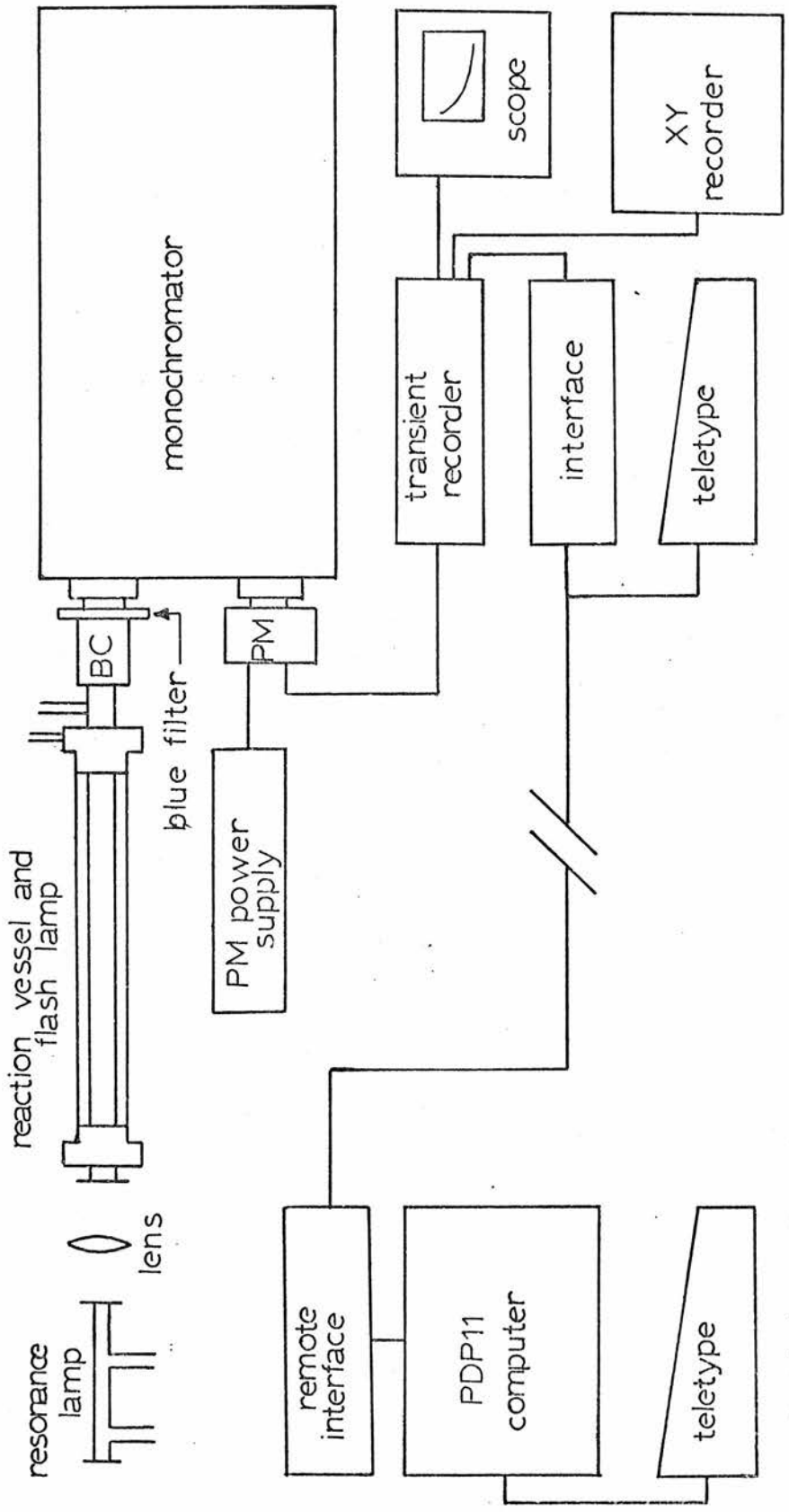

FIG.2.01 DIAGRAM OF APPARATUS

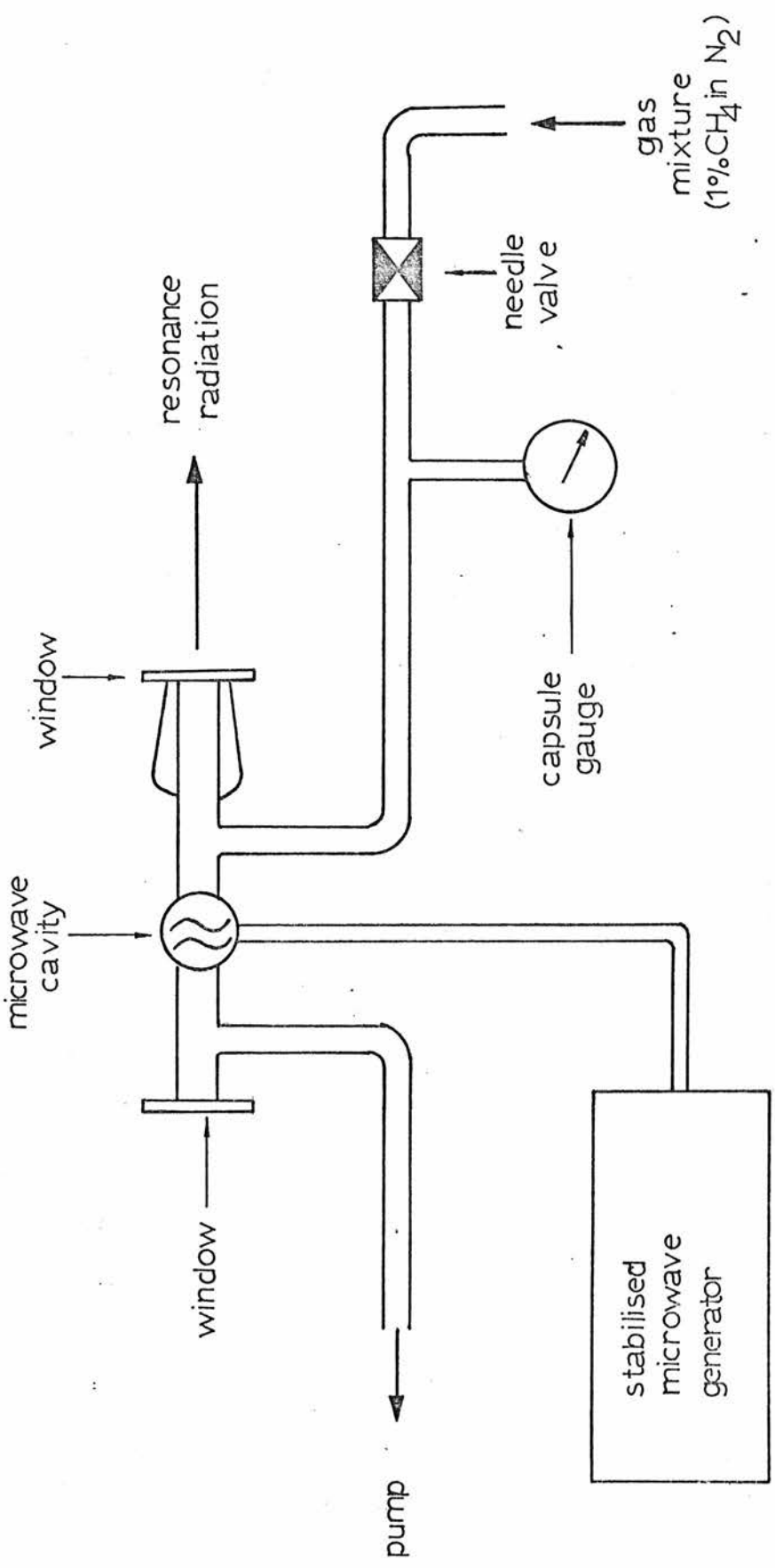

FIG. 2.02 CN DISCHARGE LAMP

Both 9 mm and 12 mm o.d. pyrex tubing was used for the main section of the lamp and it was found that the 12 mm tubing gave a more stable discharge. Microscope slides, which gave good transmission at 400 nm (short wavelength cut-off $\sim$320 nm), were used as windows. The concentric tube arrangement used to mount the exit window prevented the black wax which secured the window from contaminating the discharge.

The microwave cavity was a quarter wave, air cooled model powered by an EMI Microwave Power Generator Type T1001 which had been modified to give a reduced output ripple of $\leqslant 0.2\%$ (a reduction of about a factor of 5). This unit was normally operated at an input power of 90 W and zero reflected power. The lamp was allowed to stabilise for a few minutes before experimental measurements were taken.

It was advantageous to obtain the most intense emission possible, since the signal to noise ratio increases with the square root of intensity.[74] Maximum emission intensity was obtained when a mixture of 1% methane and 99% nitrogen was flowed through the lamp at a pressure of 270 Nm^{-2}, indicated on a capsule gauge, and at maximum pumping speed. The above conditions were used throughout this work.

The CN ($B^2\Sigma$ — $X^2\Sigma$) $\Delta v = 0$ sequence, emitted by the lamp and observed in the third order of the monochromator, was recorded photoelectrically and is given in fig. 2.03. The wavelength scale gives the first order wavelengths and the various band heads are indicated together with two mercury lines as standards. The mercury lines[77] at 579.07 and 576.96 nm were observed in second order and are therefore equivalent to 386.04 and 384.64 nm on the wavelength scale of fig. 2.03.

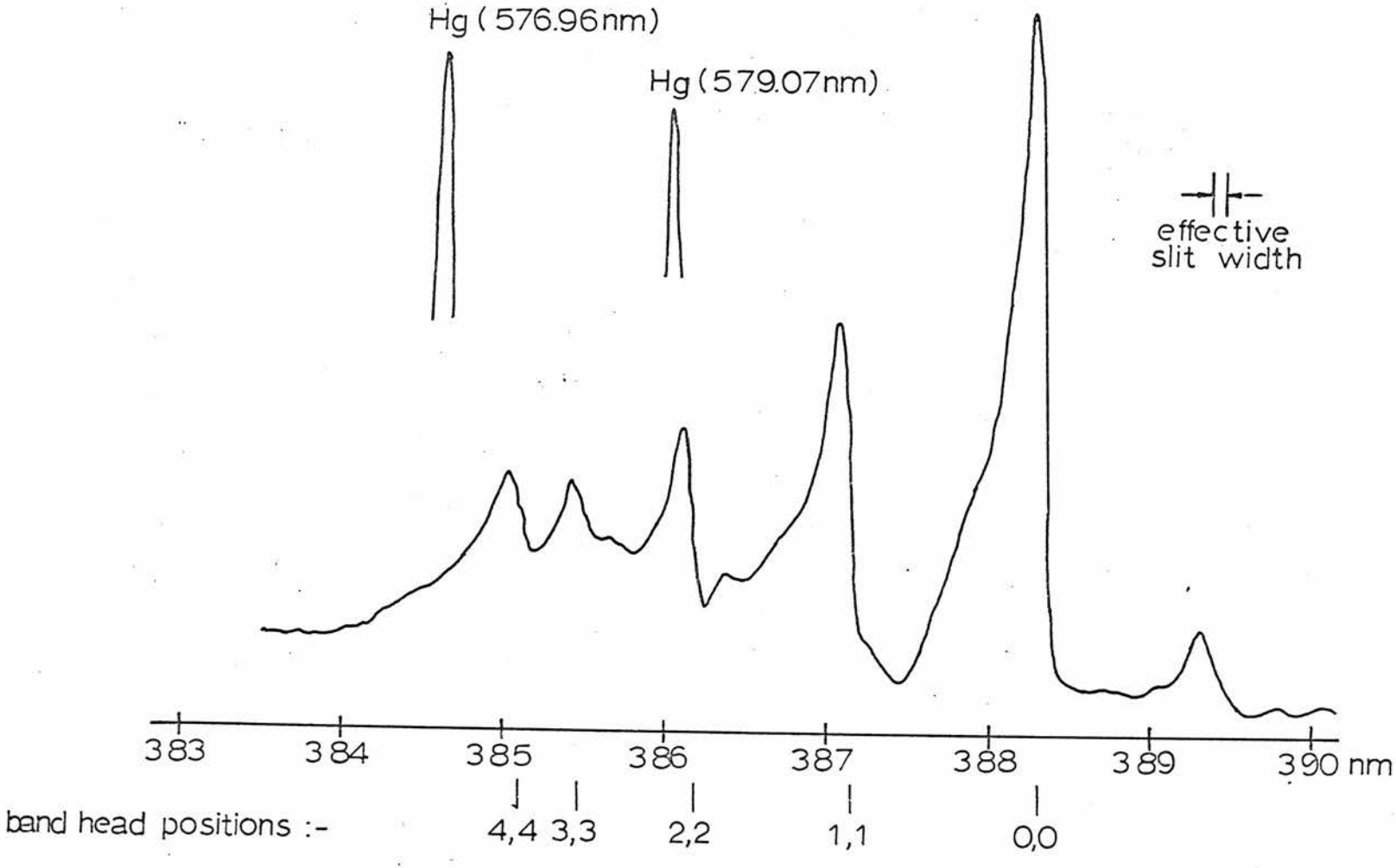

FIG. 2.03 EMISSION FROM CN LAMP

A photograph of the CN emission spectrum at higher resolution was obtained on a Bausch and Lomb 1.5 m Stigmatic Spectrograph. This spectrum is given in Chaper 3 where the rotational temperature of the CN lamp will be discussed.

2. Flash lamp

A coaxial flash lamp was used, the flash jacket concentrically surrounding the reaction vessel and separated from it at both ends by brass electrodes as shown in fig. 2.04A. The annular gap, about 2.5 mm was filled, typically, to 670 Nm^{-2} with X-grade krypton (B.O.C.) which was replaced when the lamp ceased to fire reproducibly. The outer jacket was pyrex and was fixed to the electrodes with Araldite. Rubber O-rings were used to form a vacuum seal between the electrodes and the reaction vessel.

A diagram of the capacitor and charging arrangements is given in fig. 2.05. Although, initially a 15 kV, 10 μF capacitor was used, for the majority of experiments a 15 kV, 2.5 μF capacitor was found to be adequate. An Applied Photophysics 25 kV power supply was used as a charging source, and the capacitor was charged to a potential in the range 5 to 10 kV, giving flash energies of 31 to 125 J. An advantage of this particular charging unit was that it could be preset to charge the capacitor automatically to a given potential, and so reproducible flash energies were obtainable over a series of experiments.

The lamp was fired by a simple mechanical plunger with brass electrodes. All HT cables in the flash circuit were as short as possible to reduce the inductance[74] in what is effectively an LCR circuit, and hence the duration of the flash was about 60 μs at an energy of 31 J and 90 μs at 125 J for wavelengths $230 \leqslant \lambda \leqslant 400$ nm.

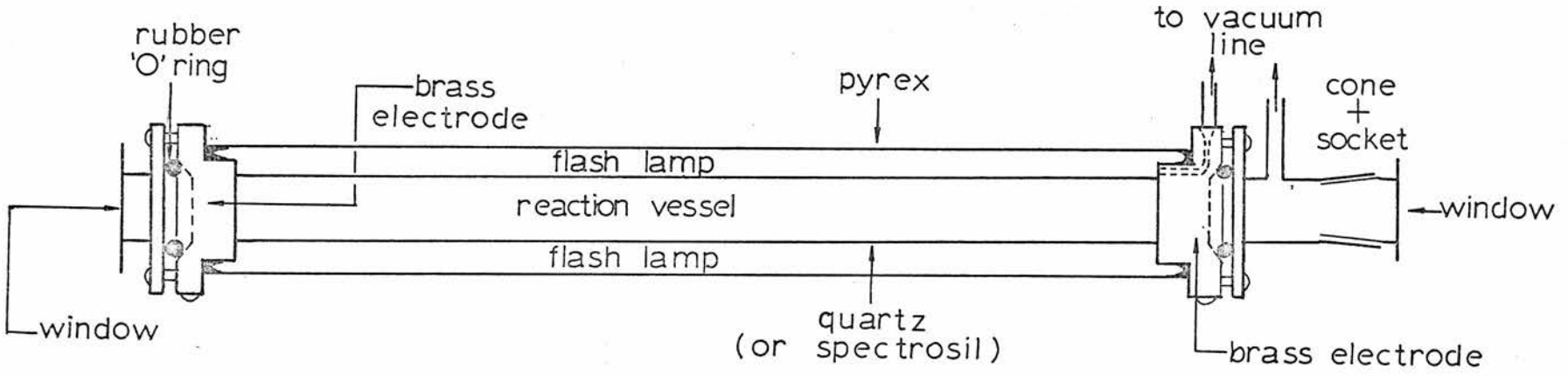

FIG. 2.04a REACTION VESSEL AND FLASH LAMP

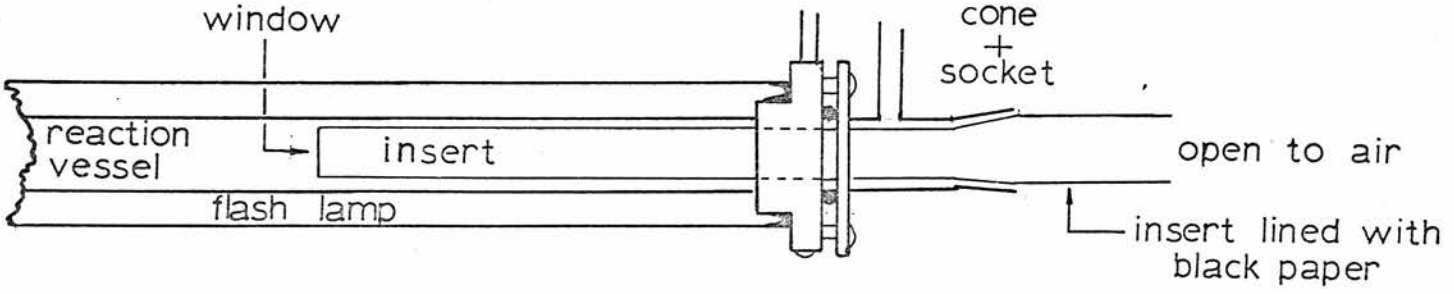

FIG. 2.04b REACTION VESSEL WITH INSERT

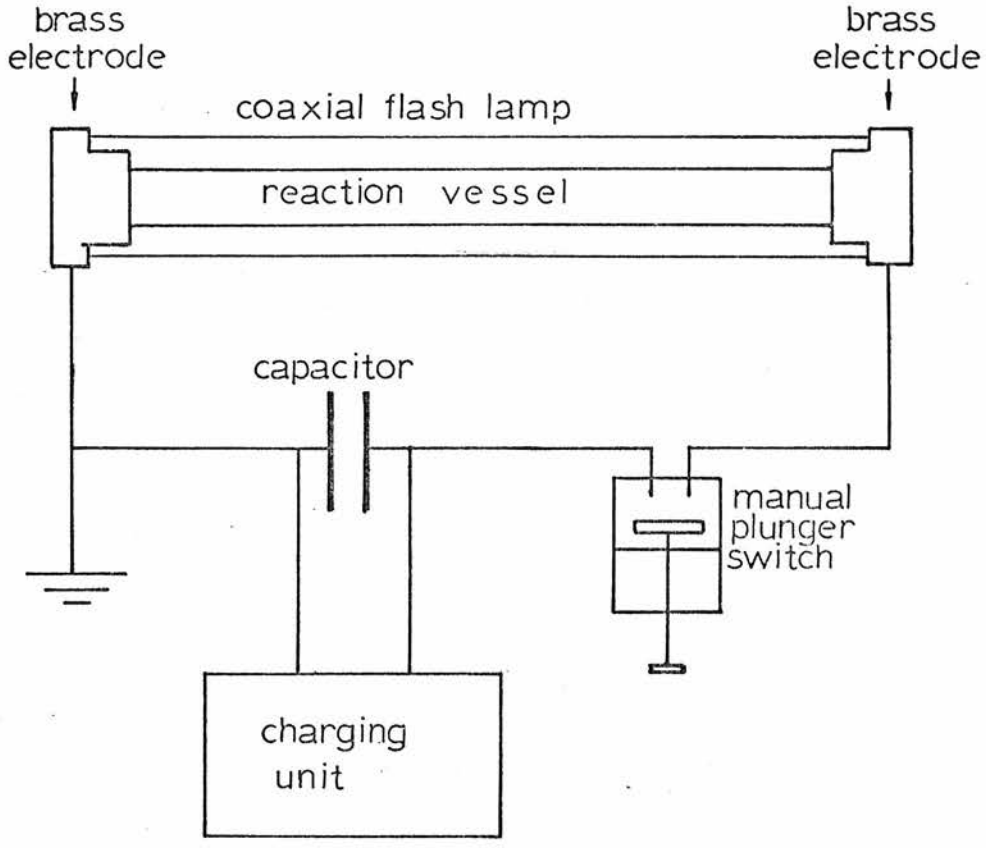

FIG. 2.05 FLASH LAMP CIRCUIT

The duration of the flash was considered to be the time taken for the intensity to return to less than 1% of the maximum intensity.

3. Reaction Vessel

The reaction vessel is illustrated in fig. 2.04A. Both quartz and spectrosil vessels were used in preliminary investigations. The short wavelength cut-off values, λ_c, for various materials are given in table 2.01 where λ_c is for 50% transmission through a 5 mm sample.

Table 2.01

Cut-off wavelengths

Material	λ_c/nm
Glass	350
Pyrex	300
Quartz	185
Spectrosil	165

For most of this work, a quartz vessel was used because there is less chance of photolysing reactant molecules than with a spectrosil vessel. Also, the extent of the vibrational excitation of the CN radical is less with a quartz vessel. The reaction vessel windows were made from microscope slides which gave good transmission at 400 nm (short wavelength cut-off $\sim$ 320 nm).

Several inserts of differing lengths were made to fit inside the vessel so that path lengths of 1.00 L, 0.67 L, 0.5 L and 0.33 L could be obtained (where L = full cell length) in order to determine any diviations from the simple form of the Beer-Lambert Law. An illustration of how these inserts fit into the reaction vessel is given in fig. 2.04 B.

4. Monochromator and optical system

The monochromator was a Hilger and Watts Monospek 1000 Grating Spectrometer D400, which utilized a symmetrical Czerny-Turner system of two mirrors and a grating to give parallel incident and exiting beams. The grating had a ruled area of 104 x 104 mm^2 with 600 lines/mm giving a dispersion of 8 Å/mm and was blazed for 1 μm. A motorised scanning facility was also incorporated.

For most kinetic experiments, the monochromator was set for maximum absorption of the CN ($B^2\Sigma$-$X^2\Sigma$) (0,0) P branch. This did not coincide with the maximum of the CN ($B^2\Sigma$-$X^2\Sigma$) emission from the lamp, as the rotational temperature of the radicals in the lamp differed from that of the radicals in the reaction vessel. These rotational temperatures will be discussed in Chapter 3. The slit width used for all kinetic work was 0.10 mm for both entrance and exit slits. Various other monochromator settings were occasionally used and details will be given in the relevant chapters.

The CN ($B^2\Sigma$-$X^2\Sigma$) $\Delta v=0$ emission bands from the CN lamp were monitored in different orders from 1st to 5th, and it was found that the CN signal was most intense with the monochromator set for 3rd order. Although the blaze wavelength was 1 μm in first order, the blaze wavelength changes with the order in a complicated manner and in fact the grating is most efficient for the CN violet system in the third order.

In general, with a monochromator, a large percentage of useful light is lost since the source and reaction vessel have a circular cross-section and the slits are narrow rectangles. To help minimise this discrepancy, various lens configurations were tested to focus as much light as possible onto the entrance slit. It was found that a symmetrical convex lens, f~10 cm, situated between the CN lamp and the reaction vessel was effective.

A diagram of the optical system is given in fig. 2.01. As indicated on this diagram, a black cardboard tube was placed between the reaction vessel and the filter holder, which was situated just in front of the monochromator entrance slit. The purpose of this was to reduce the amount of scattered light from the photolysis flash reaching the slit.

A blue R-0B10 filter, which gave good transmission at 390 nm, was placed in front of the entrance slit. This filter restricted the wavelength of the light reaching the slit to $335 \leqslant \lambda \leqslant 515$ nm and so minimised the overlap of the CN region in third order by radiation from other species present in the CN lamp.

5. Photomultiplier

An EMI 9781B photomultiplier with a Corning 9741 UV glass envelope was mounted directly on the monochromator exit slit. This tube, a modified S-5 type with a caesium-antimony cathode, gave a good spectral response between 300 and 400 nm. A Brandenburg Model 472R power supply was used to run the tube at 800 V.

Circuit designs for photomultipliers for use in kinetic spectrophotometry have been discussed by Porter and West[74]. A signal with minimal noise is essential for this type of work. Apart from dark current, the major source of noise in a photomultiplier circuit is shot noise[78], which arises when photons incident on the cathode are converted to electrons i.e. these are statistical fluctuations due to the random arrival of incident photons on the photocathode.

A means of quantifying noise is via the signal to noise ratio S/N.

$$S/N = \sqrt{I_c/(2e\Delta f)} \qquad (2.01)$$

In the above equation, S and N are the signal and noise respectively in arbitrary units, I_c is the cathode current, e is the charge on the electron and Δf is the band width. This formula applies when the electrons move freely between the dynodes in the absence of space charges.

Equation 2.01 shows that as the cathode current I_c increases, the S/N ratio increases and so the more intense the light source, the better the S/N ratio, since I_c is proportional to incident intensity. Ideally, therefore, I_c should be large. I_c is amplified along the dynode chain to give the anode current I_a which has an upper working limit (0.5 mA for the tube used in this work) determined by energy dissipation at the anode, dynode heating and space charge effects. Hence for large I_c, the gain must be restricted and this can be achieved by lowering the cathode to anode voltage, but this can lead to problems of non-linearity in the gain.

Porter and West[74] discussed the problems of reducing photomultiplier gain for tubes used in kinetic spectrophotometry. They calculated values of I_c for acceptable S/N ratios of 1000:1 and 100:1 for milli- and microsecond time scales and showed that good results could be obtained using low gains of 10^3-10^4. This means that for kinetic spectrophotometry, high gain photomultiplier tubes are not necessary.

The solution to the problem of reducing the gain and maintaining linearity is to reduce the number of dynodes. This was the case in the circuit used in this work where dynodes D7, D8 and D9 and the anode A were connected together as shown in figure 2.06. Linearity was maintained by using a Zener diode (150 V) between D5 and D6, and three decoupling capacitors between dynodes D3 to D6 to stabilise the interdynode potentials.

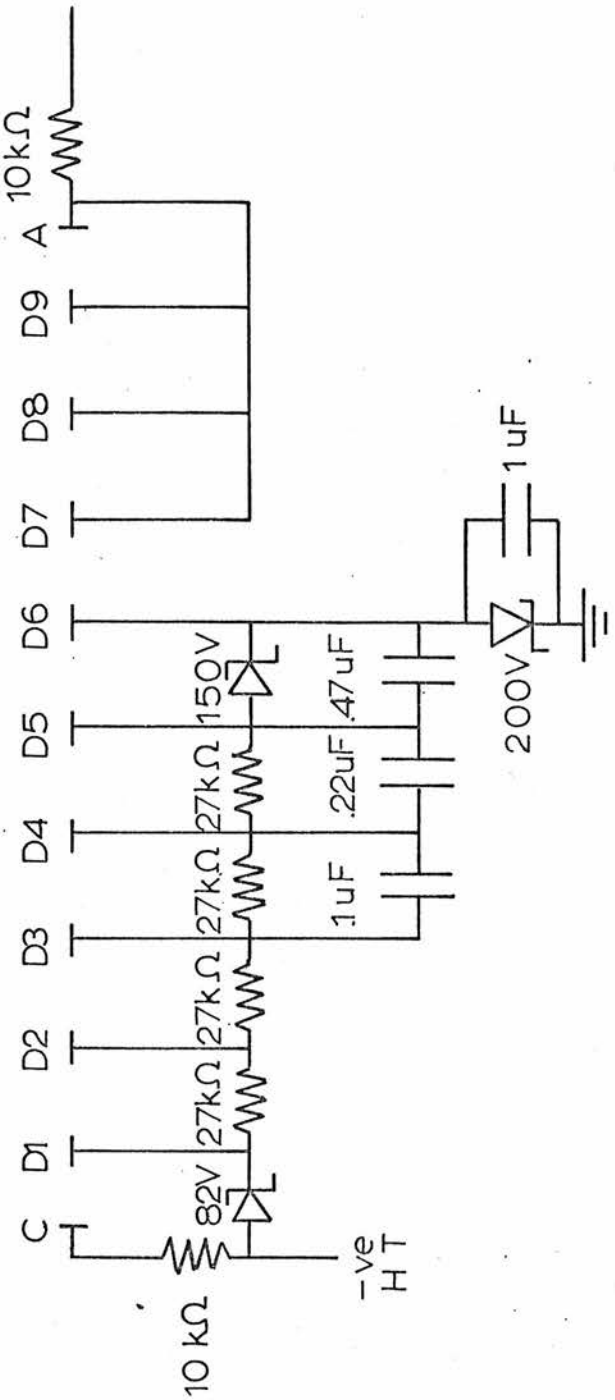

FIG. 2.06 PHOTOMULTIPLIER CIRCUIT

Operating the photomultiplier tube at low gain as described above increases its life since overheating, which can destroy dynode coatings, is avoided.

A simple circuit for obtaining current to voltage conversion of the photomultiplier output signal is given in fig. 2.07 and involves a load resistor (47 kΩ in this case). The potential dropped across the resistor will be proportional to the current flowing through it.

However, the circuit given in fig. 2.08 was used for most of this work because it converted the CN decay signal to an exponential curve (effectively a concentration against time curve) which was easier to analyse than the intensity measurements obtained using a load resistor. In this circuit, two high speed switching diodes (type 1N914) were placed in series across the photomultiplier output and the voltage drop across them was monitored.

It is well known that diodes have a logarithmic relationship between current i through the device and voltage V dropped across it. Use was made of this fact in construction of this simple logarithmic converter consisting of the two diodes, as used by Morley and Smith[72]. Fig 2.09 is a plot of current i through the two silicon diodes in series against voltage drop across them. This was measured on a Telequipment Curve Tracer Type CT 71 on the most sensitive ranges (5 nA/div, 0.1 v/div). Fig 2.10 is a plot of ln(i) against voltage drop for the same data and gives a straight line indicating that the diode device behaves as expected.

As a further check that the device operated satisfactorily, data obtained using the diode circuit were checked against the data obtained using the load resistor for a series of experiments.

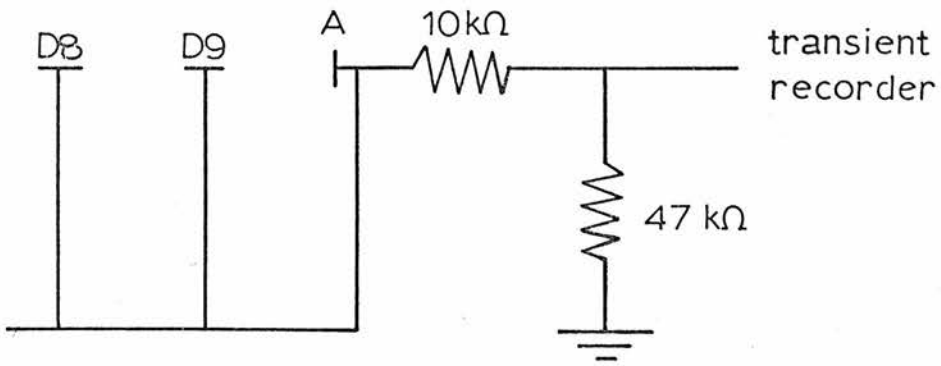

FIG.2.07 LOAD RESISTOR CIRCUIT

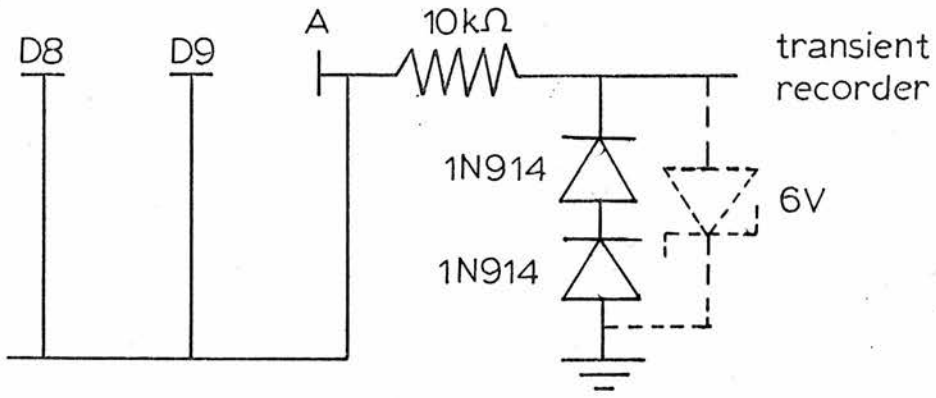

FIG.2.08 - DIODE CIRCUIT

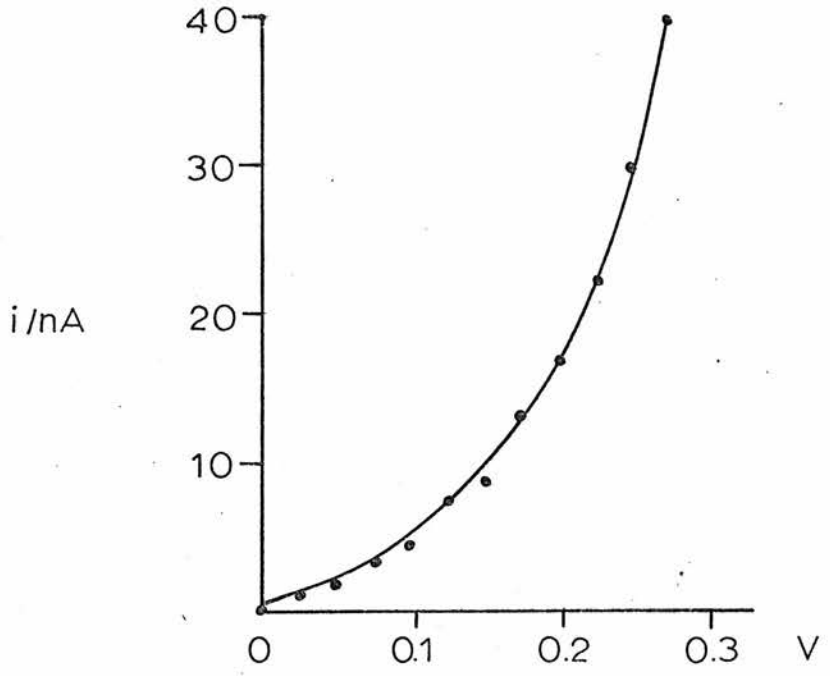

FIG. 2.09 GRAPH OF CURRENT AGAINST VOLTAGE

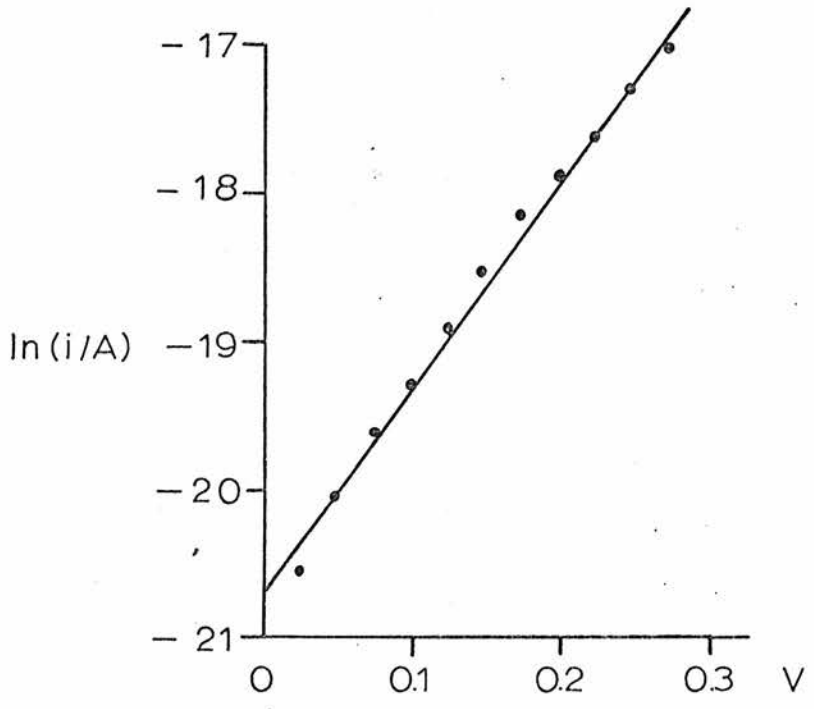

FIG. 2.10 GRAPH OF LN(CURRENT) AGAINST VOLTAGE

Four mixtures of $(CN)_2/He/H_2$ were made up to give a range of reaction rates by varying the partial pressure of H_2. The rate coefficients obtained for the removal of CN radicals for each mixture using both the load resistor and the diode circuit were in good agreement as shown in table 2.02.

Table 2.02

Rate Coefficients obtained with load Resistor and with Diode Device

Circuit	Rate Coefficient k_{obs}/s^{-1}			
	$He/C_2N_2/H_2$ mixtures			
	A	B	C	D
Load Resistor (Fig. 2.07)	458 ± 46	991 ± 109	1770 ± 223	2950 ± 437
Diode Device (Fig. 2.08)	447 ± 44	1020 ± 115	1610 ± 196	2790 ± 405

An attempt was made to reduce the shot noise in the load resistor circuit (fig. 2.07) by lowering the band width, Δf, which is given by equation 2.02 (Porter and West[74]),

$$\Delta f = 1/(2\pi RC) \qquad (2.02)$$

where R is the resistance and C is the capacitance of the external cicuit. This was achieved by placing a capacitor, C_1, across the load resistor. Morrow[78] points out the dangers of using too large a capacitance resulting in distortion of decay profiles. An optimum value of the capacitance of C_1 was found to be 0.0033 μF.

In most of this work however, the diode logarithmic device of fig. 2.08 was used in conjunction with a reverse biased 6 V Zener

diode which was found to be more effective in reducing noise than a capacitor. Fig. 2.11 is a typical decay trace obtained using the diode device and the Zener diode.

6. Signal and Data Processing

The layout of the equipment for processing the output from the photomultiplier is shown in fig. 2.01. For the most of the experiments, the output from the photomultiplier was fed into a fast transient recorder (Datalab DL905) via two silicon diodes (type 1N 914) placed in series across a BNC T-piece (no load resistor), as shown in fig. 2.08. This circuit gave rise to a logarithmic input to the transient recorder, as discussed in the previous section. A 1024 channel, 8 bit word memory stored the signal which could then be displayed in analogue form (Telequipment DM64 Oscilloscope and for permanent record, on a Bryans XY Recorder 26000 A4). The contents of the memory could also be sent in digital form to a paper tape punch (not used in this work) and direct to a Digital PDP11/20 computer for on-line processing.

For the first part of this work, direct digital processing facilities were not available and the XY plotter traces were digitised on a Ferranti Freescan Digitiser and transferred to magnetic tape for processing on an ICL 4-75 computer. However, the majority of the experimental data was sent direct to the PDP11/20 computer from the transient recorder and processed on-line. The computer programmes used for the data processing were originally written and developed by my predecessor Robin Strain[79].

The advantage of the DL905 transient recorder was that a portion of the memory could be allocated to store the pretrigger signal. In most cases, the first 200-300 channels were used for this purpose and the contents of these channels were averaged to give a value for the baseline for the post-trigger decay signal. Fig. 2.11 shows a

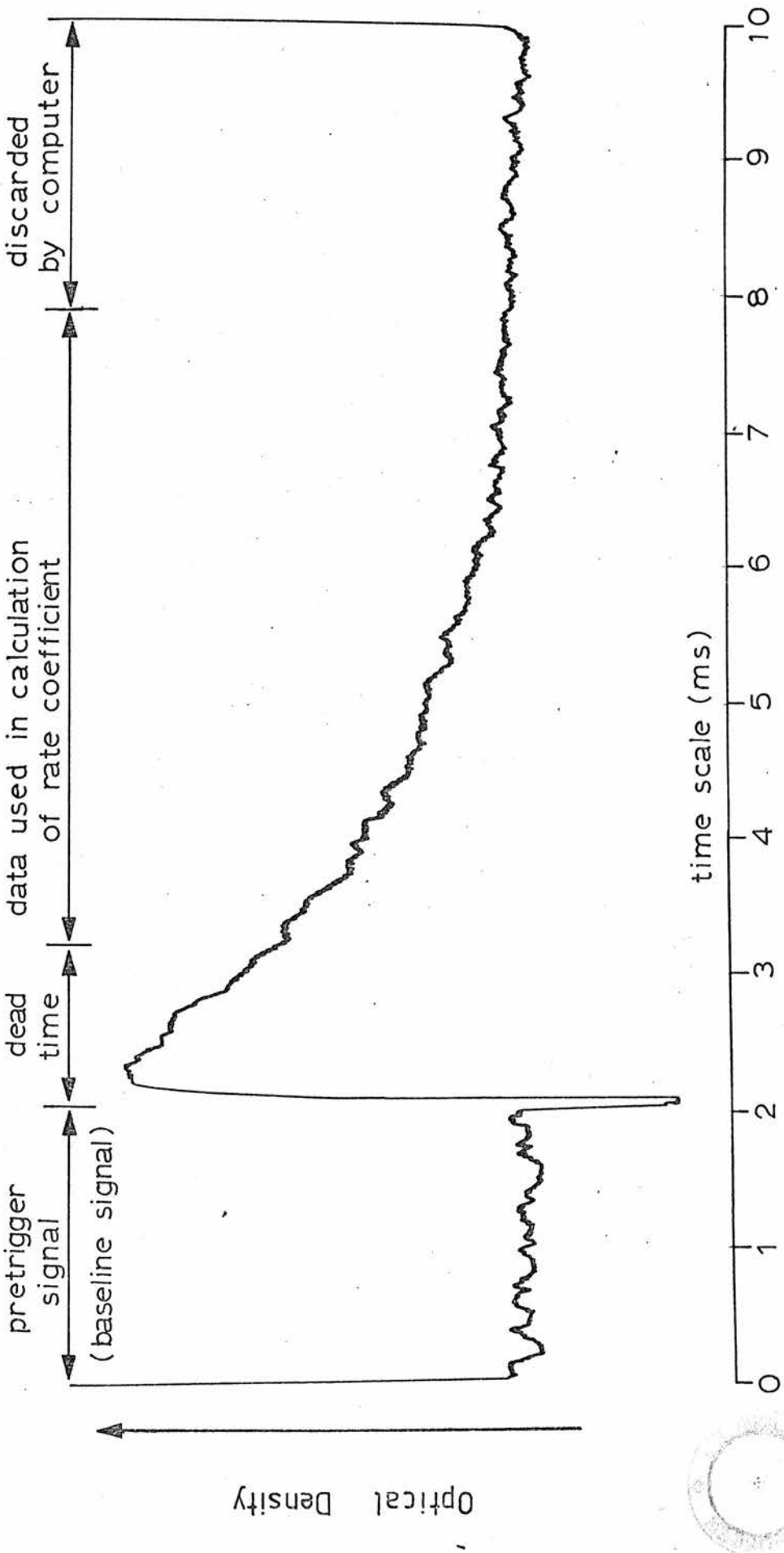

FIG.2.11 TYPICAL CN DECAY TRACE (USING DIODE DEVICE)

typical XY plotter trace of the memory contents for the decay of CN radicals. According to the time base used, about the next 100 channels after the triggering event were ignored for the rate coefficient calculations because during this time, the photomultiplier was recovering from the scattered light produced by the photolysis flash. Also, by this time, as the signal corresponds to <25% absorption, the Beer-Lambert exponent, γ, should remain constant throughout the decay. The significance and determination of γ will be discussed in chapter 3.

The contents of the remaining channels were used to calculate k_{obs}, the observed rate coefficient for the decay. Once the optical density (O.D.) had decreased to the level of the noise in the pretrigger signal (baseline), the data in the remaining channels were rejected by the computer programme.

A least squares fit of the graph of ln(O.D.) against time was used in the calculation of k_{obs}, since the optical density was proportional to the CN concentration. The gradient of this plot, multiplied by -1, gave the observed rate coefficient, k_{obs}.

In order to calculate the rate constant for reaction of CN with a reactant, the rate coefficients for several partial pressures of reactant were obtained. The gradient, obtained from a weighted least squares fit of k_{obs} against partial pressure of reactant, gave the rate constant k when divided by the Beer Lambert exponent γ.

EXPERIMENTAL PROCEDURE

The following list was the procedure normally executed for most experiments.

1. Make up gas mixtures.
2. Switch on electronic equipment.
3. Refill flash lamp with fresh Kr if the flash is erratic or not reproducible.

4. Check that detection system is triggering from the flash reproducibly.
5. Set monochrometer to the required wavelength.
6. Pump out reaction vessel.
7. Flush out reaction vessel with the gas mixture to be used for the experiment.
8. Pump out reaction vessel.
9. Fill reaction vessel to the required pressure with reaction mixture.
10. Charge capacitor to the required potential.
11. Set trigger.
12. Fire flash lamp.
13. Record result.
14. Return to 5 for further experiments.

In the following chapters, any deviation from the standard methods described here will be discussed as they are encountered. The experimental details of work carried out at Thornton Research Centre (Shell Research Ltd.) will be described in Chapter 9.

PRODUCTION OF CN RADICALS

CN radicals were generated from the flash photolysis of cyanogen in the presence of helium buffer gas. The excess helium was necessary to dissipate the kinetic energy produced in the primary photochemical step, so that the reaction mixture had a translational temperature close to room temperature.

Various $(CN)_2$/He mixtures were tested and a mixture containing 26.7 Nm^{-2} of $(CN)_2$ was found to be most suitable, since adequate absorption was obtained giving a good signal to noise ratio. At higher partial pressures, problems with saturation of the absorption

would have arisen, while at lower pressures, the signal to noise ratio would decrease.

In most experiments, helium buffer gas was added to mixtures of cyanogen plus reactant to give a total pressure of 1.33×10^{4} Nm^{-2}. The choice of this total pressure will be discussed in Chapter 4.

A rough estimate of the extent of photolysis of cyanogen was obtained by repeatedly flashing a $(CN)_2/O_2$/He mixture, until the rate was the same as for a $(CN)_2$/He mixture. Assuming a value of 10^{-11} cm^3 $molecule^{-1}$ s^{-1} for the rate constant of the reaction of CN with molecular oxygen, the amount of O_2 removed per flash was calculated. This corresponds to an upper limit of 8×10^{12} molecule cm^{-3} for the initial concentration of CN radicals produced in the quartz reaction vessel for a flash energy of 125 J.

In previous work, various parent molecules, RCN, have been photolysed to give CN radicals.[80,81] Although the strongest R-CN bond is for R = CN, the photolysis of cyanogen was chosen as the source of CN radicals for this work to avoid interference from other radicals e.g. R = Cl, Br, I etc.

As the CH_3-CN bond is weak, attempts were made to photolyse methyl cyanide. No CN radicals were observed possibly because of a fast abstraction reaction or recombination as in the following reactions.

$$CN + CH_3CN \longrightarrow HCN + CH_2CN \qquad (2.03)$$

$$CH_3 + CN + M \longrightarrow CH_3CN + M \qquad (2.04)$$

GAS HANDLING

A conventional glass vacuum line was used for gas handling, and a vacuum of $\sim 10^{-4}$ Nm^{-2} was obtained with a mercury diffusion

pump backed by a rotary pump (Edwards model 2SC20). Residual mercury was assumed to be the same in all gas mixtures and was not considered to alter the kinetics. The gas mixtures were made up in spherical bulbs and allowed to mix thermally for more than 3 hours, or stirred in a magnetically operated mixing vessel for 20 minutes.

Pressures were measured on a mercury manometer or on an oil damped glass spiral gauge. In some cases, where the determination of low pressures ($< 670\ Nm^{-2}$) was required, sharing ratios were used. Throughout the experimental work, ideal gas behaviour was assumed for all gases used.

GAS PURITIES

A list of gases used and methods of purification are given in Appendix I. The gases, except X-grade helium (B.O.C.) and certificated helium, were mostly analysed on a mass spectrometer (MS10) but it was obvious from the impossibly high levels of impurity found, that addition of these gases to the mass spectrometer was causing other gases to desorb from the metal surfaces of the mass spectrometer. Generally, IR spectra were run for most gases and no significant impurities were found. For some gases, the purity was assumed to be within the manufacturer's specification.

EXPERIMENTAL UNCERTAINTIES

Uncertainties in observed rate coefficients k_{obs} arose from two main sources, namely the uncertainty in assigning a baseline to a decay trace, like the one shown in fig. 2.11, and the random error found by repeating the same experiment several times. The uncertainty in k_{obs} is therefore a combination of the baseline uncertainty and the standard deviation calculated from a

set of identical experiments. This combined total uncertainty, which will be referred to as σ, was found to vary with k_{obs} and in general was about $\pm$ 40 s^{-1} for k_{obs} = 400 s^{-1} increasing to $\pm$ 450 s^{-1} for k_{obs} = 3000 s^{-1}. This applied for a single experiment. When the average of several identical experiments was obtained, the uncertainty became $\sigma/\sqrt{n-1}$ where n was the number of experiments averaged. ($\sigma/\sqrt{n-1}$ is equivalent to the standard error in k_{obs}).

The uncertainties in the rate constants presented in later chapters were obtained from the weighted least squares processing of plots of k_{obs} against partial pressure of reactant. The values quoted are equal to one standard deviation in the gradient. From all plots of k_{obs} against partial pressure of reactant, the assigned error bars (equivalent to the standard errors in k_{obs}) agreed well with the scatter in the points, suggesting that the assigned uncertainties were reasonable.

CHAPTER 3

CHAPTER 3

CN EMISSION AND ABSORPTION

INTRODUCTION

In this chapter, the emission of the CN resonance lamp, described in chapter 2, is discussed in detail along with the subsequent absorption of the CN resonance radiation by the radicals produced in the reaction vessel. However, before proceeding, an understanding of the spectroscopy of the CN violet system and its special features is essential.

The CN($B^2\Sigma - X^2\Sigma$) Violet System

The spectroscopy of the CN($B^2\Sigma^+ - X^2\Sigma^+$) violet system has been well characterised, and details of the various features are summarised by Herzberg [1] and the observed wavelengths of the bandheads are given by Pearse and Gaydon [76].

For CN radicals, where the equilibrium internuclear distance, r_e, is almost the same in both the $B^2\Sigma$ and $X^2\Sigma$ electronic states, the Condon parabola is extremely narrow and in fact the transition probabilities for the $\Delta v = 0$ sequence are significantly larger than for other sequences or progressions.

As the vibrational quanta of the $B^2\Sigma$ and $X^2\Sigma$ electronic states of CN radicals are of similar magnitude, the observed CN bands of the violet system are grouped in sequences rather than band progressions.

The selection rules for the change of rotational quantum number during an electronic transition depend on the coupling of the rotation and electronic motion. [1] Both the $B^2\Sigma$ and $X^2\Sigma$ states of CN radicals belong to Hund's coupling case (b), where the coupling of the spin vector S to the internuclear axis is very weak (or zero).

For Σ states, the angular momentum vector $\mathbf{N}$ of nuclear rotation is equal to $\mathbf{K}$, the vector of the total angular momentum apart from spin. The quantum number K is given by

$$K = \Lambda, \Lambda + 1, \Lambda + 2, \cdots$$

$$K = 0, 1, 2, 3 \cdots \text{ for } \Lambda = 0$$

Vector $\mathbf{J}$ is the total angular momentum including spin and is the resultant of $\mathbf{K}$ and $\mathbf{S}$. The quantum number J is given by

$$J = (K + S), (K + S - 1), (K + S - 2), \cdots, |K - S|$$

i.e. $J = K \pm \frac{1}{2}$ (for a doublet state).

The energy separation of the rotational levels is much larger than the separation of the sub-levels corresponding to $J = K + \frac{1}{2}$ and $J = K - \frac{1}{2}$.

The selection rules which apply in Hund's case (b) for a $^2\Sigma - {}^2\Sigma$ transition are

$$\Delta K = \pm 1$$

$$\Delta J = 0, \pm 1.$$

Since $\Delta K = 0$ is forbidden for $\Sigma - \Sigma$ transitions, the P and R branches are split into three components corresponding to $\Delta J = 0, \pm 1$. However for $\Delta J = 0 \neq \Delta K$, the intensity decreases dramatically with increasing K and normally only doublet P and doublet R branches may be observed under high resolution. Under low resolution, the doublets are unresolved and the spectrum corresponds to that of a $^1\Sigma - {}^1\Sigma$ transition.

Due to the relative changes in the vibrational energies of the $B^2\Sigma$ and $X^2\Sigma$ states with increasing vibrational quantum number, the band heads of the CN violet sequences turn back on themselves. In fact, a plot of v" against band head wavenumber is approximately parabolic for a given sequence. The wavenumbers of vibrational transitions are given by the following expression,[1]

$$\nu = \nu_{oo} + \omega_o' \Delta v - \omega_o' x_o' (\Delta v)^2 - (\omega_o'' - \omega_o' + 2\omega_o' x_o' \Delta v) v'' - (\omega_o' x_o' - \omega_o'' x_o'') v''^2 \quad (3.01)$$

where ν_{oo} is the wavenumber of the (0,0) band of the system, Δv is the change in vibrational quantum number, and the terms ω_o and $\omega_o x_o$ are as follows

$$\omega_o = \omega_e - \omega_e x_e + 0.75 \omega_e y_e + \cdots \quad (3.02)$$

$$\omega_o x_o = \omega_e x_e - 1.5 \omega_e y_e + \cdots \quad (3.03)$$

If the linear term in v" in equation 3.01 is small and of opposite sign to the quadratic term, then a reversal of band order can take place in a sequence.

For the $\Delta v = 0$ sequence of the CN violet system, the separation of the band heads decreases with increasing v" from the (0,0) band head at 388.34 nm to the (4,4) band head at 385.09 nm. Near the apex of the parabola mentioned above, the (5,5) to (10,10) bands are headless.[82] As v" is increased still further, band heads may again be observed at longer wavelengths and in fact, the (11,11) to (18,18) bands[82,83] have been observed at longer wavelengths than the (0,0) band. These bands are called the "tail" bands and may be observed under blue flame conditions in active nitrogen[76].

The wavenumbers of the rotational lines of a vibrational band may be obtained from the following equation[1]

$$\nu = \nu_o + (B_v' + B_v'')m + (B_v' - B_v'')m^2 \quad (3.04)$$

where ν_o is the wavenumber of the band origin, B_v' and B_v'' are the rotational constants for a given vibrational level and m is an integer (R branch for positive m, P branch for negative m).

From equation 3.04, it may be observed that if the linear term in m is of opposite sign to the term in m^2, the rotational lines can turn back on themselves and form a band head. A graphic illustration of this phenomenon in the form of a Fortrat parabola is given by Herzberg[1].

The band heads of the CN (0,0) to (4,4) bands occur in the P branch and are shaded to the violet, i.e. $B'_v > B''_v$. The tail bands however, at higher v have the band head in the R branch and are shaded toward the red i.e. $B'_v < B''_v$.

Fig. 3.01 shows the emission spectrum obtained for the CN resonance lamp under normal operating conditions. A Bausch and Lomb 1.5 m spectrograph with a slit width of 10 μm was used to photograph this spectrum. A blue filter (ROB10), which gave good transmission in the spectral region of interest, was placed between the resonance lamp and the entrance slit. The spectrum obtained will be discussed in more detail shortly.

CN EMISSION SPECTRA

Spectra of the CN violet system given by Pearse and Gaydon[76] and Herzberg[1] are useful illustrations of the spectroscopic features discussed in the previous section. The sources of these spectra were not specified, and so the discussion will be limited to more recent studies of the violet emission from CN radicals in active nitrogen flames, as this is particularly relevant to this work.

Vibrational Distributions

The emissions from CN radicals, produced in the reactions of active nitrogen with traces of carbonaceous materials have been studied by several researchers.[16,53-64] Both the CN red emission from the $A^2\Pi$ state and the CN violet emission from the $B^2\Sigma$ state were observed. Three distinct vibrational population distributions P'_1, P'_2, and P'_3 have been observed[61] for the CN violet bands.

The P'_1 distribution is charactertistic of CN ($B^2\Sigma$) produced in flames containing cyanogen derivatives,[54,61] RCN, and in this case, $v' \leq 15$. In halogenated hydrocarbon flames,[54,61] the P'_2 distribution

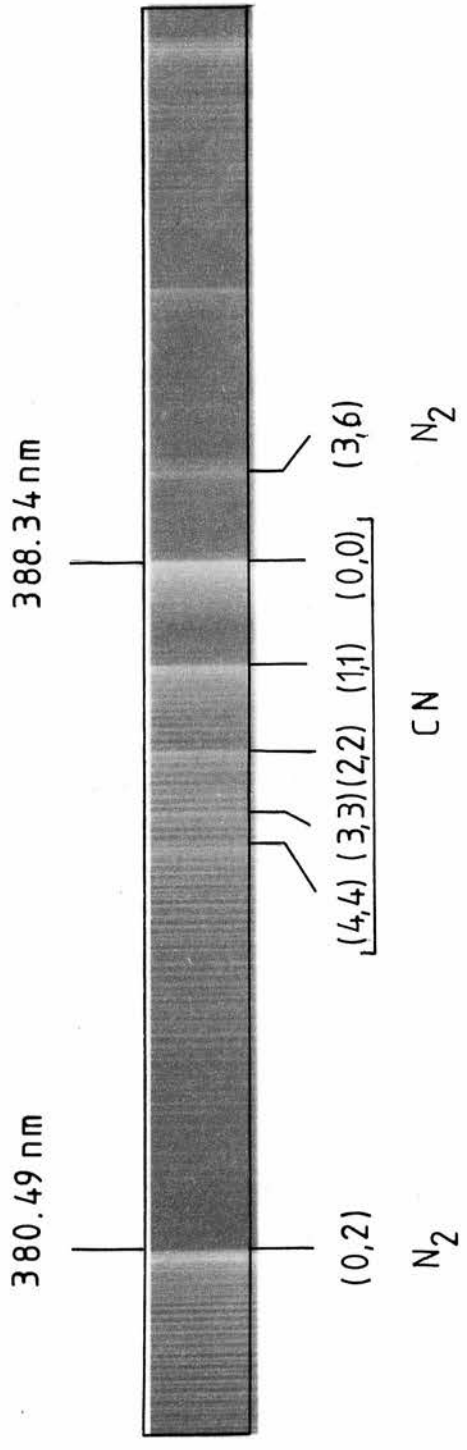

FIG. 3.01 EMISSION SPECTRUM OF CN RESONANCE LAMP ($\Delta v=0$ SEQUENCE)

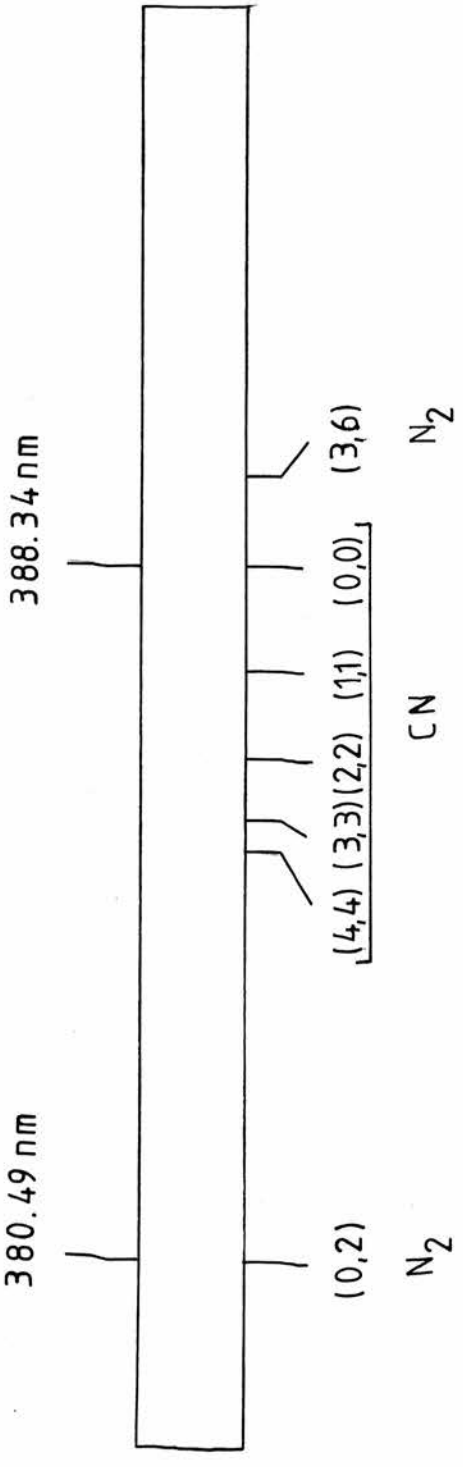

FIG. 3.01 EMISSION SPECTRUM OF CN RESONANCE LAMP ($\Delta v=0$ SEQUENCE)

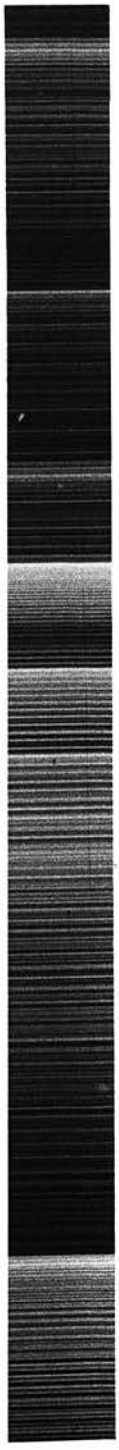

predominates and CN ($B^2\Sigma$) is produced mainly with v' = 0. The P_1' and P_2' distributions are observed for active nitrogen flames at low total pressure, whereas at pressures greater than $\sim 1.3 \times 10^2$ Nm^{-2}, the P_3' distribution predominates, corresponding to the blue flame condition.[60] In the P_3' distribution, the populations of the vibrational levels increase from v' = 0 to a maximum at about v' = 7 and then decrease again for higher values of v'.

Although the P_1' distribution was originally thought to arise from the excitation of previously formed CN radicals by energy transfer from N_2 ($A^3\Sigma^+$) metastable molecules,[55,59] more recent studies have shown that energy transfer occurs almost exclusively from high vibrational levels of ground state N_2 ($X'\Sigma_g^+$) molecules.[63,64] The P_2' distribution however is believed to arise from near resonant collision induced intersystem crossing[56,60] from the CN ($A^2\Pi$, v' = 10) level to CN ($B^2\Sigma$, v' = 0). The P_3' distribution is thought to occur by a similar process[60] but for higher vibrational levels of the $A^2\Pi$ state, produced by a different chemical mechanism.

The CN resonance lamp used in this study was similar to that used by Boden and Thrush,[16] although their total pressure of ~ 150 Nm^{-2} was slightly less. Fig. 3.01 shows the emission from the CN lamp used for this work for a total pressure of ~ 270 Nm^{-2} of 1% CH_4 in nitrogen. The wavelengths of the band heads are given in appendix II.A.

The visible emission from the CN resonance lamp was characteristic of the blue flame condition[60] but the tail bands of the violet system, which should accompany the blue flame, were not significantly developed. Hence the vibrational distribution obtained corresponds to the P_1' and P_2' distributions obtained in previous work.

The intensities of the bands of the $\Delta v = 0$ sequence were adequately suitable for this study of CN ($X^2\Sigma$) radicals and decreased with increasing v.

Rotational Distributions

The rotational energy distribution of the CN ($B^2\Sigma$) radicals produced in the resonance lamp used in this work is likely to be close to a Boltzmann distribution. Although the radicals were produced by chemical reaction and were excited by energy transfer processes, and not purely by thermal excitation, rotational relaxation is likely to be rapid leading to near equilibrium between rotational and translational modes.

Evanson and Broida[84] studied rotational relaxation of CN ($B^2\Sigma$, $v' = 0$) in active nitrogen, and observed changes in rotational quantum number varying from 1 to 10 (contrary to the optical selection rule, $\Delta K = \pm 1$). Change of rotational state was observed to occur at nearly every collision for CN ($B^2\Sigma$) in He and N_2. A rotational lifetime of 1.2×10^{-7} s was calculated for a total pressure of 1.33×10^2 Nm^{-2} for CN ($B^2\Sigma$, $v' = 0$, $K = 4$).

For this present study, at twice the pressure, the rotational lifetime would be about the same as the radiative lifetime of 6×10^{-8} s determined by Luk and Bersohn[66] in the absence of collisional quenching. Hence the rotational energy distribution of the CN ($B^2\Sigma$) radicals should be approximately Boltzmann-like and the rotational and translational temperatures should be nearly equal.

A method of determining the rotational temperature of an excited electronic state of a diatomic molecule is given by Herzberg[1] and involves measuring the relative emission intensities of each rotational line. The intensity of a given rotational line is as follows,

$$I_{em} = \frac{2\, C_{em} \nu^4}{Q_r} S_K \exp\left(-hcB'K'(K' + 1)/kT\right) \qquad (3.05)$$

The terms in the above expression are

ν wavenumber of the transition.

S_K rotational line strength.

Q_r rotational partition function of excited state.

B' rotational constant of excited state.

K' rotational quantum number

C_{em} a constant

h, c, k and T have their conventional meanings.

A plot of $\ln (I_{em}/S_K \nu^4)$ against $K'(K' + 1)$ should be a straight line for a thermal rotational distribution, and the rotational temperature may be calculated from the gradient which equals hcB'/kT.

The above method was used by Bulewicz et al.[85] to determine the rotational temperature of CN ($B^2\Sigma$) radicals produced in combustion processes. Similar methods were used by Iwai et al.[62] and Cody et al.[86] to determine the rotational temperatures of CN ($X^2\Sigma$) radicals.

An attempt was made to determine the rotational temperature of the CN ($B^2\Sigma$) radicals produced in the resonance lamp used in this work. However, overlap of the CN (0,0) rotational lines by emission from some other species in the discharge prevented the assignation of a meaningful rotational temperature to the CN ($B^2\Sigma$) radicals. This was particularly obvious from the densitometer trace of the CN (0,0) band, given in appendix II.B, where a line is observed at the band origin where there should be a gap.

As the CN resonance lamp used in this work was very similar to that used by Boden and Thrush,[16] the rotational and translational temperatures of CN ($B^2\Sigma$) should be similar to their values i.e. 1700 K and 1200 K respectively. The band envelope for the CN violet $\Delta v = 0$ sequence, emitted by the resonance lamp and shown in fig. 2.03, agrees well with the band envelopes calculated by Tokue et al.[87] for rotational temperatures between 1000 and 2000 K. The rotational intensity distribution given in appendix II.B for the (0,0) band is similar to the high temperature

spectrum given by Cody et al.[86], which corresponds to a rotational temperature of ~1400K. Hence a rotational temperature around 1500 K is reasonable for the CN ($B^2\Sigma$) radicals produced in the resonance lamp.

ABSORPTION BY CN RADICALS

For CN radicals produced by photolysis of cyanogen in the reaction vessel, complete rotational relaxation[86] of the CN ($X^2\Sigma$) radicals will have taken place by the time the photomultiplier detector has recovered from the photolysis flash i.e. for delay times in excess of 900 μs. As will be discussed in chapter 4, almost complete vibrational relaxation has also taken place by this time. Hence the energy distribution throughout the observed decay of the CN radicals will be entirely Boltzmann.

Although the intensity of the vibrational bands is sufficient for absorption experiments, a problem arose due to the mismatch of rotational temperatures of the radicals in the resonance lamp and the radicals produced in the reaction vessel i.e. the observed absorption was less than that expected had the rotational temperatures been equal.

To overcome this problem, CN ($X^2\Sigma$, v" = 0) radical absorption was monitored at a wavelength of 388.1 nm corresponding to the maximum absorption of the (0,0) band and not at 388.3 nm which corresponds to the maximum emission intensity of the resonance lamp.

As the rotational temperature of the CN emission lamp was high (∿ 1500 K), heating the reaction vessel in a thermostatically controlled oven would have reduced the rotational mismatch. The system worked well enough without recourse to this measure, which would certainly have given rise to other problems.

It was not necessary to know the absolute concentrations of CN radicals in the reaction vessel to determine kinetic data, relative concentrations were sufficient. The Beer-Lambert law provides an easy

method of relating transmitted light intensity to the concentration of an absorber, and a modified version of this relationship was adopted for this study.

The Beer-Lambert Law

For most chemical systems, the following empirical relationship, known as the Beer-Lambert Law was found to apply for incident intensity I_o, transmitted intensity I_t (at delay time t), absorber thickness 1, and absorber concentration c.

$$I_t/I_o = \exp(-\alpha\ c1) \qquad (3.06)$$

The term α is the natural extinction coefficient, the units of which must be compatible with those of c and 1.

However, there is a restriction on the applicability of equation 3.06 to a given absorption system, namely that the range of wavelengths to which I_t refers is small compared to the width of the absorption band i.e. α is constant over this range. The term α is a measure of the probability that quantum - molecule interaction will lead to absorption of the quantum, and strictly speaking, the incident light should be monochromatic.

For atomic emission sources, self reversal of the emitted lines can alter the line shape[88] and equation 3.06 no longer strictly applies. This problem should not be of importance for the emission from CN molecules in the resonance lamp, as the intensity is distributed throughout all the rotational lines and is not concentrated into one line as is the case for atoms.

As mentioned above, the emitted line should be narrow compared with the absorption line. Several types of broadening, applicable to both emission and absorption may occur in the type of system under investigation. They are natural broadening, Doppler broadening, and pressure broadening which can be sub-divided into Lorentz and Holtsmark broadening. These

phenomena are all discussed by Mitchell and Zemansky[89] who deal with a more fundamental approach to the absorption of resonance radiation.

In this study, the CN resonance lamp is essentially a line emitter and hence the resolution of the monochromator will not affect the absorption. The absorption is however affected by the relative line shapes of the emitting and absorbing lines. For the CN resonance lamp, the emitted lines will be broader than the absorbing lines mainly due to Doppler broadening[16]. Hence the equation 3.06 will not strictly apply in this case.

The mismatch of rotational temperatures of the emitting and absorbing species can lead to some lines being absorbed extensively while the absorption of other lines is small or zero. This again deviates from the ideal situation for which equation 3.06 was intended.

To accommodate the deviations from ideal line shapes and mismatch of rotational temperature, a modified form of the Beer-Lambert Law may be used, which introduces the empirical coefficient, γ, which can have values between zero and one.

$$\ln (I_o/I_t) = \alpha(cl)^{\gamma} \qquad (3.07)$$

The γ coefficient may be determined empirically by varying the concentration of absorber or by varying the length of absorber. The latter method was used in this study.

If $\ln (I_o/I_t)$ is monitored as a function of time for a given initial absorber concentration for two values of l, say l = L and l = L/2, then the following equations describe the decay of the absorber.

$$\left[\ln (I_o/I_t)\right]_L = \alpha(cL)^{\gamma} \qquad (3.08)$$

$$\left[\ln (I_o/I_t)\right]_{L/2} = \alpha(cL/2)^{\gamma} \qquad (3.09)$$

$$\frac{\left[\ln (I_o/I_t)\right]_L}{\left[\ln (I_o/I_t)\right]_{L/2}} = 2^{\gamma} \qquad (3.10)$$

Hence a plot of $\left[\ln (I_o/I_t)\right]_L$ against $\left[\ln (I_o/I_t)\right]_{L/2}$, for a range of values of t, has a gradient of 2^γ for the decay of the absorber. If instead of 1 = L/2, the value of 1 = L/3 was used, then a gradient of 3^γ would be obtained.

The reaction vessel length was varied by using inserts, allowing values of 1 = L, 2 L/3, L/2, L/3 to be obtained. A diagram of the reaction vessel used in this mode is given in fig. 2.04B. Care was taken to obtain a good vacuum each time a different insert was placed in the reaction vessel.

The flash lamp was freshly filled and flashed about ten times to ensure reproducible emission. The flash lamp was not refilled throughout a series of experiments to determine γ, as this would have given an alteration in the spectral output, as was observed in preliminary experiments.

Three separate determinations of γ were carried out. For each, a large volume of helium/cyanogen mixture, 500 : 1, was prepared and allowed to mix thoroughly, so that this standard mixture, at a total pressure of 1.33×10^4 Nm^{-2} could be used for the two path lengths used in each determination. The removal of CN ($X^2\Sigma$, v'' = 0) radicals was monitored for each pair of 1 values at 388.1 nm corresponding to the (0,0) P branch.

Fig. 3.02 shows the values of $\left[\ln (I_o/I_t)\right]_1$ values obtained for each pair of 1 values used to determine γ. Each point is the average of 5 experiments and the uncertainties are the standard errors. As the uncertainties in each point are almost the same, most of the error bars have been omitted from the graphs for clarity.

Table 3.01 gives the γ values obtained from the gradients of the graphs in fig. 3.02, together with the average rate coefficients for the removal of CN radicals. The average value of γ was 0.57 ± 0.03 and this value will be used throughout this research.

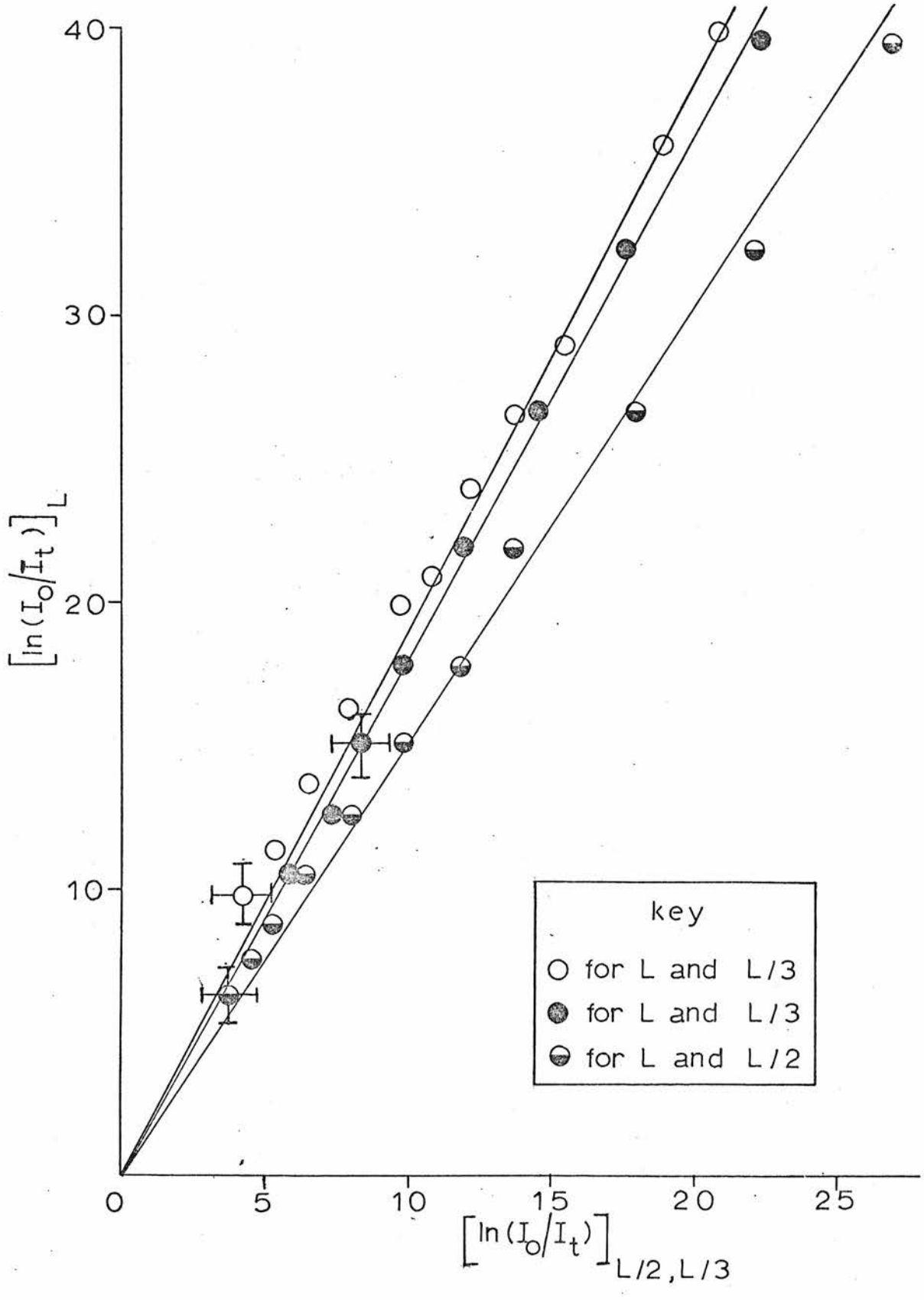

FIG. 3.02 GRAPH OF $\left[\ln(I_o/I_t)\right]_L$ vs $\left[\ln(I_o/I_t)\right]_{L/2,L/3}$

Table 3.01

γ Values and Rate Coefficients

	Path lengths		Path lengths		Path lengths	
	L	L/3	L	L/3	L	L/2
Beer-Lambert Coefficient γ	0.60±0.02		0.54±0.03		0.58±0.03	
Average Rate Coefficient k_{obs}/s^{-1}	416±21	471±24	419±21	410±20	419±21	445±23

The average rate coefficients are in excellent agreement for all values of path length l, and indicate that for a reproducible photolysis flash, the CN decay profiles should be reproducible.

For pseudo first order kinetics, the observed rate coefficient, k_{obs}, must be divided by γ to give the correct rate coefficient. However, throughout this thesis instead of correcting the values of k_{obs} for each experiment, it was more convenient to correct the rate constants obtained i.e.

$$k = k' / \gamma \qquad (3.11)$$

where k is the actual rate constant and k' is the observed rate constant (calculated from the gradient of a plot of k_{obs} against reactant concentration). For convenience, the uncertainties in the values of the rate constants k, quoted in subsequent chapters, do not contain a contribution from the uncertainty in γ.

The above treatment is based on the assumption that γ is constant over the range of CN concentrations studied, and this appears to be valid, as the graphs in fig. 3.02 are good straight lines.

Absolute CN Concentrations

An absolute determination of absorber concentrations is possible by equating the experimentally measured fractional absorption of a resonance line with the theoretical equivalent. Such a determination is not essential for the study of pseudo first order kinetics, but it is useful to have some idea of the concentrations of the species under observation.

Paul and Dalby[13], Iwai et al.[62] and Boden and Thrush[16] have all calculated the absolute CN concentrations produced in

their experiments on CN radical reactions. The methods used were essentially the same, but as the resonance absorption study of Boden and Thrush was similar to this work, only their method will be discussed in detail.

The method they used was based on the work of Ladenburg and Reiche which is described by Mitchell and Zemansky[89] It applies strictly for:-

a. small absorptions at the centre of a resonance line under conditions where absorption at the edges of the line is negligible.

b. conditions where line shape is determined purely by Doppler broadening i.e. in the absence of all other types of broadening or when they are negligible.

This method was therefore applicable to the work of Boden and Thrush[16] where absorptions were $\leq 4\%$ and where Doppler broadening was about three orders of magnitude greater than the natural line width.

For simplicity, the absorption of resonance radiation by a single rotational line will be described initially. Under the conditions described above, the fractional absorption coefficient, A_α, for a single rotational line is given by the following expression[89]

$$A_\alpha = \frac{k_o l}{\sqrt{1+\alpha^2}} - \frac{(k_o l)^2}{2!\sqrt{1+2\alpha^2}} + - - - - + \frac{(-1)^{n+1}\,(k_o l)^n}{n!\sqrt{1+n\alpha^2}} \qquad (3.12)$$

The terms in the above equation are as follows,

k_o (cm^{-1}) is the maximum absorption coefficient for pure Doppler broadening.

l (cm) path length of the absorption cell.

n is a positive integer.

α is the ratio of the emission line width to the absorption line width. It is equal to the square root of the ratio of the absolute temperatures of the emitting and absorbing radicals for a resonance lamp with a thin emitting layer.

The background leading up to the derivation of equation 3.12 above is given in appendix II.C.

In the notation of Boden and Thrush[16], k_o for a single rotational line of the $CN(B^2\Sigma-X^2\Sigma)$ (0,0) band is given by the following expression

$$k_{O,K} = \left(\frac{\ln 2}{\pi}\right)^{\frac{1}{2}} \frac{N \lambda^2 q_{0,0} S_K \exp(-K(K+1)/Q_R)}{4 \pi \tau \Delta\nu_a Q_V Q_R} \qquad (3.13)$$

The terms of the above expression are:-

N concentration of absorber (molecule cm^{-3}).

λ wavelength absorbed (cm).

$q_{0,0}$ Franck-Condon factor for the transition[90]

S_K rotational line strength.

τ radiative lifetime of the excited state (s).

$\Delta\nu_a$ Doppler width of the absorbing line.

Q_V vibrational partition function

Q_R rotational partition function

K quantum number of total angular momentum apart from spin.

Hence if A_α is measured experimentally, N may be determined if all the other parameters in equations 3.12 and 3.13 are known.

Boden and Thrush used the experimental oscillator strength ($f = 0.027 \pm 0.003$) determined by Bennett and Dalby[91] to calculate τ and hence the $k_{0,K}$ values. Knowing the rotational intensity distribution of their resonance lamp from the determination of its rotational temperature, Boden and Thrush then calculated the integrated fractional absorption for the whole of the (0,0)P branch, allowing for overlap of the absorbing lines. From this information and their experimental absorption measurements, they then calculated the absolute CN concentration.

A rough calculation by the method described above is given in appendix II.D for the fractional absorption of a single rotational line under the conditions used for this present work. The value obtained for the initial CN concentration was $>5 \times 10^{13}$ molecule cm^{-3} compared to the value of 8×10^{12} molecule cm^{-3} given in chapter 2. The discrepancy is not surprising considering that the calculations apply only for small absorptions and the absorption measured experimentally was large.

SUMMARY

It is possible to calculate good kinetic data for this study of $CN(X^2\Sigma, v''=0)$ radicals using a modified form of the Beer-Lambert Law, for which a value of $\gamma = 0.57 \pm 0.03$ has been obtained.

The rate constants, k, given in the following chapters were obtained from the following expression, $k = k'/\gamma$, where k' was the observed rate constant. The quoted uncertainties in the values of k do not include a contribution from the uncertainty in γ.

CHAPTER 4

CHAPTER 4

PRELIMINARY EXPERIMENTS

Removal of CN Radicals in Cyanogen/Helium Mixtures

INTRODUCTION

The photolysis of cyanogen/helium mixtures was chosen as the source of CN radicals for the reasons given in chapter 2. It is therefore important to characterise fully the removal of CN in such mixtures to obtain optimum conditions for observing CN radical decay in the presence of reactants.

The following possible pathways have been considered for the removal of $CN(X^2\Sigma, v'' = n)$:-

1. Removal of CN by diffusion to the walls of the reaction vessel.
2. Vibrational relaxation of $CN(X^2\Sigma, v'' = n)$ to $CN(X^2\Sigma, v'' = n-1)$.
3. Recombination of CN radicals by the third order process

$$CN + CN + M \longrightarrow C_2N_2 + M \qquad (1.18)$$

4. Removal of CN by the third order reaction

$$CN + C_2N_2 + M \longrightarrow C_3N_3 + M \qquad (4.01)$$

5. Reaction of CN radicals with impurities.

By assessing the contribution of each of the above processes under various conditions, it should be possible to choose conditions where removal of CN radicals, in the presence of reactant molecules, occurs predominantly by reaction with these molecules. This should enable rate constants to be determined accurately.

It is also essential that removal of CN radicals is pseudo first order, as this simplifies the calculation of kinetic data. In

particular, since the aim of this work is to study the removal of $CN(X^2\Sigma, v'' = 0)$ in the absence of feeding by vibrational relaxation, care must be taken in finding a suitable system to do this.

A discussion of the vibrational distributions produced in previous flash photolysis studies, followed by a detailed account of the theoretical and experimental aspects of the removal processes listed earlier, will now be given.

CN VIBRATIONAL DISTRIBUTIONS

Previous Work

Although Paul and Dalby[13] produced $CN(X^2\Sigma)$ radicals by photolysis of C_2N_2 and cyanogen chloride, they give no indication of the CN vibrational distributions produced. Basco et al.[15] and Basco[14] produced vibrationally excited $CN(X^2\Sigma)$ with $v'' \leqslant 6$ by photolysis of cyanogen, cyanogen bromide and cyanogen iodide in a quartz vessel at a flash energy of 1600 J. They observed the excited radicals spectroscopically via the $\Delta v = 0, \pm 1$ and -2 sequences of the $CN(B^2\Sigma-X^2\Sigma)$ system. The absorptions of $v'' = 5$ and 6 could not be separated and in fact overlapped the tail of $v'' = 4$. Transient population inversions were observed which relaxed rapidly as the intensity of the photolysis flash decayed.

Engleman[92] photolysed BrCN in a twenty fold excess of helium at total pressures of $1.3 \times 10^2 - 1.3 \times 10^4$ Nm^{-2} in a quartz vessel. He observed $CN(X^2\Sigma)$ with $v'' \leqslant 7$ in absorption via the $\Delta v = 0$ and $+1$ sequences. Mixtures of BrCN and He, N_2, CO_2, Xe, etc. were also studied at a higher total pressure of 8×10^4 Nm^{-2}. For helium, a strong population inversion was produced between $v'' = 3$ and $v'' = 2$, and this is yet to be explained. For He, N_2 and CO_2 the (0,0) band of the CN violet system was strong, with the (1,1) band weak or absent.

No higher vibrational bands were observed for these diluents.

Schacke et al.[21] photolysed cyanogen in a Suprasil vessel (λ >165 nm) using flash energies between 20 and 4000 J. They observed $CN(X^2\Sigma)$ radicals in excited vibrational levels up to $v'' = 7$, which was energetically possible in the primary photochemical step for $\lambda > 165$ nm.

West and Berry[67] studied both electronic and vibrational laser emissions of CN radicals produced by the photodissociation and predissociation of a variety of RCN precursors including cyanogen. The following mechanism, involving near resonant collision induced intersystem crossing, explained most of their observations including the preferential population of $CN(X^2\Sigma, v''=4)$.

$$RCN + h\nu \longrightarrow R + CN(A^2\Pi_i, \text{ primarily } v' = 0) \qquad (4.02)$$

$$CN(A^2\Pi_i, v' = 0) + M \longrightarrow CN(X^2\Sigma, v'' = 4 \text{ primarily}) + M \qquad (4.03)$$

Laser action was observed for the following transitions, the $v'' = 4 \rightarrow v'' = 3$ transition being the first to reach threshold.

$$CN(X^2\Sigma, v'') \longrightarrow CN(X^2\Sigma, v'' - 1) + h\nu, \quad v'' = 5,4,3,2 \qquad (4.04)$$

Population of $CN(X^2\Sigma, v'' = 5)$ was thought to occur via near resonant intersystem crossing from $CN(A^2\Pi, v' = 1)$.

Jackson and Cody[93], in their laser induced fluorescence study of the fragments produced on photodissociation of cyanogen, found evidence to support the above mechanism for the production of the CN vibrational energy distributions.

The collision induced intersystem crossing mechanism supercedes the optical pumping mechanism, suggested by Basco et al.[15] and given by Pollack[94] to explain the vibrational energy distributions obtained in his CN photochemical laser studies.

This Work

Experiments were carried out to determine the extent of vibrational excitation of the $CN(X^2\Sigma)$ radicals produced in this photolysis study of cyanogen/helium mixtures.

A mixture containing a partial pressure of 26.7 Nm^{-2} of cyanogen, made up to a total pressure of 1.33×10^4 Nm^{-2} with helium, was photolysed in the quartz reaction vessel at a flash energy of 125 J. The absorptions at time t = 0 (found by extrapolation) are given for several wavelengths in table 4.01 along with the corresponding absorption bands.[95]

Table 4.01

$CN(B^2\Sigma \leftarrow X^2\Sigma)$ Absorptions

Wavelength/nm	Bands observed	% Absorption at time t = 0
388.10	(0,0) P	89
386.96	(0,0) R + (1,1) P	54
385.70	(1,1) R + (2,2) P	trace*
385.00	(2,2) R + (3,3) P	none
384.32	(3,3) R + (4,4) P	none

*difficult to extrapolate to t = 0 accurately

This indicates that there is very little vibrationally excited CN present after the photomultiplier has recovered from the photolysis flash i.e. after $\sim$ 900 μs. It is possible that substantial populations of $CN(X^2\Sigma, v'' > 0)$ were produced initially, but if this was the case, decay was very rapid. No absorption by $CN(X^2\Sigma, v'' > 1)$ was observed at delay times > 900 μs. Only a trace absorption was observed at 385.70 nm corresponding to the (1,1) R + (2,2) P branches. This was assumed to be due entirely to $v'' = 1$ since no absorption corresponding to the (2,2) R branch was observed.

After due consideration of the uncertainties involved, an upper limit of $P(v'' = 1) < 5\%$ of $P(v'' = 0)$ at time $t = 0$ was determined, assuming no higher levels were populated initially ($P(v'' = 1)$ and $P(v'' = 0)$ are the populations of levels $v'' = 1$ and $v'' = 0$ respectively). Hence the decay of the absorption signal at 386.96 nm, corresponding to the (0,0) R + (1,1) P branches should approximate well to the decay of the (0,0) P branch at 388.10 nm.

This system was therefore ideal for studying the removal of $CN(X^2\Sigma, v'' = 0)$ in the absence of vibrationally excited CN, since by the time the CN (0,0) absorption decayed to <25% (so that γ remains constant throughout the decay), no trace of the CN (1,1) R + (2,2) P branches was observed. Hence it was possible to study the removal of $CN(X^2\Sigma, v'' = 0)$ in the absence of vibrationally excited species for the above experimental conditions.

DIFFUSION

As diffusion to the walls of a reaction vessel can be the principal pathway for removal of transient species at low pressures, it is essential to determine a suitable working pressure above which diffusion is negligible compared to other collisional processes.

For radical concentrations C_0 and C_t at times $t = 0$ and $t = t$, Mitchell and Zemansky[89] gave the following equation for removal of radicals by diffusion.

$$C_t = C_0 \exp(-\beta t) \qquad (4.05)$$

The rate coefficient β (s^{-1}), given in the above equation, has been derived for diffusion in a cylindrical vessel by the equation

$$\beta = D(\pi^2/l^2 + 5.81/r^2) \qquad (4.06)$$

where D is the diffusion coefficient ($cm^2\ s^{-1}$), l is the length of the reaction vessel (cm), and r is its radius (cm).

The rate coefficient for removal of CN radicals by diffusion in a helium/cyanogen mixture may be calculated from equation 4.06 if the value of D is known. To simplify the calculations, the system was considered to be a binary mixture of CN radicals in a large excess of helium, since the cyanogen partial pressures used in this work were low.

The diffusion coefficient D for such a binary mixture may be calculated from the following equation given by Hirschfelder, Curtiss and Bird,[96] which was derived from the Chapman-Enskog theory of transport phenomena.

$$D = 0.0026280 \frac{\sqrt{T^3 (M_1 + M_2)/2 M_1 M_2}}{p \sigma^2 \Omega} \qquad (4.07)$$

The symbols used in this equation are as follows:

D diffusion coefficient ($cm^2 s^{-1}$) for diffusion of component 2 in excess of component 1.

p total pressure (atm).

T absolute temperature (K).

T_{12}^* reduced temperature ($= kT/\varepsilon_{12}$)

M_1 and M_2 molecular weights of gases 1 and 2

σ_{12} (Å) and ε_{12}/k (K) are the molecular potential energy parameters characteristic of a 1 - 2 interaction.

Ω integral used in the determination of transport coefficients (see appendix III).

Although the above treatment applies strictly for a Lennard-Jones intermolecular potential, it will suffice to give an estimate of the diffusion of CN in helium. The molecular potential energy parameters for the CN - He interaction were taken to be equal to those for the

N_2 - He interaction as a rough approximation.

The values of all the parameters used to determine D and β are given in Appendix III. At 1 atm pressure and 295 K, D and β were calculated to be $0.69\ cm^2\ s^{-1}$ and $4.0\ s^{-1}$ respectively.

D and hence β are inversely proportional to total pressure, and fig. 4.01 shows a plot of β against total pressure for diffusion of CN in helium. This plot is useful, in conjunction with the results of the following experiments, in determining the relative contributions for the removal of CN radicals by diffusion and removal by other collisional processes.

The rate coefficient for removal of $CN(X^2\Sigma, v'' = 0)$ was measured experimentally for mixtures containing a fixed partial pressure of cyanogen ($26.7\ Nm^{-2}$). The total pressure, made up with helium, was varied from 26.7 to $1.33 \times 10^4\ Nm^{-2}$. Both the (0,0) P and (0,0) R branches of the $CN(B^2\Sigma-X^2\Sigma)$ system were monitored, and a plot of the observed rate coefficients, k_{obs}, against total pressure is given in fig. 4.01.

At total pressures of $< 7 \times 10^2\ Nm^{-2}$, good agreement was obtained between the calculated values and experimental data, showing that diffusion dominates CN removal in this pressure region. For total pressures $> 7 \times 10^2\ Nm^{-2}$, collision processes other than diffusion dominate the removal of CN.

For this study of CN radical reactions, a total pressure of $1.33 \times 10^4\ Nm^{-2}$, corresponding to $\beta \simeq 30\ s^{-1}$, was considered high enough for removal of CN by diffusion to be negligible. This total pressure was in fact used for the majority of this study.

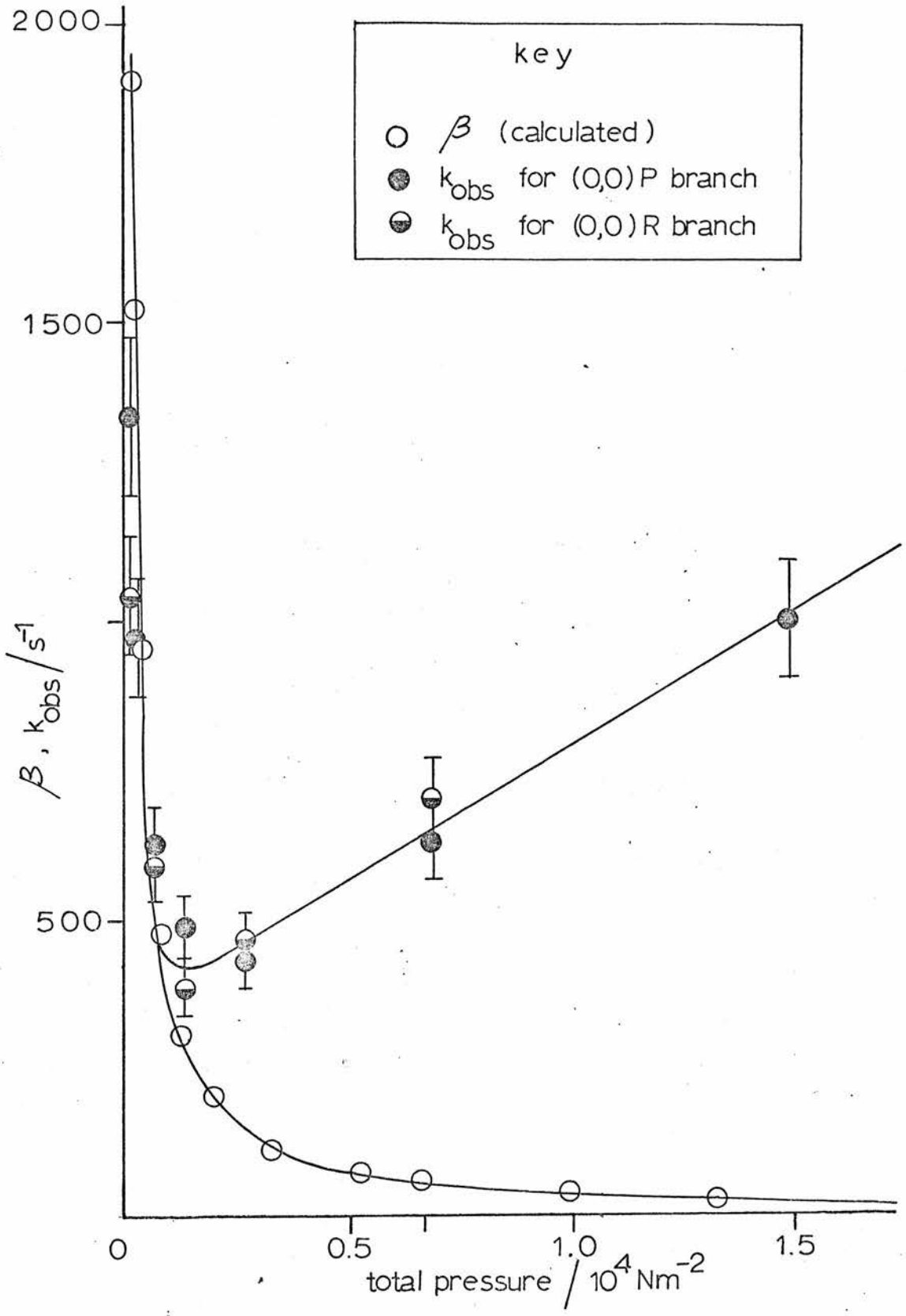

FIG.4.01 GRAPH OF β AND K_{OBS} VS TOTAL PRESSURE

VIBRATIONAL RELAXATION OF CN RADICALS

There is a lack of good experimental data on the vibrational relaxation of CN radicals. However, several theories of vibrational relaxation of diatomic molecules have been evolved, and some empirical relationships have been derived for some cases. Vibrational relaxation processes are discussed in reviews by Moore [97], Amme[98] and Callear,[99] and a useful text covering energy transfer processes has been written by Levine and Bernstein[100].

It should be possible to obtain an estimate of the importance of CN vibrational relaxation in the helium/cyanogen mixtures used in this study.

Vibrational relaxation of $CN(X^2\Sigma, v'')$ radicals may occur by several of the following inelastic collision processes.

1. Transfer of CN vibrational energy to translational energy of helium atoms (V → T process).
2. Transfer of CN vibrational energy to cyanogen molecules by
   a. V → T process.
   b. V → V process, where CN vibrational energy is converted to vibrational energy of cyanogen.
3. Energy transfer to other CN radicals by
   a. V → T process.
   b. Near resonant V → V exchange reactions.

$$CN(v'' = n) + CN(v'' = m) \longrightarrow CN(v'' = n - 1) + CN(v'' = m + 1) \quad (4.08)$$

In general, V → T processes are inefficient at ∿ 300K, occuring at the low velocity adiabatic limit. Near resonant V → V processes however will be orders of magnitude more efficient.[100] There will be some nominal energy release, Q, from these processes. If Q is positive, the exoergicity is dissipated in rotational and translational modes, and if Q is negative, rotational and translational energy are utilised to supply the endoergicity.

Before discussing further the possible relaxation processes, it is worthwhile to consider previous work on the vibrational relaxation of $CN(X^2\Sigma)$ radicals.

Previous Work

Basco et al.,[15] in their flash photolysis study of CN, obtained a rate constant of $\sim 1.7 \times 10^{-12}$ cm^3 $molecule^{-1}$ s^{-1} for vibrational relaxation of $CN(X^2\Sigma, v'' = 4)$ by BrCN, under conditions where the populations of levels with $v'' \geq 5$ were negligible. The removal rate was found to obey the following equation.

$$-d\left[CN(v'' = 4)\right]/dt = k\left[BrCN\right]\left[CN(v'' = 4)\right] \qquad (4.09)$$

However, k can include a contribution for removal of $CN(v'' = 4)$ by reaction with BrCN as well as relaxation i.e.

$$k = k\ (\text{relaxation}) + k\ (\text{reaction}). \qquad (4.10)$$

Hence the rate constant obtained may be regarded as an upper limit. The disposal of the vibrational energy was not considered.

Schacke et al.[21] gave the lifetimes of CN radicals in levels up to $v'' = 7$ produced by photolysis of helium/cyanogen mixtures. The values obtained are given in Table 4.02 along with the rate constants for relaxation calculated in two ways:-

a. assuming removal of $CN(X^2\Sigma, v'')$ took place exclusively by $V \rightarrow T$ transfer to helium diluent i.e. in the absence of feeding from higher v'' levels and in the absence of reaction with cyanogen.

b. as in a. but for energy transfer to cyanogen, including both $V \rightarrow T$ and $V \rightarrow V$ processes i.e. the calculated rate constants correspond to the total relaxation cross-section.

The values calculated by the two methods above are entirely reasonable for the processes considered, and relaxation by both He and C_2N_2 probably takes place.

Table 4.02

Estimated Rate Constants

v"	Lifetime $\tau/10^{-4}$ s	Relaxation by He		Relaxation by C_2N_2	
		$p\tau/10^{-6}$ atm s	$k/10^{-14}$ cm^3 $molecule^{-1}$ s^{-1}	$p\tau/10^{-8}$ atm s	$k/10^{-12}$ cm^3 $molecule^{-1}$ s^{-1}
1	6.7	2.64	1.51	3.52	1.14
2	4.2	1.66	2.42	2.21	1.82
3	2.9	1.14	3.5	1.53	2.6
4	2.1	0.83	4.9	1.11	3.6
5	1.6	0.63	6.4	0.84	4.8
6	1.1	0.43	9.3	0.58	6.9
7	0.8	0.32	13	0.42	9.5

The rate constant obtained for the removal of CN (v" = 4) by energy transfer to C_2N_2, based on the assumptions given in b. above, was 3.6×10^{-12} cm^3 $molecule^{-1}$ s^{-1} which agrees within a factor of ~ 2 with the value obtained by Basco et al.[15] for relaxation of CN(v" = 4) by BrCN.

This may be entirely fortuitous, as the reactions competing with relaxation, together with the experimental conditions, radical concentrations etc., are completely different for the two studies. In the work of Basco et al. the exothermic reaction competing with relaxation was

$$CN + BrCN \longrightarrow C_2N_2 + Br \qquad (4.11)$$

which is similar to the following reaction studied by Clyne and Cruse,[101] for which a rate constant of $(1.45 \pm 0.20) \times 10^{-11}$ cm^3 $molecule^{-1}$ s^{-1} was obtained.

$$Cl + ClBr \longrightarrow Cl_2 + Br \qquad (4.12)$$

The rate constant for reaction 4.11 will be of similar magnitude to that for reaction 4.12. Hence for removal of $CN(X^2\Sigma, v" = 4)$ in BrCN, reaction 4.11 should dominate i.e. k (reaction) >> k (relaxation).

In the study by Schacke et al.,[21] an addition reaction to an unsaturated system, reaction 4.01, was the process competing with vibrational relaxation of $CN(X^2\Sigma, v" = 4)$. In this case, it is likely that CN could form a relatively long-lived collision complex with cyanogen, allowing the CN vibrational energy to be dissipated throughout the internal modes of the intermediate. The collision complex may then dissociate to give vibrationally relaxed CN radicals, or be deactivated by collisions to give C_3N_3 product.

The mechanism given below is similar to that for recombination of halogen atoms[102] and will be discussed more fully later on in this chapter.

($^{\neq}$ denotes excitation of internal modes).

$$CN + C_2N_2 \rightleftharpoons C_3N_3^{\neq} \qquad (4.13)$$

$$C_3N_3^{\neq} + M \longrightarrow C_3N_3 + M \qquad (4.14)$$

If, at the low total pressure (4.0×10^2 Nm^{-2}) used by Schacke et al.[21], step 4.14 of this mechanism is rate determining, several CN radicals may be relaxed for every C_3N_3 product molecule formed i.e. k (relaxation) >> k (reaction).

Care must therefore be taken in interpreting experimental data on the vibrational relaxation of CN radicals. It is worthwhile to consider calculated rate constants for vibrational relaxation of CN radicals as an aid to assessing the validity of experimental values.

Empirical Calculations

It is relatively easy to estimate the extent of V→T relaxation of CN radicals by CN - M collisions. The estimation of efficiencies for V →V processes and near resonant vibrational energy exchange is much more difficult and will only be discussed briefly. However, the fundamental transitions of cyanogen[103] and the energies of the $CN(X^2\Sigma)$ vibrational levels are given in appendix IV.A.

The calculation of V → T transfer from CN to the inert gas helium was accomplished using the empirical equations given by Millikan and White[104] and Lifshitz,[105] which are based on the temperature dependence relationship of Landau and Teller[106]. Details of the calculations are given in appendix IV.B. Calculations were also carried out for vibrational relaxation of NO by He to check out the empirically determined rate constant with the value determined experimentally by Stephenson[107].

A value of $k_{1\rightarrow 0} = 2.0 \times 10^{-17}$ cm^3 molecule $^{-1}s^{-1}$ was obtained for relaxation of CN(v'' = 1) → (v'' = 0) by collision with helium.

This is about a factor of 10^3 less than the value calculated from the data of Schacke et al.[21]

The calculated rate constant for the relaxation of NO (v" = 1) by He is within ± 50% of the experimental value obtained by Stephenson.[107] The value of $k_{1\rightarrow 0}$ calculated for the relaxation of CN by He should therefore be a reasonable approximation. This indicates that in the work of Schacke et al.,[21] vibrational relaxation was occurring by processes which were much more efficient than V → T transfer to helium, e.g. V → V transfer to cyanogen and near resonant vibrational energy exchange of CN radicals.

It is essential that good experimental data are obtained before a precise value may be quoted for $k_{1\rightarrow 0}$ for vibrational relaxation of CN radicals.

The V → V transfer of CN vibrational energy to cyanogen, and near resonant V → V exchange between CN radicals (reaction 4.08) will be about 2 - 4 orders of magnitude more efficient than V → T transfer to helium. Hence the V → V transfer and exchange reactions will be the dominant processes for vibrational relaxation of CN radicals. These processes may involve long range multipolar interactions, and as estimation of their efficiencies is difficult, this will not be attempted here.

For the standard cyanogen/helium mixtures used in this work (26.7 Nm^{-2} of cyanogen, total pressure 1.33×10^4 Nm^{-2}) vibrational relaxation of CN radicals is likely to be rapid, except for CN (v" = 1) which occurs by V → T processes which are less efficient. At delay times >900 μs, no CN radicals with v" > 1 were observed experimentally and only a trace of CN (v" = 1) was detected, indicating

almost complete relaxation.

Hence at delay times >900 μs removal of CN($X^2\Sigma$,v"=0) was unaffected by feeding from the v"=1 level.

RECOMBINATION OF CN RADICALS

Significant recombination of CN radicals, to give cyanogen, would give a deviation from the pseudo first order decay of CN radicals. The mechanism, analogous to that for atomic recombination is as follows

$$CN + CN + M \xrightarrow{k_{rec}} C_2N_2 + M \qquad (1.18)$$

No deviation from pseudo first order decay was observed for mixtures containing 26.7 Nm^{-2} of cyanogen at total pressures varying from 26.7 to $4x10^4$ Nm^{-2} using helium diluent.

As a check for the absence of radical-radical processes, the decay of CN was monitored for identical mixtures of cyanogen diluted with helium over a range of flash energies. The observed rate coefficients showed no dependence on flash energy over the range 31-125 J. No dependence on flash energy was also observed for the decay of CN radicals in the presence of reactant molecules.

Basco et al.[15] obtained a value of $k_{rec} = 4.7x10^{-32}$ cm^6 $molecule^{-2}$ s^{-1} for reaction 1.18 with N_2 as third body. This value agrees well with typical halogen atom recombination rate constants, and indicates the halogen-like nature of CN radicals.

In their pulse radiolysis study, Bullock and Cooper[18] observed a second order component in the pseudo first order decay of CN radicals in C_2N_2/Ar mixtures at short delay times. The decay became fully first order at longer delay times. This may be interpreted as a manifestation

of the importance of CN recombination, occuring at high [CN] and short delay times.

The initial CN concentrations monitored by Basco et al.[15] and Bullock and Cooper[18] were $> 6 \times 10^{14}$ molecule cm^{-3}, substantially greater than the value of $\sim 8 \times 10^{12}$ molecule cm^{-3} given in chapter 2 for this work.

Hence at the low CN concentrations used in this study, the contribution of CN radical recombination to the net removal of CN radicals should be low. In fact, the experiments described earlier show no evidence of recombination under the conditions studied.

REACTION OF CN WITH CYANOGEN

The following reaction was considered as a possibility for the overall removal of CN radicals in cyanogen/helium mixtures (M = He).

$$CN + C_2N_2 + M \xrightarrow{k'} C_3N_3 + M \qquad (4.01)$$

The determination of the third order rate constant for this reaction was carried out as follows:

a. For a fixed total pressure of 1.33×10^4 Nm^{-2} (made up with helium diluent), the dependence of k_{obs}, the rate coefficient for removal of $CN(X^2\Sigma, v'' = 0)$, on the partial pressure of cyanogen was monitored and the results are plotted in fig. 4.02. This yielded a second order rate constant† $k_a = (7.4 \pm 1.4) \times 10^{-15}$ cm^3 molecule $^{-1}$ s^{-1}.

†All the experimental rate constants given in this chapter are the corrected values i.e. the Beer-Lambert coefficient, γ, has been taken into account.

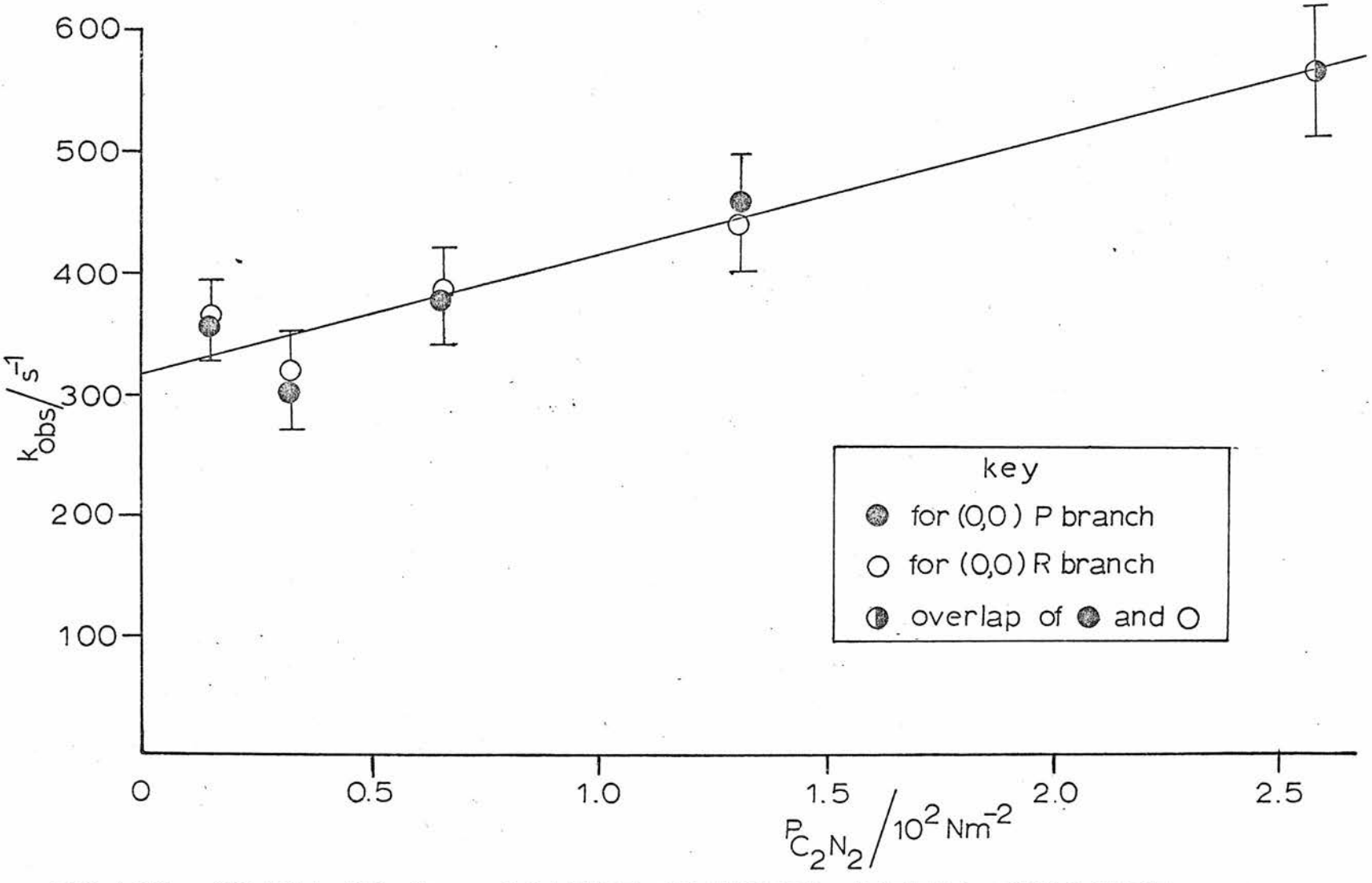

FIG.4.02 GRAPH OF K_{OBS} AGAINST CYANOGEN PARTIAL PRESSURE

However, $k_a = k' [He]$ where k' is the third order rate constant for reaction 4.01. A value of $k' = (2.3 \pm 0.4) \times 10^{-33}$ cm^6 molecule $^{-2}$ s^{-1} was obtained by this method.

b. For a fixed partial pressure of cyanogen (26.7 Nm^{-2}), the total pressure was varied from $(1.33 - 4.00) \times 10^4$ Nm^{-2} by addition of helium diluent. The observed rate coefficients, k_{obs}, are plotted against total pressure in fig. 4.03 , and a second order rate constant $k_b = (4.05 \pm 0.18) \times 10^{-17}$ cm^3 molecule $^{-1}$ s^{-1} was determined. Since $k_b = k' [C_2N_2]$, a value of $k' = (6.2 \pm 0.3) \times 10^{-33}$ cm^6 molecule $^{-2}$ s^{-1} was obtained.

Clearly there is a discrepancy between the two values of k' determined by the above methods. A consideration of other feasible mechanisms may resolve the problem.

It is very probable that the reaction of CN with cyanogen is similar to halogen atom recombination[102] where there is a transition from third to second order kinetics with increasing total pressure.[108]

The reaction mechanism may be explained as follows where $C_3N_3^{\neq}$ is a quasi-bound energy-rich collision complex.

$$CN + C_2N_2 \underset{k_{-1}}{\overset{k_{+1}}{\rightleftharpoons}} C_3N_3^{\neq} \qquad (4.13)$$

$$C_3N_3^{\neq} + M \xrightarrow{k_2} C_3N_3 + M \qquad (4.14)$$

At low total pressures, reaction 4.14 is rate determining (3rd order kinetics) but at higher pressures, the reaction becomes less sensitive to [M] and reaction 4.13 is rate determining (2nd order kinetics). At intermediate pressures, CN decay would be by kinetics between second and third order.

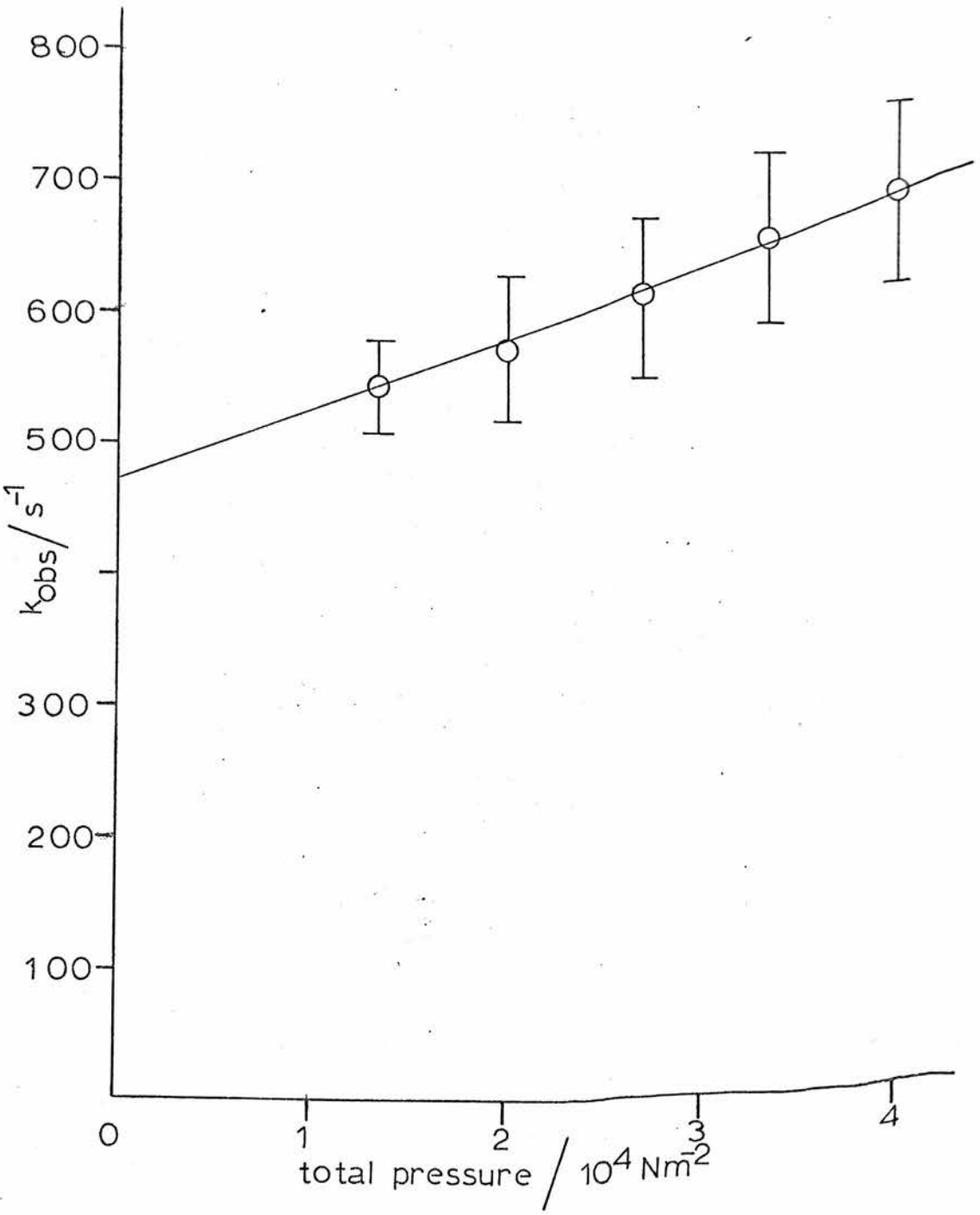

FIG.4.03 GRAPH OF K_{OBS} VS TOTAL PRESSURE

It may be that for the above mechanism, the high pressure second order limit is reached at pressures below 1.33×10^{4} Nm^{-2}, in which case the variation of k_{obs} with total pressure could be due to trace impurities in the helium. The gradient of the plot in fig. 4.03 can in fact be accounted for by an impurity level of $\sim$6 ppm of oxygen in the helium diluent. This could explain the fact that the third order rate constant, determined by varying the total pressure, was greater than the value obtained for a fixed total pressure. According to the mechanism described by reactions 4.13 and 4.14, the reverse order should be expected for the relative magnitudes of the two third order rate constants.

A further complication arises from the fact that the pressure broadening of CN rotational lines will increase over the range $(1.33 - 4.00) \times 10^{4}$ Nm^{-2} for fig. 4.03. This means that the Beer-Lambert coefficient γ will change also, and this was not accounted for in the above determinations. Hence the results obtained by varying total pressure may not be quantitatively meaningful.

The most precise result that can be given for these experiments is that for the second order high pressure regime, a rate constant of $(7.4 \pm 1.4) \times 10^{-15}$ cm^{3} $molecule^{-1}$ s^{-1} was obtained for reaction 4.01 in excess helium for a total pressure of 1.33×10^{4} Nm^{-2}. This corresponds to a third order rate constant of $(2.3 \pm 0.4) \times 10^{-33}$ cm^{6} $molecule^{-2}$ s^{-1} for the same total pressure with helium as third body, which is a reasonable value for this type of process.

The bimolecular rate constant given above is much smaller than the rate constants summarised in chapter 1, for the reactions of CN radicals with molecules like O_2, CH_4, NH_3 etc.. Hence for

experiments with reactant present, removal of CN by reaction with cyanogen should not dominate the CN decay.

Previously obtained values for the second order limit of reaction 4.01 are summarised in table 4.03 along with the partial pressures of the gases used. From their temperature dependence study of this reaction, Paul and Dalby[13] obtained an activation energy of 8.8 kJ mol^{-1} for the temperature range 300 - 450 K. A slightly higher value was obtained by Bullock and Cooper[18] (See Chapter 1).

The high temperature rate constant obtained by Boden and Thrush[16] is about two orders of magnitude greater than the value calculated at 687 K from the data of Paul and Dalby[13]. This may be explained if reactions other than the addition of CN to cyanogen became important at higher temperatures e.g.

$$CN + C_2N_2 \longrightarrow N_2 + C_3N \qquad (1.15)$$

The rate constant in table 4.03 given by Dunn et al.[24] was only approximate and will **not** be discussed further. However the other values obtained at ∿300 K are lower than obtained in this work.

In the studies by Paul and Dalby[13] and Bullock and Cooper[18], higher CN concentrations were produced and the observed decay times were much less than observed in this work (<1 ms). Hence under these conditions, it is likely that reaction and vibrational relaxation are competing processes. For this to be the case, the rate constant for the removal of $CN(X^2\Sigma, v'')$, strictly by reaction with cyanogen, would have to decrease with increasing v" so that vibrational relaxation of CN (v") to CN (v" - 1) would cause significant feeding of level v" - 1. The measured values of

Table 4.03

Rate Constants for Reaction 4.01

(second order limit)

Rate Constant k/cm^3 molecule^{-1} s^{-1}	T/K	$P_{C_2N_2}/Nm^{-2}$	P_{total}/Nm^{-2}	Ref.
3.5×10^{-15}	301	$(0.13\text{-}7.5) \times 10^4$	$(0.13\text{-}7.5) \times 10^4$	13
3.0×10^{-12}	687	0.13-3.1	$(2.0\text{-}6.7) \times 10^2$	16
$\sim 10^{-14}$	300	1.4 -3.5	$(0.9\text{-}1.6) \times 10^2$	24
4.9×10^{-15}	300	$(2.72\text{-}5.00) \times 10^2$	$\sim 10^5$	18
$(7.4 \pm 1.4) \times 10^{-15}$	295	$(0.13\text{-}2.67) \times 10^2$	1.33×10^4	this work

the rate constants for removal of $CN(X^2\Sigma, v'' = 0)$ will therefore be lower than those expected in the absence of feeding from the $v'' = 1$ level.

The rate constant for the second order regime of reaction 4.01, obtained in this work for the removal of $CN(X^2\Sigma, v'' = 0)$ in the absence of feeding by vibrational relaxation of $CN(X^2\Sigma, v'' = 1)$, is therefore faster than the previous values at $\sim$300 K.

REACTION OF CN WITH IMPURITIES

An indication of the contribution of impurities to the rate coefficients for removal of CN radicals may be obtained from a consideration of the intercepts of the graphs plotted in figs. 4.02 and 4.03.

The intercept in fig. 4.02 corresponds to the sum of all the removal processes in the absence of cyanogen.

$$\text{intercept} = \beta + \Sigma_i k_i c_i \qquad (4.15)$$

where β is the diffusion rate coefficient and k_i is the bimolecular rate constant for reaction of CN with impurity i, c_i being the concentration of impurity i. The most likely impurity was oxygen, but it was not possible to separate the contributions of the various removal processes quantitatively, thus they will not be discussed further.

In fig. 4.03, extrapolation to zero pressure gives an intercept corresponding to removal of CN in the absence of helium including reaction with C_2N_2 and impurities. However, the actual situation encountered at low helium pressures corresponds to the low pressure region of fig. 4.01 where diffusion is the dominant removal process for CN radicals.

In figs. 4.02 and 4.03, the rate coefficients for a mixture containing 26.7 Nm^{-2} of cyanogen at a total pressure of 1.33×10^4 Nm^{-2} do not agree. This was due to different amounts of trace impurities in the two sets of experiments.

REACTION PRODUCTS

The C_3N_3 produced in the reaction of CN with cyanogen may diffuse to the reaction vessel walls, and react heterogeneously as suggested by Boden and Thrush[16] or homogeneously, to form larger polymer molecules by combination with other C_nN_n units. In this work, a brown film characteristic of paracyanogen, was observed on the reaction vessel walls after extensive use of the system to photolyse cyanogen mixtures. The deposits were removed using a solution of 4% HF.

Hogness and Ts'ai[109] found similar deposits in their experiments on the photolysis of cyanogen. They determined the quantum yield of C_2N_2 photolysis to be 3, which is consistent with the formation of C_3N_3 as a precursor to the formation of the brown paracyanogen deposits. Safrany and Jaster[110] analysed the brown deposits produced in their flow system, and obtained a C : N ratio of 1.25 : 1 for cyanogen flames.

Hence the brown film observed as a product in this study of CN radicals is likely to be paracyanogen, as observed in previous work.

CONCLUSIONS

The work of this chapter provided a good basis for the planning of future experiments with gas mixtures containing cyanogen, helium and reactant. The basic mixture of cyanogen and helium chosen for these experiments was a partial pressure

of 26.7 Nm^{-2} of cyanogen and total pressure of 1.33×10^4 Nm^{-2}.

In the presence of sufficient reactant, removal of $CN(X^2\Sigma, v'' = 0)$ should occur predominantly by collision with reactant molecules, allowing the determination of accurate rate constants for the reactions of $CN(X^2\Sigma, v'' = 0)$ in the absence of feeding from the $v'' = 1$ level.

CHAPTER 5

CHAPTER 5

REACTIONS OF $CN(X^2\Sigma, v''=0)$ WITH SMALL MOLECULES CONTAINING O, N, C AND S ATOMS

INTRODUCTION

The reaction of CN with molecular oxygen has already been extensively studied. However, the rate constant determined here is strictly for the reaction of $CN(X^2\Sigma, v''=0)$ in the absence of vibrational feeding processes, and it will be useful to compare this result with those obtained previously.

Reaction of CN with molecules like CO, NO and CO_2, which are present in combustion processes, should provide useful kinetic data to aid the understanding of reactions in flames. The reactions of CN radicals with OCS and N_2O, which are isoelectronic with CO_2, were studied in an attempt to understand the relative reactivities of these isoelectronic molecules.

In the gas mixtures used for this work, the partial pressure of cyanogen (26.7 Nm^{-2}) and the total pressure (1.33×10^4 Nm^{-2}, helium diluent) were kept constant and the reactant partial pressures were varied. For the NO and CO reactions, the total pressure was also varied for a fixed partial pressure of reactant.

The ΔH° values given in this chapter were calculated for a temperature of 298 K using the data given in the JANAF tables[111]. The value of $\Delta H^\circ f(NCO) = 154 \pm 14$ kJ mol^{-1} determined by Okabe[112] was used along with the value of $\Delta H^\circ f(CN) = 418$ kJ mol^{-1} determined in this work (see Chapter 6).

RESULTS

1. Reaction with O_2

From the plot of observed rate coefficients, k_{obs}, against partial pressure of oxygen (fig. 5.01), the rate constant† for the removal of $CN(X^2\Sigma, v''=0)$ by reaction with molecular oxygen (reaction 1.20) was calculated to be $(1.85\pm0.40)\times10^{-11}$ cm^3 molecule^{-1} s^{-1} at 295 K. This value is about a factor of 2 greater than the previous room temperature values which are reviewed in Chapter 1 and summarised in Table 5.01.

$$CN + O_2 \rightarrow NCO + O(^3P), \Delta H^\circ_{298} = -14.0 \text{ kJ mol}^{-1} \qquad (1.20)$$

Two explanations for this situation were considered. The first is that, at the delay times studied in this work, and under the experimental conditions chosen, the decay of $CN(X^2\Sigma)$ exclusively in level $v''=0$ was monitored in the absence of feeding by vibrational relaxation. Previous work involved shorter delay times under conditions where vibrationally excited CN radicals were present and the net removal of $CN(X^2\Sigma, v''=0)$ could be reduced by feeding, resulting in slower rate constants.

The second explanation considered was that oxygen atoms, produced by reaction 1.20, could react with the CN precursor, cyanogen, producing more CN radicals. Thus reaction 5.01 would have given a reduction in the net rate of removal of CN radicals, which depended on the actual compositions of the gas mixtures used in the studies listed in table 5.01.

† All the rate constants given in this chapter are the corrected values i.e. the Beer-Lambert coefficient, γ, has been taken into account.

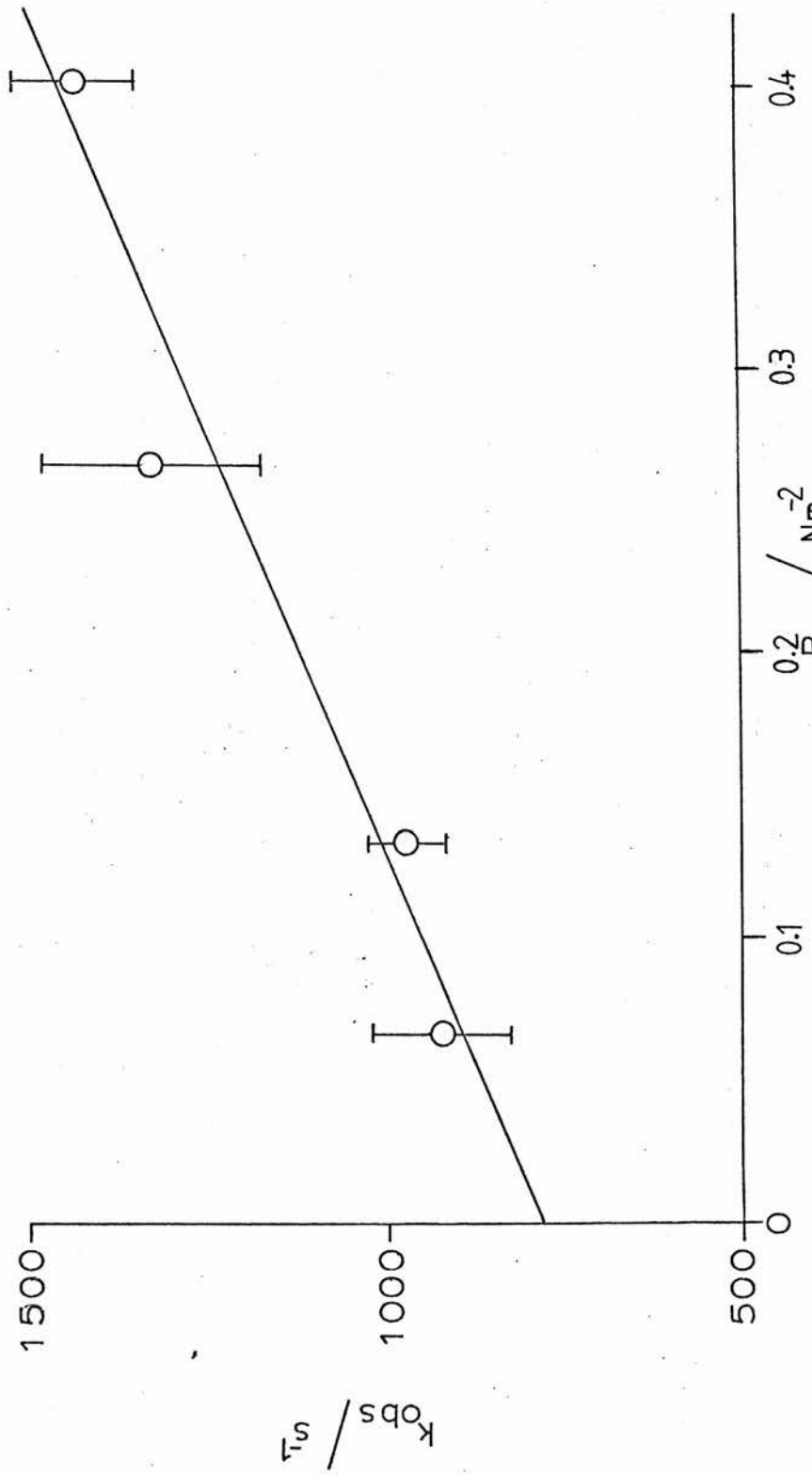

FIG. 5.01 GRAPH OF K_{OBS} AGAINST OXYGEN PARTIAL PRESSURE

Table 5.01

Rate Constants for Reaction with Oxygen

Investigator	T/K	P_{total}/Nm^{-2}	Rate Constant k/cm^3 molecule^{-1} s^{-1}	Ref.
Paul and Dalby	295†	not specified	9.1×10^{-12}	13
Basco	295†	$(2.67\text{-}4.00) \times 10^{4}$	$>7.6 \times 10^{-12}$	14
Boden and Thrush	687	2.0×10^{2}	$(7.3 \pm 3.3) \times 10^{-12}$	16
Bullock and Cooper	303	$\sim 10^{5}$	$(1.12 \pm 0.03) \times 10^{-11}$	18
Bullock and Cooper	377	$\sim 10^{5}$	$(1.05 \pm 0.04) \times 10^{-11}$	18
Schacke et al.	298	$\sim 5.3 \times 10^{2}$	1.0×10^{-11}	21
this work	295	1.33×10^{4}	$(1.85 \pm 0.40) \times 10^{-11}$	-

† Room temperature assumed to be 295 K

$$O(^3P) + C_2N_2 \rightarrow NCO + CN \quad \Delta H^o_{298} = 20 \text{ kJ mol}^{-1} \qquad (5.01)$$

Reaction 5.01 is however endothermic, and Morrow and McGrath[25] have shown that it is not significant at room temperature. Hence this explanation may be discounted in favour of the former explanation given earlier.

2. Catalysed recombination of CN radicals

Two sets of experiments were carried out to investigate the reactions of CN radicals with the molecules CO and NO. The details of these experiments are as follows where for simplicity, XO is used to represent either CO or NO:-

a. The reaction mixtures contained a fixed partial pressure of cyanogen (26.7 Nm^{-2}). The rate coefficients, k_{obs}, for removal of $CN(X^2\Sigma, v''=0)$ are plotted against XO partial pressure in figs. 5.02 and 5.03 for NO and CO respectively. Good straight lines were obtained in both cases. The second order rate constants, k_a, are given in table 5.02 along with the third order rate constants k_a'. Assuming the reaction to be third order, $k_a' = k_a/[He]$.

Table 5.02

Rate constants for reaction of CN with XO

XO	k_a /cm^3 $molecule^{-1}$ s^{-1}	k_a' /cm^6 $molecule^{-2}$ s^{-1}
NO	$(5.28\pm0.27)\times10^{-12}$	$(1.61\pm0.08)\times10^{-30}$
CO	$(9.86\pm0.78)\times10^{-14}$	$(3.01\pm0.24)\times10^{-32}$

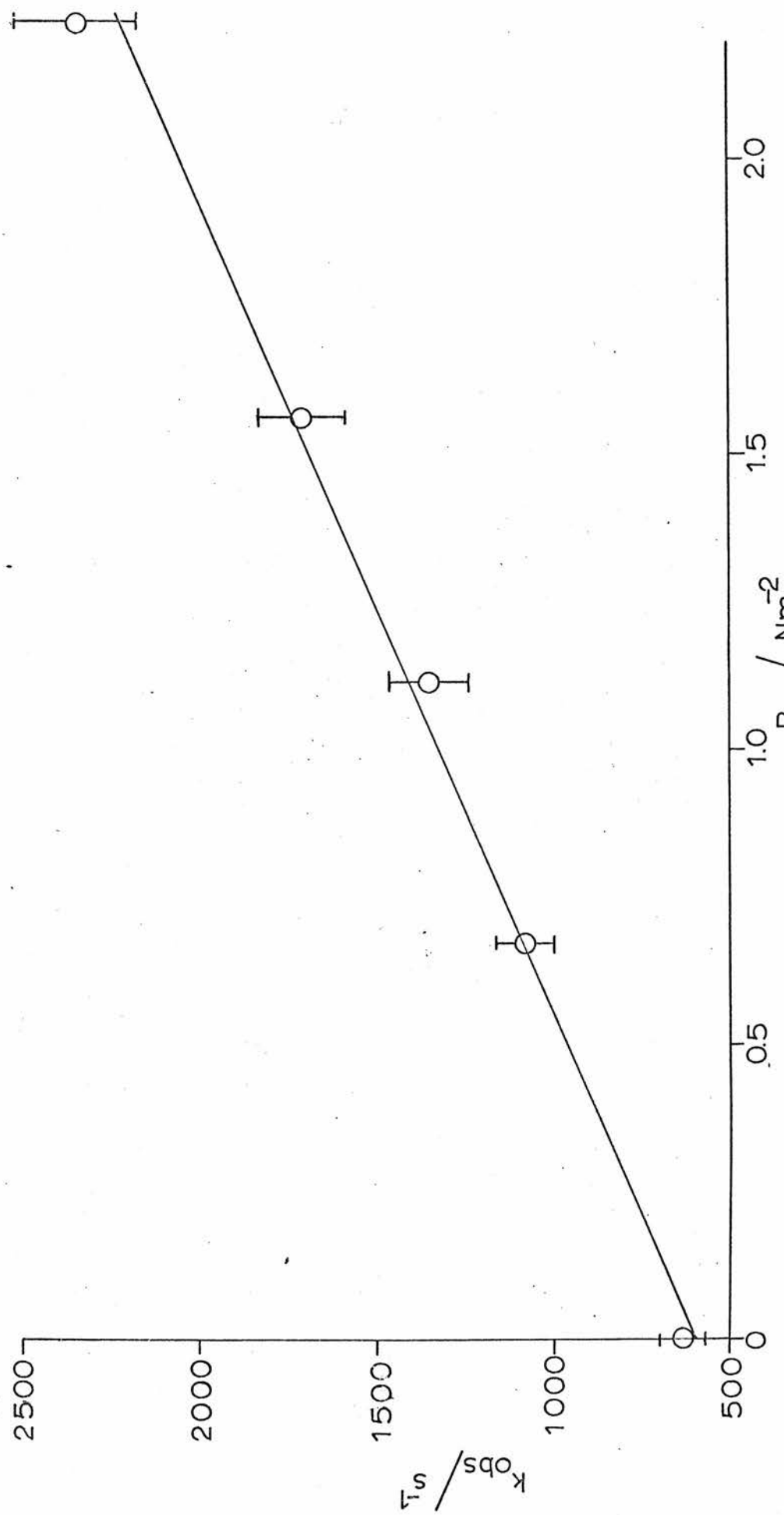

FIG. 5.02 GRAPH OF K_{OBS} AGAINST PARTIAL PRESSURE OF NITRIC OXIDE

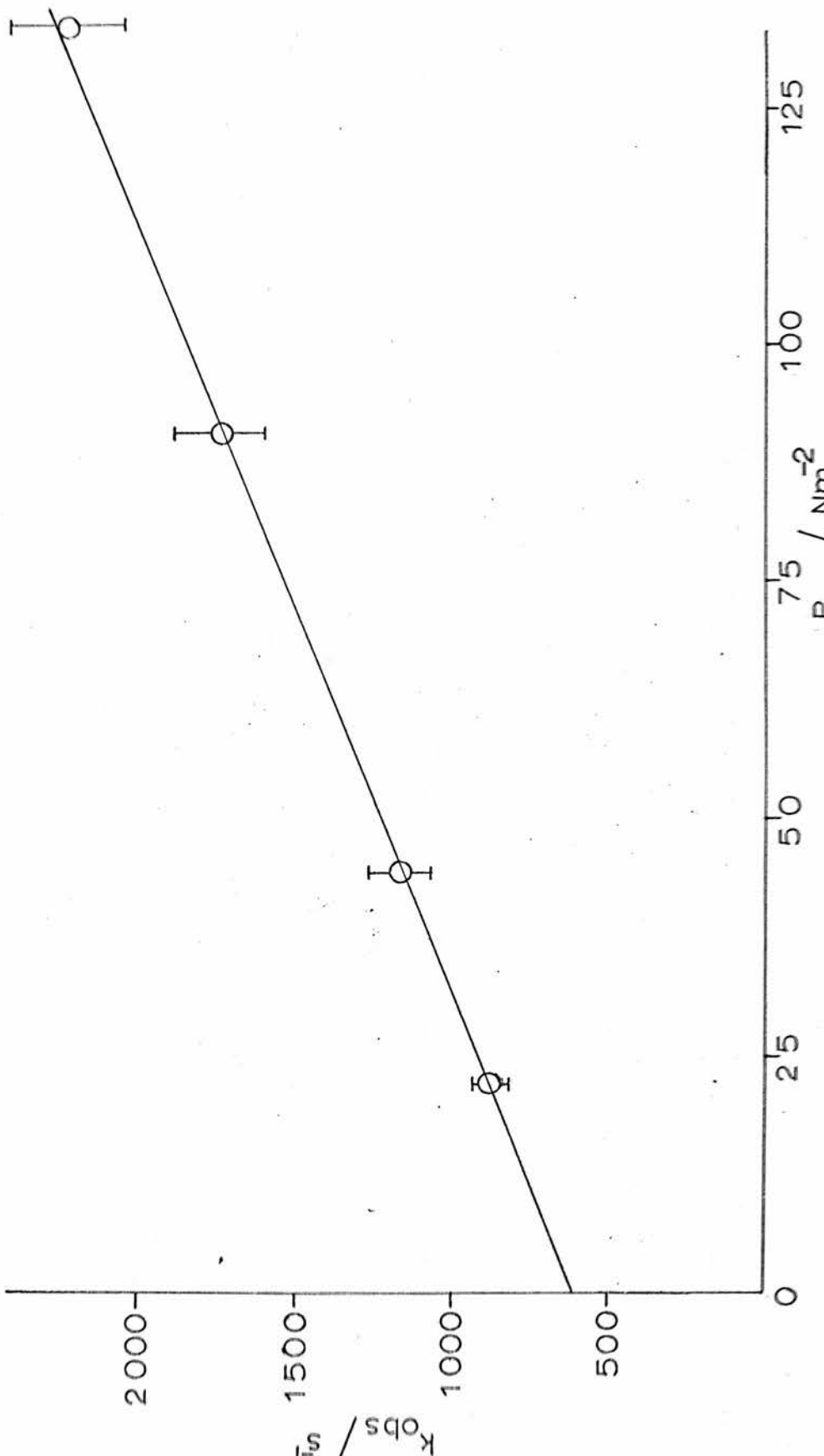

FIG.5.03 GRAPH OF K_{OBS} AGAINST PARTIAL PRESSURE OF CARBON MONOXIDE

b. The total pressures of the gas mixtures were varied by adjusting the amount of excess helium added to a fixed partial pressure of XO (see table 5.03) and a fixed partial pressure of cyanogen (26.7 Nm^{-2}). The observed rate coefficients for the removal of $CN(X^2\Sigma, v''=0)$ under these conditions are plotted against total pressure in figs. 5.04 and 5.05 for NO and CO respectively (upper traces).

The lower traces on these graphs correspond to control experiments where no XO was added to the helium/cyanogen mixtures. By calculating the rate constants from the difference between the lower and upper traces i.e. from a plot of Δk_{obs} against total pressure, any effects from impurities in the helium diluent were eliminated.

Table 5.03 gives the second order rate constants, k_b, for this method together with the third order rate constant, k_b', where $k_b' = k_b / [XO]$.

Table 5.03

Rate constants for reaction of CN with XO

XO	P_{XO}/Nm^{-2}	k_b /cm^3 $molecule^{-1}$ s^{-1}	k_b' /cm^6 $molecule^{-2}$ s^{-1}
NO	1.56	$(2.08\pm0.51)\times10^{-16}$	$(5.43\pm1.33)\times10^{-31}$
CO	44.4	$(1.62\pm0.19)\times10^{-16}$	$(1.49\pm0.17)\times10^{-32}$

The observed results may be interpreted as XO catalysed recombination of CN radicals, similar to the catalysed recombination of halogen atoms observed by Clark et al.[113] and Van den Bergh and

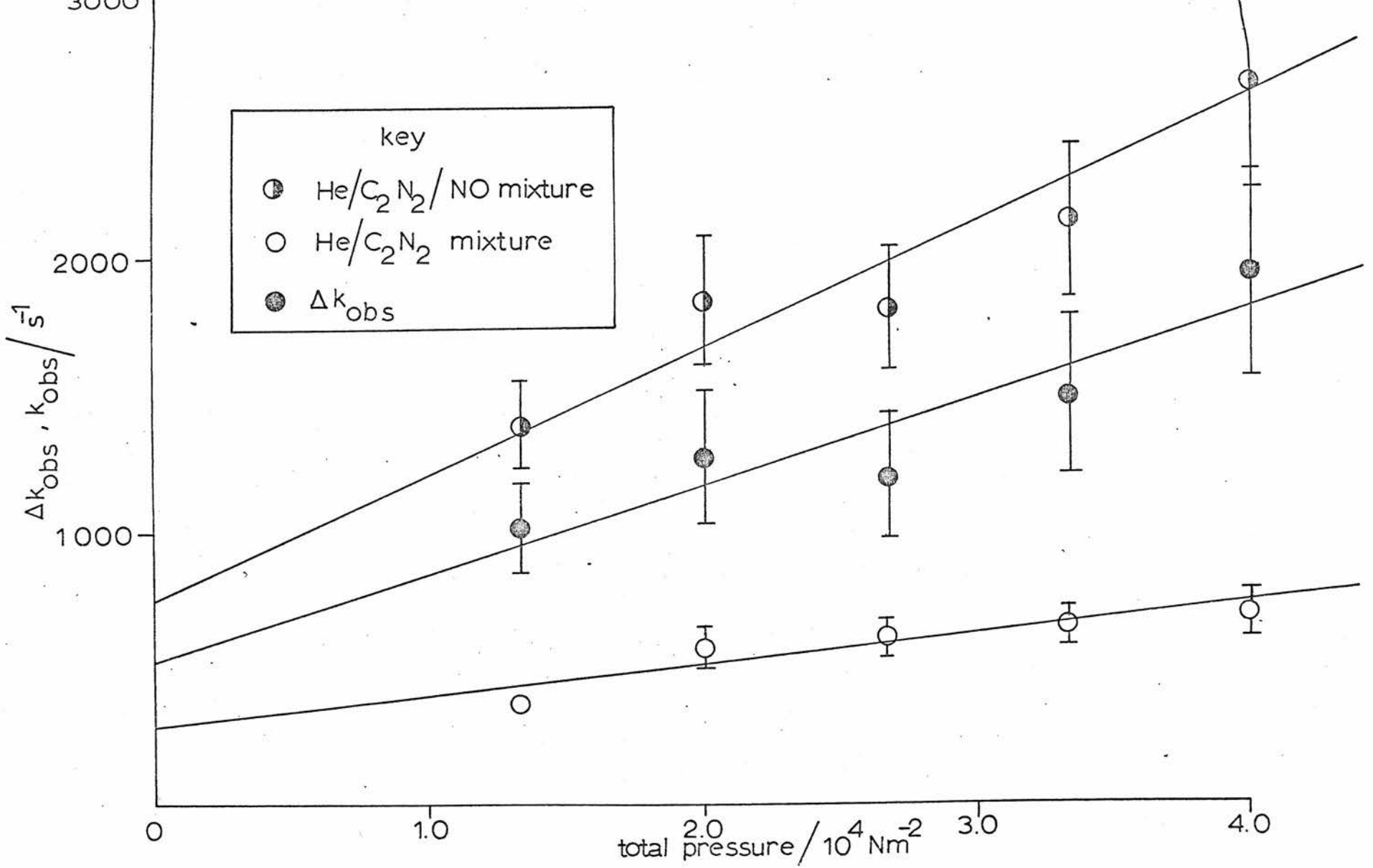

FIG.5.04 GRAPH OF K_{OBS} AND ΔK_{OBS} AGAINST TOTAL PRESSURE

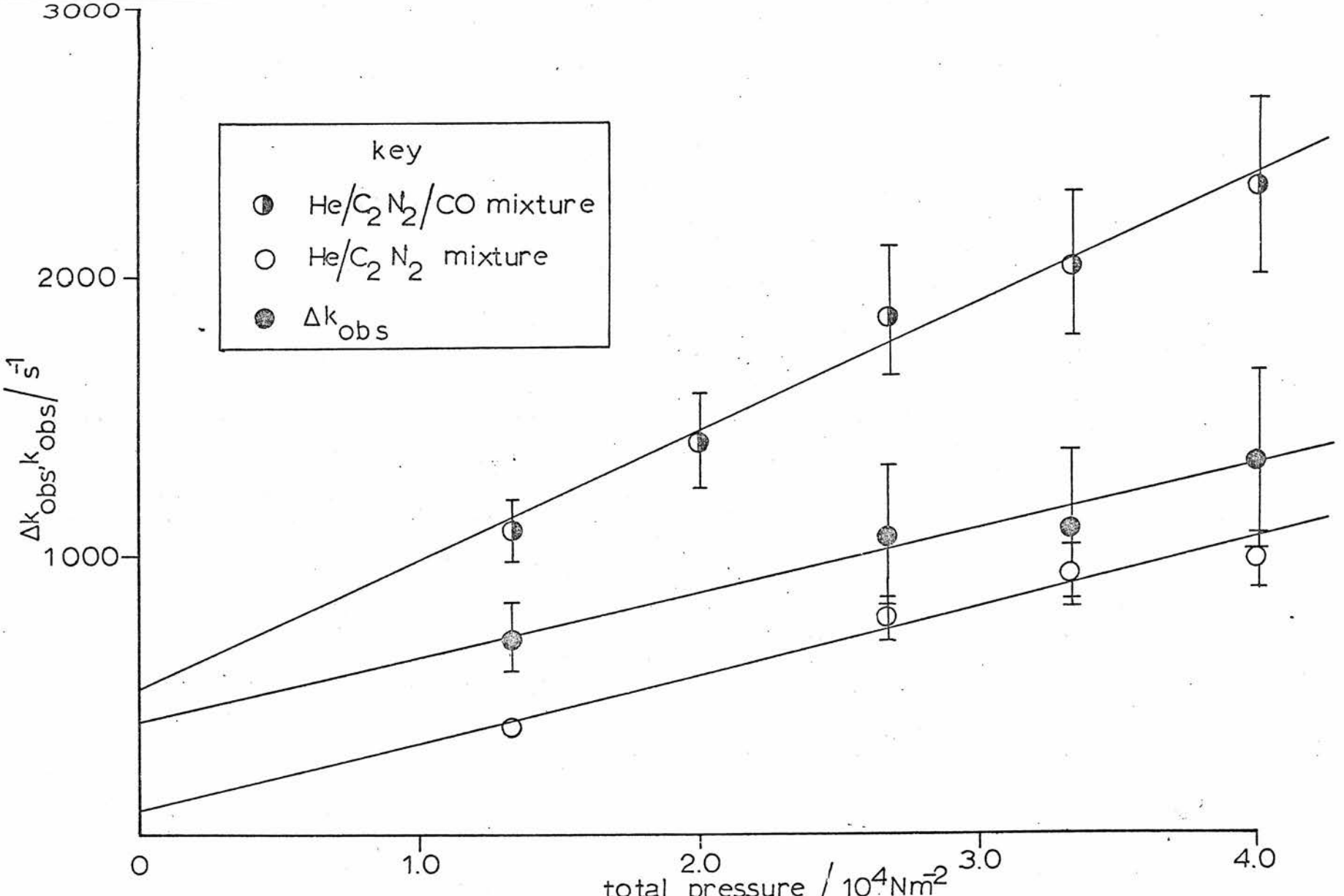

FIG. 5.05 GRAPH OF K_{OBS} AND ΔK_{OBS} AGAINST TOTAL PRESSURE

Troe[108]. Reaction of CN with XO is thought to occur by the following mechanism given by Clark et al.[113] for the recombination of Cl atoms in the presence of CO and NO.

$$CN + XO + M \underset{k_{-1X}}{\overset{k_{1X}}{\rightleftharpoons}} OXCN + M \qquad (5.02)$$

$$CN + OXCN \xrightarrow{k_{2X}} C_2N_2 + XO \qquad (5.03)$$

The molecule XO therefore acts as a chaperone by forming an intermediate with the CN radical. It is therefore worthwhile to consider the properties of these intermediates.

The existence of NOCN, a blue-green gas, was discovered by Norrish and Smith[33] in their photolysis study of C_2N_2/NO mixtures. The molecule was later identified mass spectrometrically by Galvin and Pritchard[34], and spectroscopic evidence[35,36] suggests a bent planar structure with the atoms arranged ON-CN.

The halogen analogues, YNO, are well characterised (Y≡halogen) and may be prepared readily in the laboratory[114]. However, the corresponding YCO molecules are much less stable and have been prepared and studied using matrix isolation techniques[115,116]. Nevertheless, it is likely that the molecule OC-CN is produced as a transient species in this photochemical study (c.f. ClCO in Cl atom recombination[113]).

From the bond energies given in table 5.04, the bond energy D(OC-CN) should be less than D(Cl-CO).

Table 5.04

Bond Energies

Bond	Bond Energy /kJ mol $^{-1}$	Ref.
D(Cl-CO)	∿26	113, 117
D(Cl-NO)	∿159	118
D(I-NO)	96±13	108
D(NC-NO)	120.5±11.5	119

There is a discrepancy between the third order rate constants, k_a' and k_b', calculated by the two methods described earlier and given in tables 5.02 and 5.03. This will be discussed later. More important is the fact that the third order rate constants obtained for NO catalysed CN recombination are larger than those for CO catalysed recombination.

This is a direct consequence of the stronger bond strength of the ON-CN bond compared to the OC-CN bond. For NO catalysed recombination, the equilibrium reaction 5.02 is well over to the right, and if reaction 5.03 is rapid, the decay of CN radicals will obey the following equation.

$$-d[CN]/dt = 2k_{1X}[CN][NO][He] \qquad (5.04)$$

For the CO case, equilibrium lies more to the left for reaction 5.02, and depending on the relative importance of reaction 5.03 and the reverse reaction of 5.02, then the following two extremes are possible (where K is the equilibrium constant for reaction 5.02).

$$-d[CN]/dt = 2k_{1X}[CN][CO][He] \qquad (5.05)$$

$$-d[CN]/dt = 2Kk_{2X}[CN]^2[CO] \qquad (5.06)$$

In this work, the decay of CN will occur by kinetics which are intermediate between the two extremes described by equations 5.05 and 5.06. Analysis of such behaviour is very complex[108,113] and no marked deviation from pseudo first order decay was observed. Hence the decay of CN in the presence of CO is assumed to be described by equation 5.05.

In this study, at a total pressure of 1.33×10^{4} Nm^{-2}, reaction 5.02 should be in the third order regime, which occurs at total pressures of less than one atmosphere for NO catalysed recombination of iodine atoms[108]. As the total pressure is increased, the decay of CN becomes less sensitive to helium pressure until at the high pressure limit (1000 atm. for I atom recombination[108]), the decay becomes second order and independent of helium pressure.

Hence the rate constants k_b' are less than the corresponding k_a' values due to a slight deviation from third order behaviour as the helium pressure was increased. The value of $0.5\ k_a'$ is therefore the best approximation to the low pressure limiting value of k_{1X} that can be given for this work. These limiting values are given in table 5.05. They are in good agreement with

Table 5.05

Low Pressure Rate Constants

XO	low pressure limit $k_{1X}/cm^6\ molecule^{-2}\ s^{-1}$
NO	$(8.0 \pm 0.4) \times 10^{-31}$
CO	$(1.5 \pm 0.1) \times 10^{-33}$

the values obtained by Clark et al.[113] for the catalysed recombination of Cl atoms, and with value of 3.3×10^{-31} cm^6 molecule^{-2} s^{-1} obtained by Basco and Norrish[32] for reaction 1.35 with nitrogen as third body.

$$CN + NO + (M) \longrightarrow ONCN + (M) \qquad (1.35)$$

A negative activation energy of -10 ± 4 kJ mol^{-1} was estimated for the removal of CN radicals in the presence of NO using the value of $k_a = (5.28 \pm 0.27) \times 10^{-12}$ cm^3 molecule^{-1} s^{-1} (295 K) obtained in this work, along with the value of $(5.0 \pm 3.3) \times 10^{-13}$ cm^3 molecule^{-1} s^{-1} obtained by Boden and Thrush[16] at 687 K. Negative activation energies have been observed as a characteristic of similar catalysed recombination reactions[113]. However, the validity of the estimated activation energy must be questioned as other mechanisms may dominate at higher temperatures.

3. Reaction with CO_2, N_2O and OCS

In the study of $CN(X^2\Sigma)$ radicals reacting with the isoelectronic molecules CO_2, OCS and N_2O, it is important to consider the possibility and consequence of photolysis of these reactants[120]. Secondary reactions of primary products from photolysis of these reactants could also be important.

For the molecule CO_2, no photolysis can occur at the wavelengths transmitted by the walls of the quartz reaction vessel[120]. The observed rate coefficients for removal of $CN(X^2\Sigma, v''=0)$ are plotted against the partial pressure of carbon dioxide in fig. 5.06.

$$CN + CO_2 \longrightarrow NCO + CO, \quad \Delta H^\circ = +19.7 \text{ kJ mol}^{-1} \qquad (5.07)$$

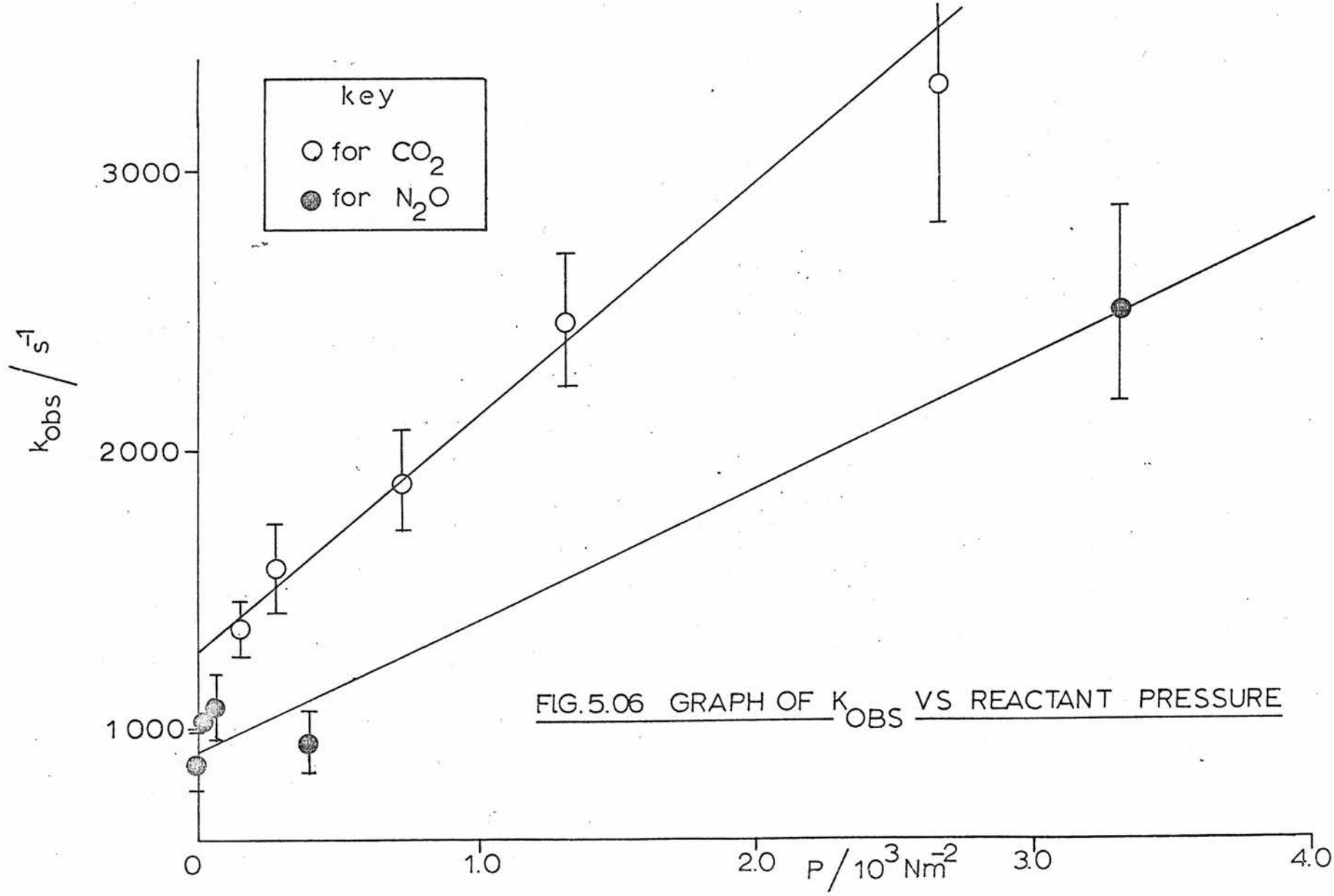

FIG. 5.06 GRAPH OF K_{OBS} VS REACTANT PRESSURE

The rate constant for the above reaction was calculated to be $(6.48\pm0.82)\times10^{-15}$ cm^3 $molecule^{-1}$ s^{-1} at 295 K. More realistically however, due to the possibility of trace impurities in the CO_2, an upper limit of 7.3×10^{-15} cm^3 $molecule^{-1}$ s^{-1} is given for this rate constant at 295 K. It is not surprising that the rate constant for reaction 5.07 is low considering the high bond strength of the C=O bond in carbon dioxide[81] (531 kJ mol^{-1}).

As the upper limit for the rate constant for the CN + CO_2 reaction is small and the reaction is slightly endothermic (ΔH°_{298} = +19.7 kJ mol^{-1}), a study of the effect of vibrational excitation of CN on this reaction would be interesting. It would also be possible to study the effect of vibrational excitation of the CO_2 molecule on this reaction.

The flash photolysis of C_2N_2/He/OCS mixtures is much more complicated, as photolysis of OCS will occur. Black et al.[121] give the absorption spectrum of OCS, which has an absorption maximum at ~223.7 nm, and this absorption corresponds to the following primary products.

$$OCS(^1\Sigma^+) + h\nu \longrightarrow CO(^1\Sigma^+) + S(^1D_2) \qquad (5.08)$$

The secondary reaction of $S(^1D_2)$ with OCS is rapid[122] and leads to the formation of S_2 molecules. Deactivation of $S(^1D_2)$ is also rapid.

$$S(^1D_2) + OCS(^1\Sigma^+) \longrightarrow CO(^1\Sigma^+) + S_2(a^1\Delta_g) \qquad (5.09)$$

$$S(^1D_2) + OCS(^1\Sigma^+) \longrightarrow OCS + S(^3P_J) \qquad (5.10)$$

The reaction of $CN(X^2\Sigma, v''=0)$ with OCS is thought to occur as follows.

$$CN + OCS \longrightarrow SCN + CO \qquad (5.11)$$

However, interference of S atom reactions makes the determination of quantitatively meaningful results difficult. Not only will $S(^1D)$ atoms remove OCS, but they may also react with cyanogen to produce SCN and more CN radicals.

Table 5.06 gives the average observed rate coefficients for the removal of $CN(X^2\Sigma, v''=0)$ radicals produced in the photolysis of C_2N_2/He/OCS mixtures.

Table 5.06

Rate Coefficients for OCS Reaction

$P_{OCS}/10^{-2}$ Nm^{-2}	Average k_{obs}/s^{-1}	No. of Results averaged
0	660±120	4
6.67	1070±260	4
13.3	1350±360	4

The reaction of CN with OCS was one of the fastest reactions studied in this work. In order to observe the CN decay for such a fast reaction, the amount of reagent present must be limited by the dead time of the photomultiplier detector. Hence only low partial pressures of OCS could be used (see table 5.06). In view of this limitation, which could cause deviations from pseudo first order decay kinetics, a lower limit of $\sim 5\times10^{-11}$ cm^3 molecule^{-1} s^{-1} is given for the rate constant of reaction 5.11.

Spectroscopic evidence for the production of SCN by the reaction of CN with OCS has recently been obtained by Addison et al.[151], who

give a lower limit of 306.4 kJ mol^{-1} for the C-S bond strength of SCN. By measuring the rate constant ratio for the reactions of CN + OCS and CN + C_2H_6, they found evidence to support the value of $k > 5x10^{-11}$ cm^3 $molecule^{-1}$ s^{-1} obtained in this work at 295 K.

The photolysis of $C_2N_2/He/N_2O$ mixtures, at wavelengths corresponding to the continuous absorption band of N_2O, which has a maximum at ~180 nm, can lead to the following primary photochemical process[120].

$$N_2O + h\nu \longrightarrow N_2 + O(^1D) \qquad (5.12)$$

The following secondary reactions have approximately the same rate constants which are close to the collision limit[123-125].

$$O(^1D) + N_2O \longrightarrow N_2 + O_2 \qquad (5.13)$$

$$O(^1D) + N_2O \longrightarrow 2NO \qquad (5.14)$$

Hence, for the delay times monitored in this work (>900 μs), all the $O(^1D_2)$ will have reacted beforehand. Therefore the decay of $CN(X^2\Sigma, v''=0)$ is monitored for removal by N_2O and removal by the products of reactions 5.13 and 5.14.

However, N_2O is a weak absorber in the spectral region above the quartz cut-off[120], and since the observed rate coefficient, k_{obs}, did not change with flash energy, negligible O_2 resulted from the photolysis of N_2O.

Hence CN radicals are removed exclusively by reaction with N_2O molecules. The following two reactions were considered, but as reaction 5.16 is substantially endothermic, reaction 5.15 is expected to predominate at 300 K.

$$CN + N_2O \longrightarrow NCO + N_2 \qquad \Delta H^{\circ} = -345 \text{ kJ mol}^{-1} \qquad (5.15)$$

$$CN + N_2O \longrightarrow NCN + NO \qquad \Delta H^{\circ} = +20.8 \text{ kJ mol}^{-1} \qquad (5.16)$$

The observed rate coefficients are plotted against partial pressure of N_2O in fig. 5.06, giving an upper limit of 3.7×10^{-16} cm^3 $molecule^{-1}$ s^{-1} for the rate constant of this reaction.

Addendum

For the decay of CN radicals in a large excess of CO_2 and N_2O, a possible alternative mechanism is that the molecules CO_2 and N_2O act as chaperones in the recombination of CN radicals.

Although it is difficult to distinguish between pseudo first and second order kinetics, an attempt to do this, for the decay of CN in CO_2 and N_2O, showed significant curvature of the second order plots, in contrast to linear first order plots. Hence the kinetics were first order with respect to CN, and the major channel for removal was most probably the abstraction reaction to form NCO in both cases.

Analysis of the reaction products would clarify the situation, and indicate the relative contributions of the two mechanisms for the removal of CN radicals.

CHAPTER 6

CHAPTER 6

REACTIONS WITH H_2O, HCl AND HCN

INTRODUCTION

None of the rate constants given in this chapter has been measured previously, with the exception of that for the reaction of CN with H_2O, for which only an estimate has been obtained[13]. The rate constants for the reactions of CN with H_2O and HCN are of use in the modelling of combustion processes where these molecules are known to be present.

The reactions of $CN(X^2\Sigma, v''=0)$ with the fully deuterated equivalents of H_2O and HCl were also studied to determine the extent of the isotope effect.

The values of ΔH which follow were calculated for 298 K using the thermochemical data given in the JANAF tables[111]. The value of $\Delta H^\circ_f(HNCO) = 23.1 \pm 3.2$ kJ mol^{-1} which was used in one of the calculations was determined by Okabe[112]. Later in this chapter, the value of $\Delta H^\circ_{f_{295}}(CN) = 417.6 \pm 1.3$ kJ mol^{-1} is derived from experimental data and this value has been used in the ΔH calculations given in this thesis.

RESULTS AND DISCUSSION

1. Reaction with H_2O and D_2O

Care was taken in handling H_2O and D_2O in the vacuum line to avoid problems of condensation since the vapour pressure of H_2O is only 2.64×10^3 Nm^{-2} at 295 K.

The observed rate coefficients for the removal of $CN(X^2\Sigma, v''=0)$ by reaction with H_2O and D_2O are plotted against the partial

pressures of these molecules in fig. 6.01. The rate constants† determined for the reactions of CN with H_2O and D_2O were $(1.71\pm0.09)\times10^{-13}$ and $(1.67\pm0.13)\times10^{-13}$ cm^3 $molecule^{-1}$ s^{-1} respectively. These values are in good agreement and no isotope effect was measurable.

The following products may be obtained for the reaction of CN with H_2O.

$$CN + H_2O \longrightarrow NCO + H_2 , \quad \Delta H^\circ = -21.4 \text{ kJ mol}^{-1} \qquad (6.01)$$

$$\longrightarrow HCN + OH , \quad \Delta H^\circ = -1.2 \text{ kJ mol}^{-1} \qquad (6.02)$$

$$\longrightarrow HNCO + H , \quad \Delta H^\circ = -54.3 \text{ kJ mol}^{-1} \qquad (6.03)$$

As product analysis was not carried out, and since the activation energies for the reactions are not known, it is not possible to specify which of these pathways predominates. However, reaction 6.03 may be considered unlikely if it occurs by a four centre mechanism, and reaction 6.01, where two O-H bonds are broken, seems unlikely as an elementary reaction. Hence it is possible that the least thermodynamically favoured reaction, reaction 6.02, is favoured kinetically.

2. Reactions with HCl and DCl

The rate coefficients for the removal of $CN(X^2\Sigma, v''=0)$ by HCl and DCl are plotted against the partial pressures of these molecules in fig. 6.02. The rate constants were calculated to be $(4.4\pm1.2)\times10^{-15}$ and $(5.7\pm0.7)\times10^{-15}$ cm^3 $molecule^{-1}$ s^{-1} respectively

† The rate constants given in this chapter are the corrected values, i.e. the Beer-Lambert coefficient, γ, has been taken into account.

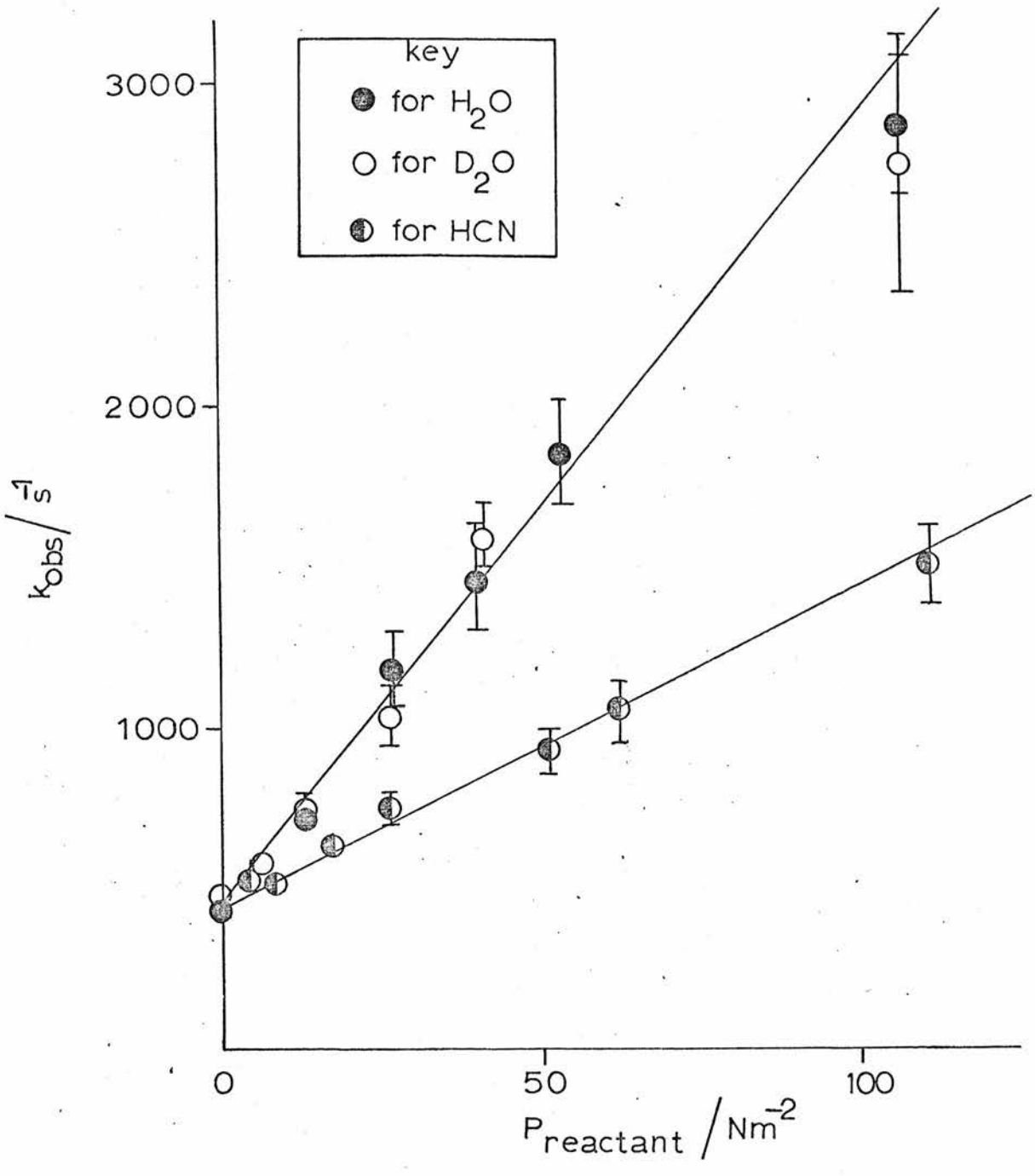

FIG.6.01 GRAPH K_{OBS} AGAINST REACTANT PRESSURE

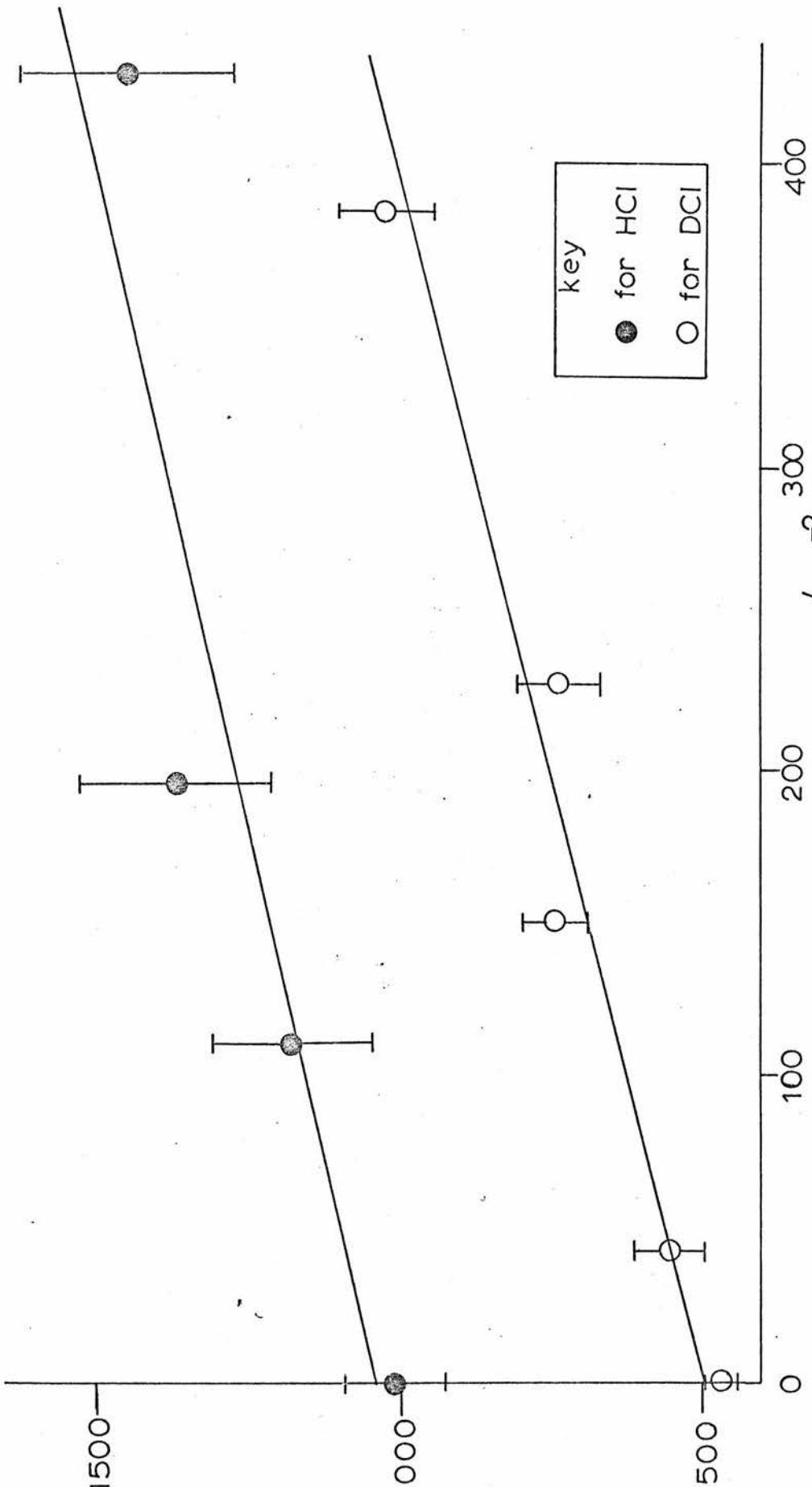

FIG. 6.02 GRAPH OF K_{OBS} AGAINST PARTIAL PRESSURE OF REACTANT

for the reaction of CN with HCl and DCl. Hence within the experimental uncertainties, no isotope effect was again observed.

For the HCl experiments, ordinary cylinder helium was used and this is reflected in the large intercept in fig. 6.02 caused by impurities. Pure helium (<1 ppm O_2) was used for the DCl experiments for which the usual intercept value was obtained.

The following reaction products were considered for the CN + HCl reaction.

$$CN + HCl \longrightarrow HCN + Cl \quad , \quad \Delta H^{o}_{298} = -69.1 \text{ kJ mol}^{-1} \qquad (6.04)$$

$$\longrightarrow ClCN + H \quad , \quad \Delta H^{o}_{298} = +30.6 \text{ kJ mol}^{-1} \qquad (6.05)$$

As reaction 6.05 is substantially exothermic, reaction 6.04 will predominate. This is in line with the following analogous halogen atom reactions studied by Kompa and Wanner[126] and Bergmann and Moore[127].

$$F + HCl \longrightarrow HF + Cl \quad , \quad \Delta H^{o} = -138 \text{ kJ mol}^{-1} \qquad (6.06)$$

$$Cl + HBr \longrightarrow HCl + Br \quad , \quad \Delta H^{o} = -65 \text{ kJ mol}^{-1} \qquad (6.07)$$

$$Cl + HI \longrightarrow HCl + I \quad , \quad \Delta H^{o} = -133 \text{ kJ mol}^{-1} \qquad (6.08)$$

These reactions are effectively H atom exchange reactions and the rate constant determined for reaction 6.04 is much smaller than the values given for reactions 6.06 to 6.08 at 295 K.

It therefore appears that the exchange reaction, 6.04, is much less efficient than the analogous halogen atom reactions, for which significant isotope effects have been observed[127].

3. Reaction with HCN

The rate constant for the removal of $CN(X^2\Sigma, v''=0)$ by reaction with HCN was calculated to be $(7.67 \pm 0.35) \times 10^{-14}$ cm^3 $molecule^{-1}$ s^{-1}

from the plot of the observed rate coefficients against partial pressure of HCN given in fig. 6.01.

$$CN + HCN \longrightarrow C_2N_2 + H \ , \ \Delta H^{\circ} = -25.7 \text{ kJ mol}^{-1} \qquad (6.09)$$

The above reaction is reversible and Dunn et al.[24] obtained a rate constant of $(8.6\pm3.0)\times10^{-16}$ cm^3 molecule^{-1} s^{-1} for the reverse process.

It was therefore possible to calculate ΔG°_{298} from the equilibrium constant of reaction 6.09. Hence, using the thermochemical data given in the JANAF tables[111], a value of $\Delta H^{\circ}_{f_{295}}(CN) = 417.6\pm1.3$ kJ mol^{-1} was obtained. This is in excellent agreement with some of the more recent values given in the literature[16,80,128]. It would therefore appear that the value of 435 kJ mol^{-1} given in the JANAF tables requires revision.

Addendum

An isotope effect was observed by Bullock and Cooper[19] for the reactions of CN with CH_4 and CD_4, where a rate constant ratio, k_H/k_D of $\sim$2 was obtained. The absence of an isotope effect, as found in the work of this chapter, is unusual. However, a fortuitous cancellation of the terms in the expressions for k_H and k_D (activated complex theory), at a particular temperature, can lead to $k_H/k_D = 1$, indicating an apparent absence of an isotope effect.

The absence of an isotope effect may also point to the molecules H_2O, D_2O, HCl and DCl acting as efficient chaperones for the recombination of CN radicals (c.f. similar reactions in Chapter 5). Departure from pseudo first order kinetics was looked for but was not detected.

CHAPTER 7

CHAPTER 7

REACTIONS WITH H_2, CH_4 AND C_2H_6

INTRODUCTION

The reactions of cyanide radicals with molecular hydrogen and small saturated hydrocarbons are of interest in the study of combustion processes. These reactions can be classed as hydrogen atom abstraction reactions, analogous to halogen atom reactions with saturated hydrocarbons.

In this work, the rate constants given are strictly for the removal of $CN(X^2\Sigma, v''=0)$ in the absence of feeding by vibrational relaxation. All the values quoted are the corrected values i.e. the Beer Lambert coefficient, $\gamma = 0.57$, has been taken into account.

The ΔH values given in this chapter were calculated for 298 K from the thermochemical data given by Calvert and Pitts[120] and the JANAF tables[111]. The value of $\Delta H^{\circ}_{f_{298}}(CN) = 418$ kJ mol^{-1}, given in this thesis, was used in the calculations.

RESULTS AND DISCUSSION

1. Reaction of $CN(X^2\Sigma, v''=0)$ with H_2

The reaction of CN radicals with molecular hydrogen was studied at a total pressure of 1.33×10^4 Nm^{-2} for both helium and argon diluents, and at a total pressure of 1.27×10^3 Nm^{-2} for helium diluent. The observed rate coefficients for these three sets of experiments are plotted against the partial pressure of hydrogen in fig. 7.01. The rate constants for these experiments, corresponding to the following reaction, are given in table 7.01.

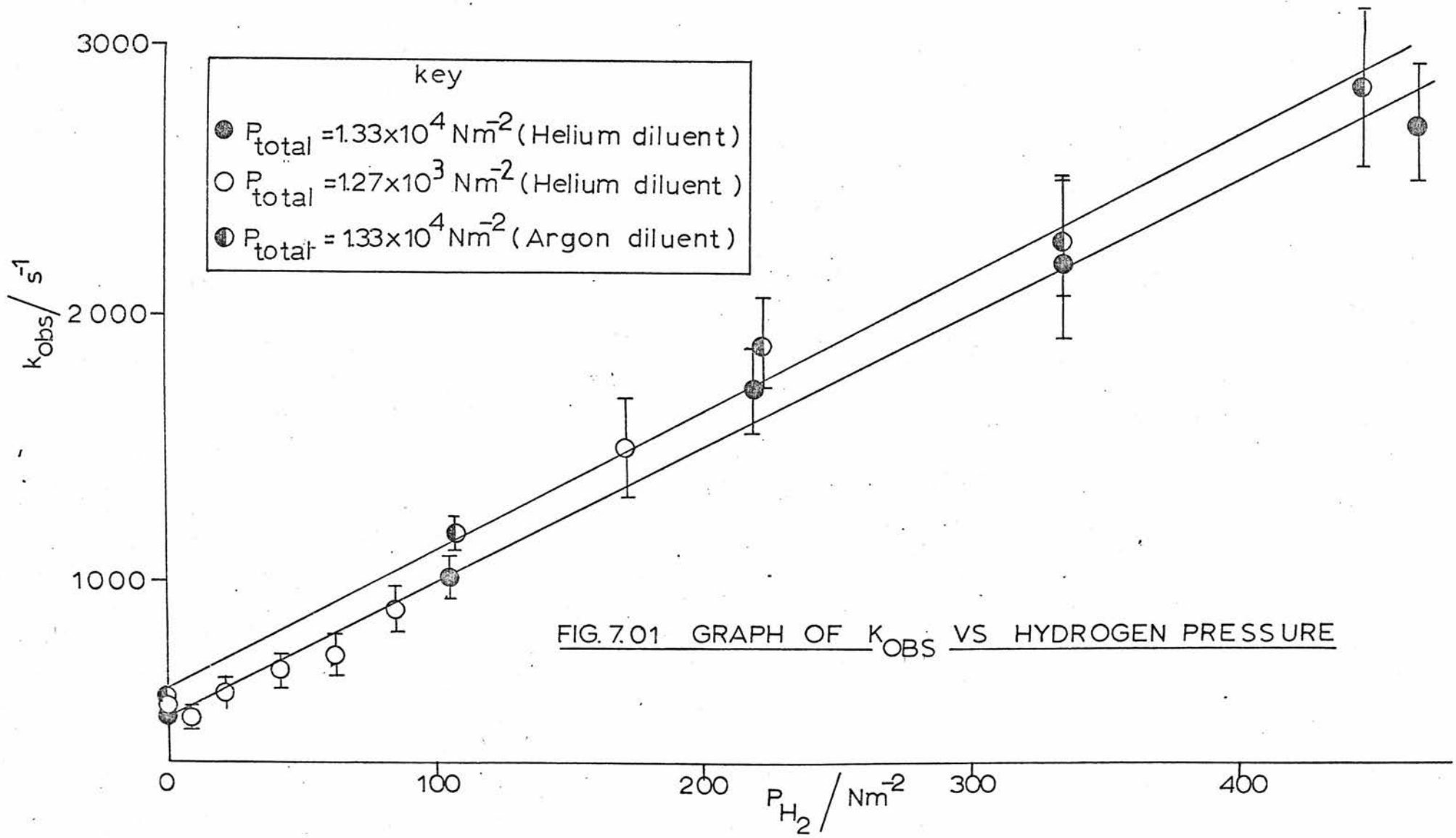

FIG. 7.01 GRAPH OF K_{OBS} VS HYDROGEN PRESSURE

Table 7.01

Rate Constants for Reaction with H_2

Investigator	T/K	P_{total}/Nm^{-2}	Rate Constant k/cm^3 molecule^{-1} s^{-1}	Ref.
Boden and Thrush	687	2.0×10^2	$<3.3 \times 10^{-13}$	16
	295	2.0×10^2	$<4.9 \times 10^{-14}$	†
Schacke et al.	295	7.7×10^2	$(1.17 \pm 0.39) \times 10^{-14}$	22
This work (He diluent)	295	1.27×10^3	$(3.97 \pm 0.41) \times 10^{-14}$	-
This work (He diluent)	295	1.33×10^4	$(3.60 \pm 0.18) \times 10^{-14}$	-
This work (Ar diluent)	295	1.33×10^4	$(3.73 \pm 0.17) \times 10^{-14}$	-

† calculated from the limit given by Boden and Thrush[16] using the activation energy of 29 kJ mol^{-1} given by Hartel and Polanyi[27].

$$CN + H_2 \longrightarrow HCN + H \ , \ \Delta H^{\circ} = -64.5 \text{ kJ mol}^{-1} \qquad (1.26)$$

The rate constants obtained at both high and low total pressures using helium diluent are in excellent agreement. So also are the rate constants for both argon and helium diluents at 1.33×10^{4} Nm^{-2} total pressure. These results confirm that feeding of the $CN(X^2\Sigma, v''=0)$ level by vibrational relaxation is unimportant under the experimental conditions chosen for this work. Had feeding been important, the rate constants for removal of CN would have been different for the two diluents, argon and helium, which have different vibrational relaxation efficiencies.

Previously determined rate constants for reaction 1.26 are also given in table 7.01. The results obtained here agree well with the upper limit proposed by Boden and Thrush[16] but are about a factor of three greater than the value given by Wolfrum and coworkers.[22,23] It is likely that feeding of the $CN(X^2\Sigma, v''=0)$ level was occurring at the short delay times observed by Wolfrum and coworkers, especially since their system allowed photolysis by shorter wavelength radiation ($\lambda > 165$ nm) than the quartz vessel used in this study. This would allow relatively more vibrationally excited CN radicals to be produced in their system, leading to a significant increase in the feeding of lower vibrational levels by relaxation.

2. Reaction of $CN(X^2\Sigma, v''=0)$ with CH_4

The reaction of CN radicals with methane was studied at two total pressures, 1.33×10^{4} and 1.27×10^{3} Nm^{-2}, using helium diluent. The observed rate coefficients are plotted against methane partial pressure in fig. 7.02. Table 7.02 gives the rate constants obtained, together with previous values.

$$CN + CH_4 \xrightarrow{k_{28}} HCN + CH_3 \quad \Delta H^{\circ} = -61.9 \text{ kJ mol}^{-1} \qquad (1.28)$$

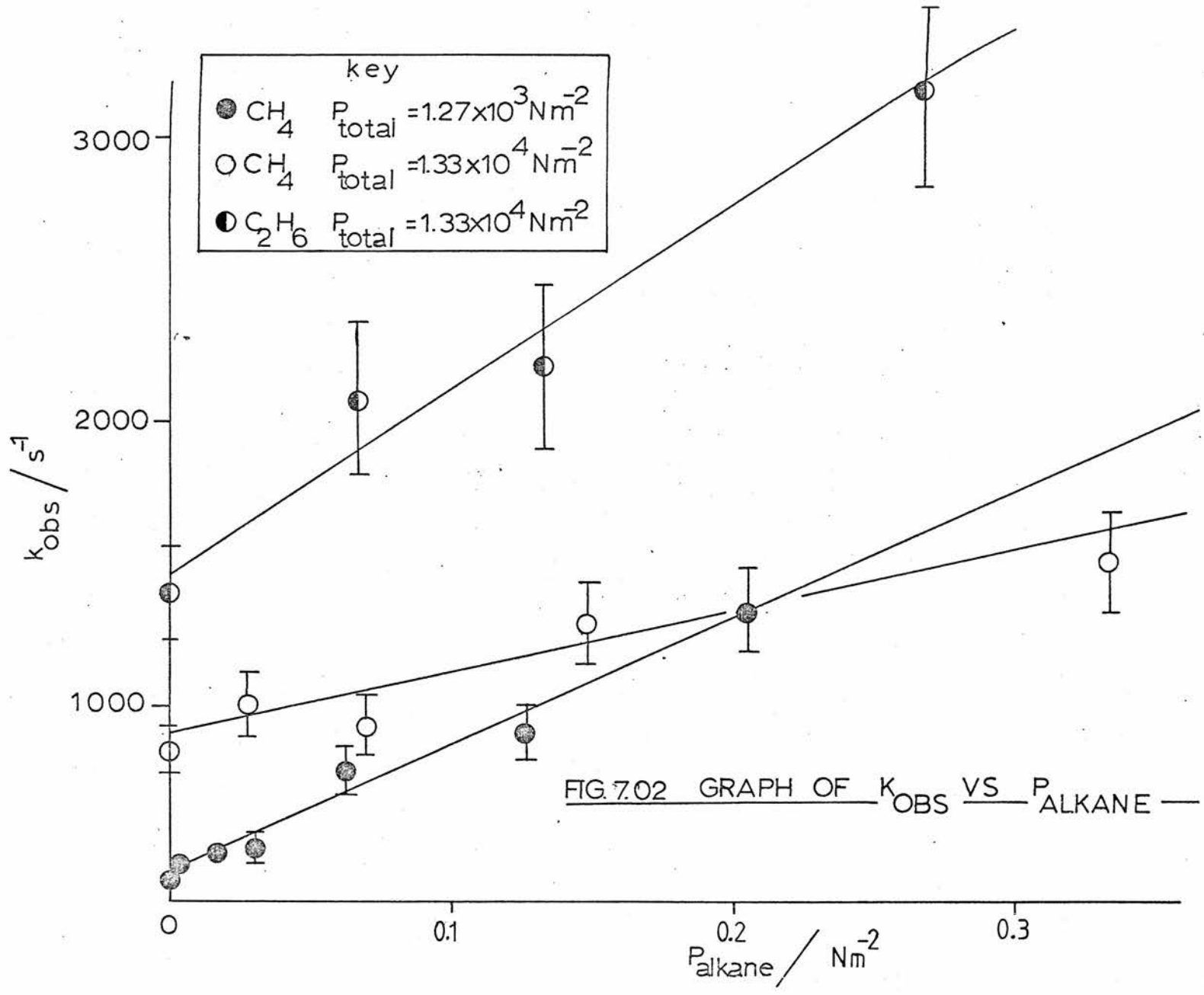

FIG. 7.02 GRAPH OF K_{OBS} VS P_{ALKANE}

Table 7.02

Rate Constants for Reaction with Methane

Investigator	T/K	P_{total}/Nm^{-2}	Rate Constant k/cm^3 molecule^{-1} s^{-1}	Ref.
Boden and Thrush	687	2.0×10^2	$<1.2 \times 10^{-12}$	16
	295	2.0×10^2	$<1.7 \times 10^{-13}$	†
Bullock and Cooper	300	$\sim 10^5$	$(7.40 \pm 0.16) \times 10^{-13}$	19
Schacke et al.	295	6.0×10^2	2.8×10^{-13}	22
This work	295	1.27×10^3	$(3.21 \pm 0.23) \times 10^{-12}$	-
This work	295	1.33×10^4	$(1.49 \pm 0.31) \times 10^{-12}$	-

† calculated from the limit given by Boden and Thrush[16] using the activation energy of 8.3 kJ mol^{-1} given by Bullock and Cooper[19].

The rate constants obtained at high and low total pressure differ by a factor of ~ 2. They were calculated on the assumption that the Beer-Lambert coefficient, γ, was the same at both pressures. The broadening of the CN absorption lines increases with pressure and as the value of $\gamma = 0.57$ used in this work was determined for 1.33×10^4 Nm^{-2} total pressure, the high pressure rate constant of $(1.49 \pm 0.31) \times 10^{-12}$ cm^3 $molecule^{-1}$ s^{-1} will be the more exact value.

The results obtained in this work are again faster than the values obtained in previous studies which are given in table 7.02. The same explanation, given for the reaction of CN with molecular hydrogen, is offered here for the methane results i.e. feeding of the $CN(X^2\Sigma, v''=0)$ level was important in previous studies.

3. Reaction of $CN(X^2\Sigma, v''=0)$ with C_2H_6

The observed rate coefficients for the following reaction of CN with ethane are plotted against ethane partial pressure in fig. 7.02 for a total pressure of 1.33×10^4 Nm^{-2}.

$$CN + C_2H_6 \xrightarrow{k_{31}} HCN + C_2H_5 \,, \quad \Delta H^\circ = -88.2 \text{ kJ mol}^{-1} \qquad (1.31)$$

The rate constant obtained is given in table 7.03 along with previous values.

Again the results obtained in this work are consistently higher than those obtained by other workers for the reasons given in the previous two sections.

4. General Discussion

The reactions of CN with H_2, CH_4 and C_2H_6 and the halogen-like behaviour of the CN radicals have been discussed by previous workers and their conclusions are reviewed in chapter 1.

Table 7.03

Rate Constants for Reaction with Ethane

Investigator	T/K	P_{total}/Nm^{-2}	Rate Constant k/cm^3 molecule^{-1} s^{-1}	Ref.
Bullock and Cooper	300	$\sim 10^5$	$(2.41 \pm 0.17) \times 10^{-11}$	19
Schacke et al.	295	5.9×10^2	1.2×10^{-11}	22
This work	295	1.33×10^4	$(4.57 \pm 0.59) \times 10^{-11}$	-

Table 7.04 gives an indication of the relative activation energies for the abstraction of H atoms from H_2, CH_4 and C_2H_6 by F, Cl and CN radicals. The activation energies for the CN reactions range between the values for the corresponding Cl and F atom reactions.

Table 7.04

Activation Energies (kJ mol^{-1})

Reactant	Radical			Ref.
	Cl	CN	F	
H_2	22.9		7.2	31
		29		27
		22.2		22
CH_4	16		5.0	31
		12.1		22
		8.3		19
C_2H_6	4.3		1.2	31
		<1.6		19

The rate constant ratio, k_{31}/k_{28}, for the ethane and methane reactions, has been calculated by several researchers and the values obtained are summarised in table 7.05. These ratios are all in good agreement except for the value of Goy et al.[30] which is low. This may be attributed to secondary processes occurring in their steady state photolysis experiments, which were not important in pulsed systems.

Table 7.05

Rate Constant Ratio

Investigators	k_{31}/k_{28}	Ref.
Goy et al.	24.4	30
Bullock and Cooper	37.5	17
Schacke et al.	32.4	22
This work	30.7	-

CONCLUSIONS

The rate constants obtained in this work are greater than previous values. In this work, the removal of $CN(X^2\Sigma, v''=0)$ was studied in the absence of higher vibrational levels. In previous work however, the feeding of the $CN(X^2\Sigma, v''=0)$ level by vibrational relaxation may have caused a reduction in the rate constants for the net removal of $CN(X^2\Sigma, v''=0)$ radicals.

CHAPTER 8

CHAPTER 8

REACTION OF $CN(X^2\Sigma, v''=1)$ WITH H_2

INTRODUCTION

A brief summary of the work done on the reactions of vibrationally excited $CN(X^2\Sigma)$ radicals was given in chapter 1. Two conflicting reports have been given on the effect of vibrational excitation on the reaction of $CN(X^2\Sigma, v''=n)$ with molecular oxygen, which is 14.0 kJ mol^{-1} exothermic for a Boltzmann distribution of vibrational levels at 298 K. Bullock and Cooper[18] found that the rate constants increased with n, whereas Schacke et al.[21] observed a decrease.

When the experimental uncertainties are taken into account, neither of the above trends is particularly convincing, especially since no allowances were made for the effects of vibrational relaxation.

It would have been useful to resolve the situation for this reaction, but the signal to noise ratio of the decay signal of $CN(X^2\Sigma, v''\geq 1)$ would have been too low to obtain meaningful results for this fast reaction.

Hence the reaction of CN radicals with molecular hydrogen was chosen to study the effect of CN vibrational energy on reaction rates, as moderate decay rates and good signal to noise ratios were obtainable.

However, before discussing the results and implications of these experiments, it is necessary to describe the production of $CN(X^2\Sigma, v''=1)$, and the determination of the relative population of the $v''=1$ and $v''=0$ levels.

Production of $CN(X^2\Sigma, v''=1)$

The Spectrosil and not the quartz reaction vessel was used in this work to increase the initial population of $CN(X^2\Sigma)$ radicals in the v"=1 level relative to the v"=0 level, for a flash energy of 125 J. The ratio of the initial populations, P(v"=1)/P(v"=0), will be referred to as R_0.

For helium/cyanogen mixtures containing a fixed partial pressure of cyanogen (26.7 Nm^{-2}), the total pressure was varied between 1.33×10^2 and 1.33×10^4 Nm^{-2}, and the maximum value for R_0 was estimated to occur at a total pressure of 2.67×10^3 Nm^{-2}. Hence this total pressure was chosen for this present work.

For a mixture containing 26.7 Nm^{-2} of cyanogen at a total pressure of 2.67×10^2 Nm^{-2}, the absorption by $CN(X^2\Sigma, v''=0)$ at 388.1 nm was initially saturated for the Spectrosil vessel. This had no effect on the measured kinetics since the data used corresponded to absorptions of <25%. However, it did make the determination of R_0 impossible for this mixture.

To overcome this problem, R_0 was determined for cyanogen/helium mixtures at the same total pressure but containing less cyanogen. The values of R_0 obtained are given in table 8.01 along with the cyanogen pressures. From these identical results, it is reasonable to assume that R_0 for a cyanogen partial pressure of 26.7 Nm^{-2} will be the same i.e. $R_0 \simeq 0.10$. Details of the calculation of the R_0 values are given in appendix V.

Table 8.01

Relative Vibrational Population at time t=0

Cyanogen Pressure/Nm^{-2}	Optical Density (arbitrary units)		$R_0 = \frac{P(v''=1)}{P(v''=0)}$ *
	388.1 nm v" = 0	386.8 nm v" = 0 and 1	
3.33	81.5	54.6	0.09±0.02
6.67	151	102	0.10±0.02
13.3	99.5	67.4	0.10±0.02

* see Appendix V

Although the value of R_0 determined here is only approximate, it is significantly greater than the value $R_0<0.05$, estimated in chapter 4 for the quartz vessel.

RESULTS

Reaction of $CN(X^2\Sigma,v''=1)$ with H_2

To monitor the reaction of $CN(X^2\Sigma,v''=1)$ with molecular hydrogen, the time dependence of the CN absorption at 385.7 nm was observed. This wavelength corresponds to the overlap of the (1,1) R branch and the (2,2) P branch of the CN violet system[95]. No vibrational levels with v">1 were detected, so the absorption signal at 385.7 nm was strictly due to $CN(X^2\Sigma,v''=1)$.

The $C_2N_2/He/H_2$ mixtures used to study the removal of $CN(X^2\Sigma,v''=1)$ in the presence of molecular hydrogen contained a fixed partial pressure of C_2N_2 (26.7 Nm^{-2}) at a fixed total pressure of 2.67×10^2 Nm^{-2}. A plot of the observed rate coefficients against hydrogen partial pressure is given in fig. 8.01. The rate constant† obtained for the removal of $CN(X^2\Sigma,v''=1)$ was $(6.80\pm0.45)\times10^{-14}$ cm^3 $molecule^{-1}$ s^{-1}.

† All the rate constants given in this chapter are the corrected values i.e. the Beer-Lambert coefficient, γ, has been taken into account.

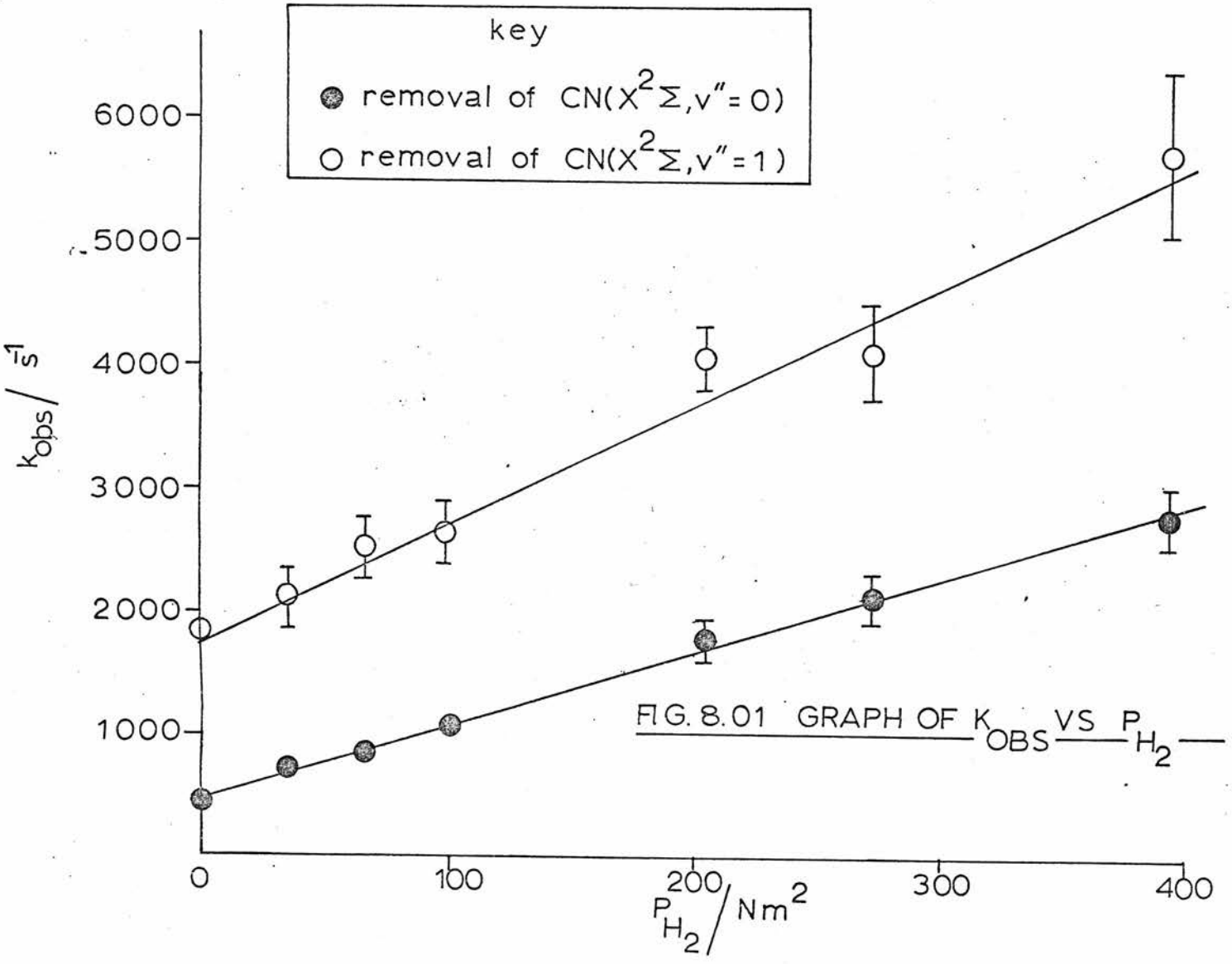

FIG. 8.01 GRAPH OF K_{OBS} VS P_{H_2}

Reaction of $CN(X^2\Sigma,v''=0)$ with H_2

This series of experiments was carried out to determine the rate constant for the removal of $CN(X^2\Sigma,v''=0)$ in the presence of H_2 for the Spectrosil vessel. It will be of interest to compare the value obtained with the rate constants given in chapter 7 for the quartz vessel.

The reaction mixtures were identical to those described in the previous section, and the decay of the CN (0,0) P branch at 388.1 nm was monitored. The observed rate coefficients are plotted against the partial pressure of molecular hydrogen in fig. 8.01. A rate constant of $(4.29\pm0.11)\times10^{-14}$ cm^3 $molecule^{-1}$ s^{-1} was calculated from the gradient of this plot. This agrees well with the value of $(3.60\pm0.18)\times10^{-14}$ cm^3 $molecule^{-1}$ s^{-1} obtained using the quartz reaction vessel (chapter 7).

DISCUSSION

The following reactions must be considered when interpreting the results obtained in this work.

$$CN(v''=0) + H_2 \longrightarrow HCN + H \qquad (8.01)$$

$$CN(v''=1) + H_2 \longrightarrow HCN + H \qquad (8.02)$$

$$CN(v''=1) + M \longrightarrow CN(v''=0) + M \qquad (8.03)$$

The net removal of $CN(v''=1)$ contains a contribution from reactions 8.02 and 8.03. The removal of $CN(v''=0)$ occurs by reaction 8.01 and $CN(v''=0)$ is produced by reaction 8.03. Any vibrational relaxation, by collision of $CN(v''=1)$ with cyanogen and helium, would contribute equally to all the observed rate coefficients for the range of hydrogen pressures given in fig. 8.01, and

would not therefore affect the measured rate constants for CN removal.

The measured rate constant for the net removal of $CN(X^2\Sigma, v''=1)$ may however contain contributions from both relaxation by H_2, as well as reaction with H_2. It is therefore only possible to give an upper limit for the ratio of the rate constants for removal of CN(v''=1) and CN(v''=0) by reaction with H_2. This ratio, $k_{v''=1}/k_{v''=0}$ was calculated to be 1.7 from the rate constants determined in this chapter.

The contribution of relaxation by H_2 to the rate constant for the removal of CN(v''=1) may be quite substantial. However, since the initial population of the v''=1 level was only 10% of that of the v''=0 level, the contribution by feeding to the decay of CN(v''=0) will fall within the uncertainty in the rate coefficient for CN(v''=0) removal, and should therefore be negligible. In fact, the rate constant for the removal of CN(v''=0) in the presence of H_2, obtained in this chapter, agrees well with the value obtained under conditions where the population of excited vibrational levels was zero (chapter 7).

Vibrational relaxation of CN(v''=1) by H_2 is likely to occur by vibrational to rotational energy transfer (V→R), similar to vibrational relaxation of CO by H_2, which has been discussed by Sharma and Kern[152]. The following equations show the energy mismatch in the two systems, ΔE_T, for no change in rotational energy of CO or CN.

$$CO(v''=1) + H_2\ (j=2) \longrightarrow CO(v''=0) + H_2\ (j=6) + 88\ cm^{-1} \qquad (8.04)$$

$$CN(v''=1) + H_2\ (j=2) \longrightarrow CN(v''=0) + H_2\ (j=6) - 12\ cm^{-1} \qquad (8.05)$$

The energy mismatch in the CN case is small, and providing the long range multipolar interactions between H_2 and CN are favourable, energy transfer (V→R) from CN to H_2 is likely to be very efficient.

By repeating the experiments in this chapter using ortho and para hydrogen, it may be possible to detect a change in the overall rate constant for the removal of CN(v"=1). If so, the relative contributions of relaxation and reaction may be quantitatively determined.

The intercept in fig. 8.01 is greater for the removal of $CN(X^2\Sigma,v"=1)$ than for removal of $CN(X^2\Sigma,v"=0)$. This suggests that vibrational excitation of CN radicals may increase the efficiency of their reaction with cyanogen molecules and with impurities in the mixtures. Alternatively, relaxation effects may be important. It is not however possible to quantitatively separate these contributions using the present data.

CHAPTER 9

CHAPTER 9

CN RADICALS IN FLAMES

The work presented in this chapter was carried out at Thornton Research Centre, Shell Research Ltd., under the supervision of Dr. C. Morley of the Combustion Division.

INTRODUCTION

In the study of combustion processes, apart from producing more efficient burners and internal combustion engines, it is important to consider the environmental aspects of exhaust gases from such processes. Combustion of nitrogenous fuels, e.g. coal and heavy fuel oils, is known to produce nitric oxide which can, in some conditions, react to form photochemical smog.[4]

Certain radicals[130] e.g. CN, CH, NH and OH, which have been observed spectroscopically in flames, are thought to participate in the kinetics of the production and removal of NO in combustion processes. It is therefore of value to study the elementary reactions of such radicals in flames, and to determine the extent to which specific radicals are involved in the production of NO. This information could then be used to devise a method of minimising NO production.

The aim of the work carried out at Thornton Research Centre was to gain more information about the role of CN radicals in the nitrogen chemistry of flames, and to provide useful rate constants for computer modelling of combustion processes. The technique of pulsed resonance fluorescence, which had not previously been used to study flames, was chosen for this study of the burnt gas region of premixed, fuel-rich ethylene flames.

A brief description of flames and their nitrogen chemistry will now be given along with a resume of the experimental technique used in this work.

Flames

Several good descriptions of flames and their characteristics are available. In particular, texts by Gaydon and Wolfhard[131], Fenimore[132], and Fristrom and Westenberg[133] are useful. The spectroscopy of flames is discussed in detail by Gaydon[134] and Lewis and von Elbe[135].

The most useful flame for kinetic work is the flat premixed laminar flame[136] where the flow of gases is essentially unidirectional and uniform across a horizontal section through the flame. Only in this type of flame does the vertical height above the burner surface correspond to the time of flow of gases from the burner. Hence kinetic data may be obtained from time resolved concentration measurements of the various species present in the flame. This easy method of time resolution is not applicable to conical laminar flames, turbulent flames, and diffusion flames which, as a result, are of limited value for kinetic experiments.

For the above reasons, a flat laminar flame was used in this work. The various zones of this type of flame are illustrated in fig. 9.01. The pre-reaction zone, reaction zone and post-reaction zone are common to most flames. The secondary reaction zone is a diffusion flame and is therefore useless for kinetic work. It occurs in fuel-rich flames due to air entrainment.

Although it is difficult to define the extent of the reaction zone of a flame, it is $\sim 10^{-2}$ cm thick for a flat laminar hydrogen flame[136]. The region of interest in this work is the post-reaction zone which can extend for several centimetres making it more amenable

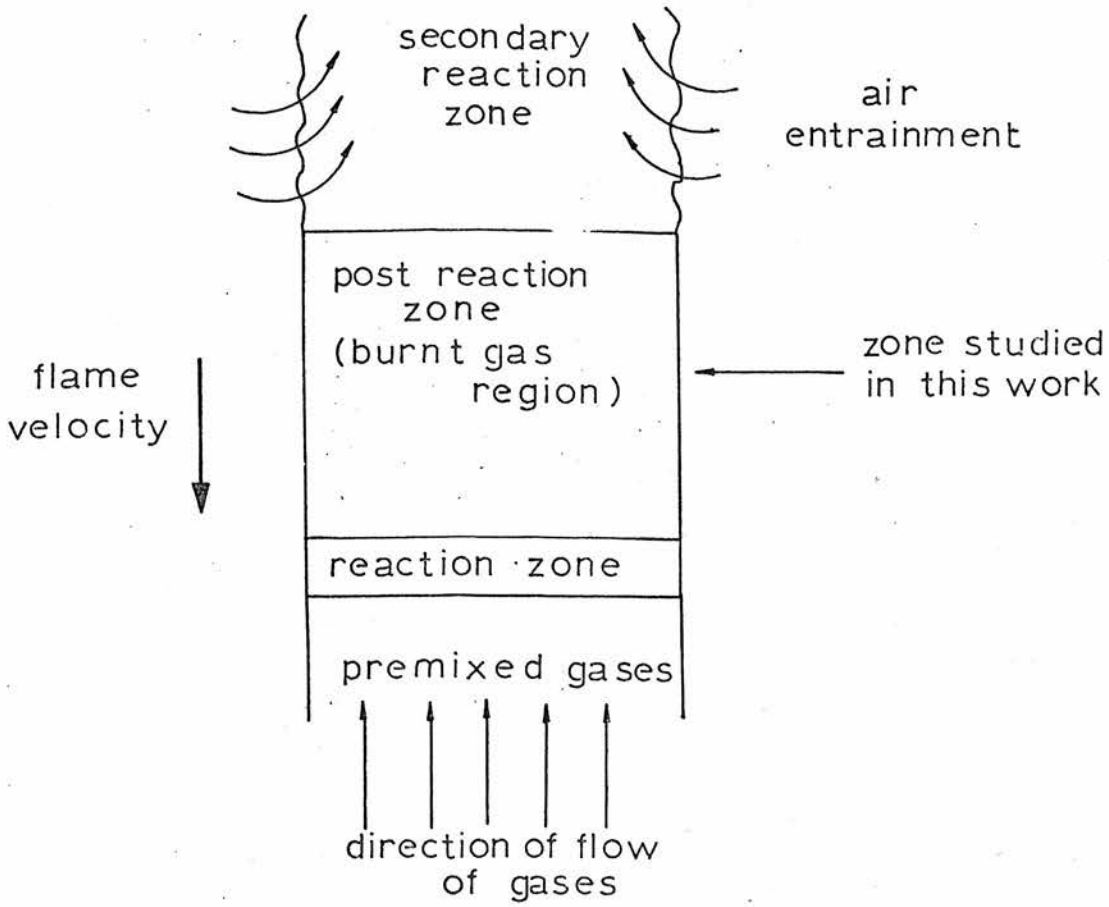

FIG. 9.01 DIAGRAMMATIC REPRESENTATION OF A FLAT PREMIXED LAMINAR FLAME

to study.

The composition and temperature of a flame may be determined experimentally by methods outlined by Gaydon and Wolfhard[131] and Fristrom and Westenberg[133] . Alternatively, the flame composition and temperature may be calculated from thermochemical data, provided the premixed gas composition is known. This is a complicated procedure however, as composition and temperature are interdependent.

A model calculation of flame composition and temperature is given by Gaydon and Wolfhard[131]. The method is essentially an iterative process based on the work of Damköhler and Edse[137] . For the calculation, the flame is assumed to be adiabatic,and initially a flame temperature is estimated. Successive approximations are made till the flame temperature correlates with the thermochemical data for the calculated composition at that temperature. It is also possible to calculate equilibrium concentrations at temperatures below the adiabatic temperature.

In most atmospheric flames, there is both vibrational and rotational relaxation of the flame gases by the time they leave the reaction zone. Hence temperature has a real meaning in the region of interest in this study i.e. Boltzmann energy distributions exist.

Flame Nitrogen Chemistry

Nitric oxide is produced in flames from two sources, namely molecular nitrogen from air and from nitrogen compounds in the fuel.

The fixation of molecular nitrogen in flames has been studied extensively and the accepted mechanism for lean or stoichiometric fuel-air mixtures, originally suggested by Zeldovich[2] , is given below.

$$O + N_2 \longrightarrow NO + N \qquad (9.01)$$

$$N + O_2 \longrightarrow NO + O \qquad (1.02)$$

An extension of this mechanism, including additional reactions for fuel-rich flames, is discussed in a review by Bowman [130].

For fuel-rich flames, the following additional alternative mechanisms were proposed by Fenimore [138] to explain the rapid production of NO from molecular nitrogen in the reaction zone ('prompt NO').

$$CH + N_2 \longrightarrow HCN + N \qquad (9.02)$$

$$C_2 + N_2 \longrightarrow 2CN \qquad (9.03)$$

Subsequent oxidation of HCN and CN, which are in fact equilibrated [139], leads to the formation of NO (this will be discussed shortly). The four centre reaction of C_2 with N_2 is unlikely, and in fact reaction 9.02 was later favoured by Hayhurst and McLean [140] in their survey of the reactions of hydrocarbon fragments with N_2.

The conversion of fuel nitrogen to nitric oxide has been a more difficult problem to solve. Fenimore [141] showed that the relative amounts of NO and N_2 produced from fuel nitrogen in fuel-rich flames varied. In general, the yield of NO was greater for leaner, hotter flames with low fuel nitrogen concentrations. To explain this, Fenimore proposed that all fuel nitrogen species could form the same intermediate I, which could react with a nitrogen-free radical species R to give NO, or react with NO to give N_2. Morley [139] has shown that for rich hydrocarbon flames, fuel nitrogen is converted quantitatively to HCN, regardless of the nature of the nitrogen compound. Thus HCN may be regarded as a precursor to the intermediate I suggested by Fenimore [141].

Since HCN is produced from both atmospheric and fuel nitrogen in fuel-rich flames, its subsequent oxidation is of interest, and a study of the processes involved may lead to the identification of intermediate I. As mentioned above, HCN and CN are equilibrated in most flames by the following reaction,

$$CN + H_2 \rightleftharpoons HCN + H \qquad (1.26)$$

which means that the removal of a CN radical is equivalent to the removal of an HCN molecule.

Morley[139] studied the decay of HCN in the burnt gas region of fuel-rich hydrocarbon flames. He showed that the removal of HCN, produced from fuel nitrogen in the reaction zone, is consistent with the following rate determining step ($2300 \leqslant T \leqslant 2560$ K).

$$CN + OH \longrightarrow NCO + H \qquad (9.04)$$

Rapid removal of NCO may then occur via the following reactions, resulting in the formation of NH_x species.

$$H + NCO \longrightarrow NH + CO \qquad (9.05)$$

$$H_2 + NCO \longrightarrow NH_2 + CO \qquad (9.06)$$

It is possible however that other mechanisms may dominate for the removal of CN at lower temperatures. Haynes[142] suggests that at temperatures below 2300 K, the removal of HCN by reaction with OH radicals may be the dominant process, leading to the formation of NH_x species.

The final step in the oxidation of HCN is the conversion of NH_x to NO and N_2. Nadler et al.[143] have shown that NH_x species ($x = 1, 2, 3$) can equilibrate by H atom transfer reactions. Thus intermediate I may be regarded as a composite of all NH_x species. The conversion of NH_x to give both N_2 and NO may occur as follows.

$$NH + OH \longrightarrow N + H_2O \qquad (9.07)$$

$$N + OH \longrightarrow NO + H \qquad (9.08)$$

$$NH_2 + NO \longrightarrow N_2 + H_2O \qquad (9.09)$$

$$NH + NO \longrightarrow N_2 + OH \qquad (9.10)$$

$$N + NO \longrightarrow N_2 + O \qquad (9.11)$$

Resonance Fluorescence

The technique of resonance fluorescence simply involves the monitoring of fluorescence from an irradiated species, the wavelength of the exciting radiation and emitted radiation being the same. One of the first observations of this type of emission was for the mercury atom $6(^3P_1) \longrightarrow 6(^1S_o)$ line at 253.7 nm. Although a change in multiplicity occurs, the radiative lifetime of the excited state is short enough for the emission to be termed 'fluorescence'.[144]

For the technique to be effective, it is essential that the molecule studied does fluoresce, that the band system observed is well characterised and that a suitable exciting source is available. The fluorescence is usually monitored at right angles to the incident exciting radiation, so that the fluorescence signal is observed against zero background signal.

The technique of resonance fluorescence was used by Braun and Lenzi[145] to study the reaction of hydrogen atoms with olefines. More recently Brewer and Tellinghuisen[146] and Strain et al.[147] have studied iodine atom reactions using this technique. A refinement, described by Zare and coworkers[148,149], is the use of a laser to excite the species under observation. They used this system to study specific product states of BaO, produced from the reaction of barium atoms with molecular oxygen in a molecular beam experiment.

The major advantage of the above technique is that it is generally more sensitive than absorption. This is because the fluorescence signal is measured against zero background, whereas the absorption signal is observed as a small decrease in a large background signal. Hence a better signal to noise ratio is expected.

In this study of flames however, some of the advantage is lost because spontaneous emission from the flame does provide a background

signal, from which the fluorescence signal must be separated.

The use of a pulsed fluorescence system was an attempt to compensate for the reduced signal to noise ratio due to the spontaneous emission, by increasing the fluorescence signal measured, relative to the spontaneous emission signal. An integrator to do just this is described in the experimental section.

EXPERIMENTAL

The layout of the pulsed resonance fluorescence system used in this flame study is illustrated in fig. 9.02. It consists of a burner, a flash lamp to excite the radicals in the flame, and at right angles to it, a monochromator and photomultiplier to detect the fluorescence.

The burner[139] was a Meker type, made up of bundles of capillary tubes (0.5 mm diam.). Flames of radius 10 or 20 mm could be produced with a shield of inert gas to prevent air entrainment. A burner of this design produces a stable, flat laminar flame of uniform velocity distribution across the burner. To aid flame stability, the burner was water cooled. The vertical height of the burner could be adjusted accurately via a motor drive unit.

Out of three systems tested, the flow flash lamp shown in fig. 9.02 was chosen as the source of CN ($B^2\Sigma - X^2\Sigma$) emission to excite the CN radicals in the flames studied. Two other systems, namely a resonance lamp similar to the one described in chapter 2, and a Garton lamp were found to lack the required intensity.

The flow flash lamp consisted of a 1 mm i.d. quartz capillary tube, tungsten electrodes, gas inlet and outlet points, and a bulb to dissipate the pressure rise when the lamp was fired. The windows were made from microscope slides which gave good transmission in the spectral region of interest. The working pressure of the lamp was typically $(1 - 7) \times 10^2$ Nm^{-2}.

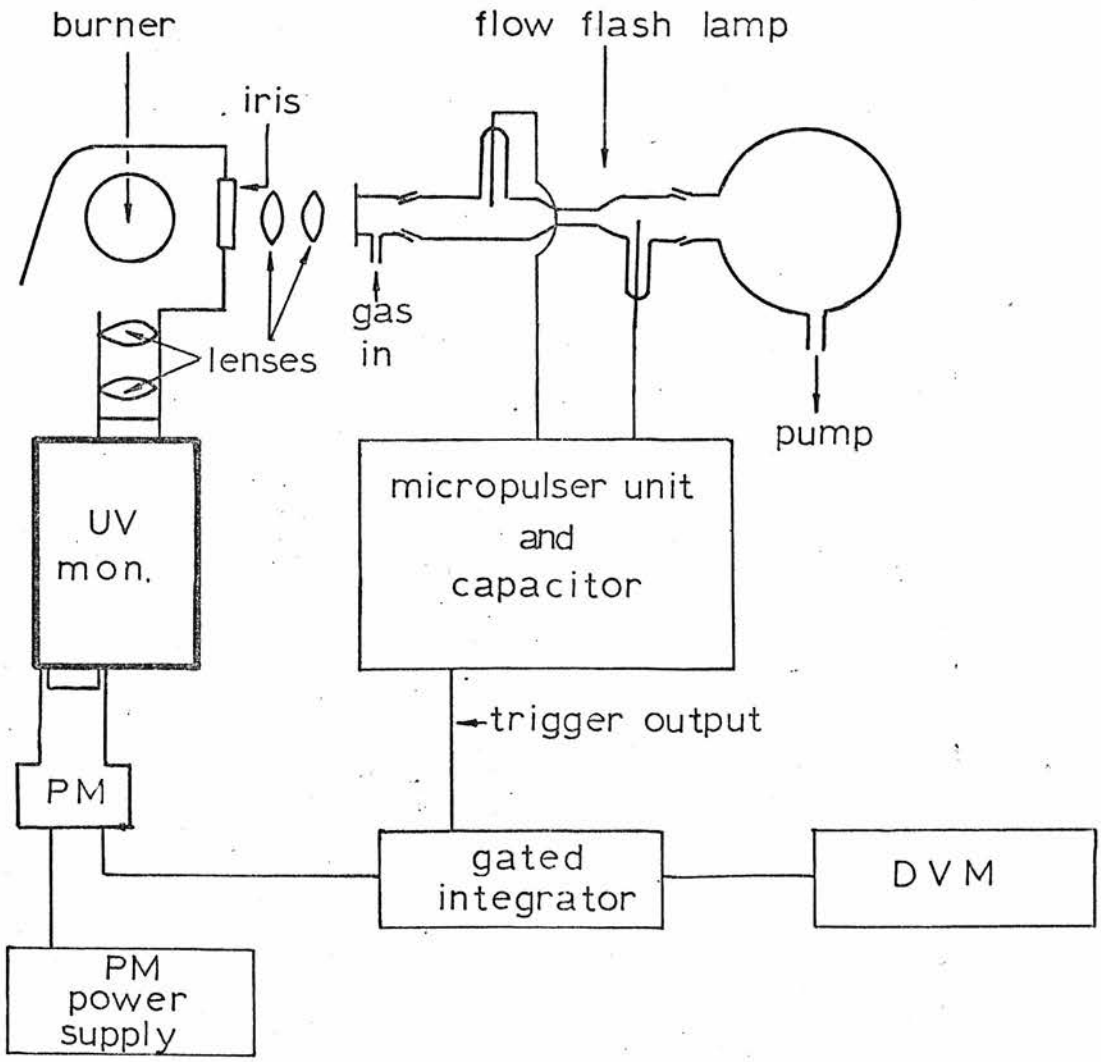

DVM: digital voltmeter
PM : photomultiplier

FIG.9.02 DIAGRAM OF RESONANCE FLUORESCENCE SYSTEM USED TO STUDY FLAMES

A micropulser (Xenon Corp. Model 368) with a 1 μF capacitor charged typically to 3 - 4 kV was used to power the lamp. Although its range was 3 - 60 pulses/s (maximum energy/pulse = 5 J, maximum power output = 300 W), a flash rate of 3 pulses/s was used because pulsing became erratic at higher rates. The micropulser and flash lamp circuit were connected to a different earthing system to that used for the photomultiplier and detection equipment. This eliminated earth loops and electrical noise problems.

The spectral output of the flash lamp was photographed on a medium quartz spectograph, and fig. 9.03 shows a densitometer trace of the emission from the lamp in the CN violet region. Several bands are overlapped at the CN ($B^2\Sigma - X^2\Sigma$) $\Delta v = 0$ sequence, making it impossible to state categorically whether or not CN bands were present.

Wavelength resolution of the fluorescence signal was achieved using a Bausch and Lomb High Intensity UV Grating Monochromator. The signal was detected on a photomultiplier (EMI 9698 QB) mounted on the exit slit of the monochromator. The photomultiplier circuit was of conventional design except that no anode load resistor was used. A stabilised power supply (Farnell Instruments Ltd.) was used to operate the photomultiplier at 1450 V.

The signal from the photomultiplier was fed into a gated integrator. The circuit for this device, shown in fig. 9.04 was designed and built by Dr. C. Morley (Thornton Research Centre). Before the operation of the device is explained, it is necessary to show the derivation of the time interval for which the gate should be open.

Because of strong collisional quenching in the flames studied in this work, the decay half-life of CN fluorescence following an infinitely short excitation pulse would only be ~5 ns. Hence the

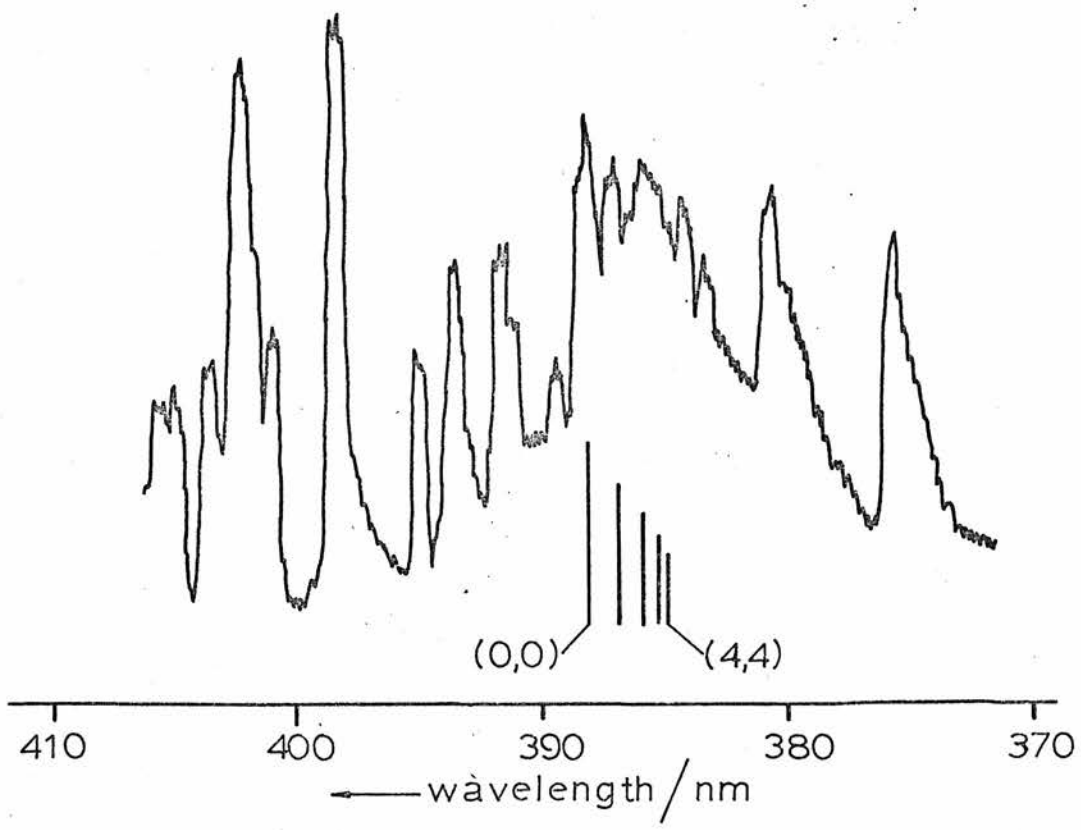

The band heads of the CN($B^2\Sigma - X^2\Sigma$) $\Delta v = 0$ sequence are shown above. For clarity, only the (0,0) and (4,4) band heads are labelled.

FIG. 9.03 DESITOMETER TRACE OF THE SPECTRAL OUTPUT OF THE PULSED FLASH LAMP

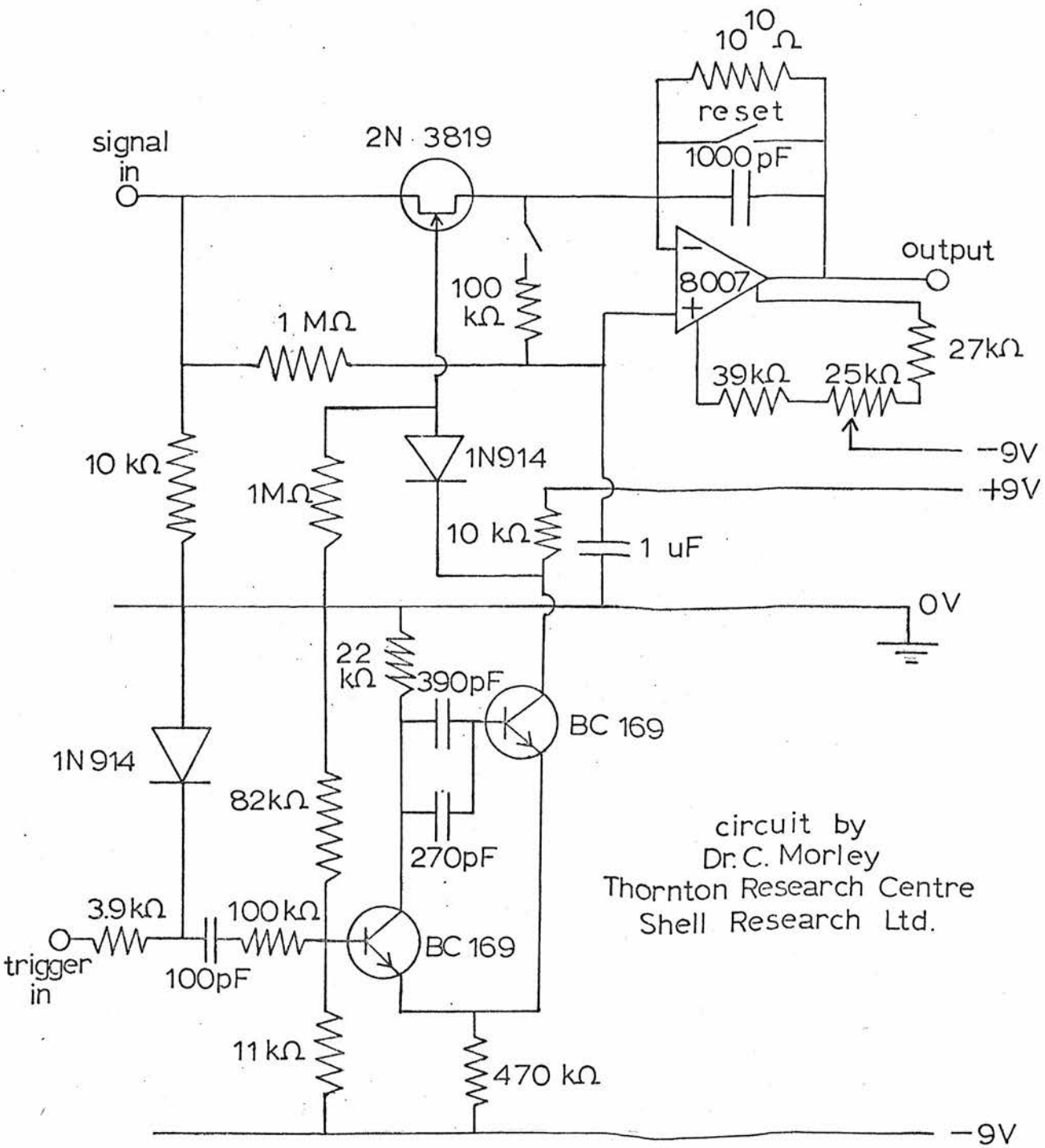

FIG. 9.04 GATED INTEGRATOR CIRCUIT

fluorescence decay follows closely the decay of the incident light from the flash lamp (half-life ~5 μs). A time interval of 10 μs is therefore sufficient time for the gate to be open.

The operation of the gated integrator is illustrated in fig. 9.05. The gate was triggered to open, at the beginning of an incident light pulse, for a period of ~10 μs. This occurred three times per second corresponding to the pulse rate of the flash lamp. The electronic circuit integrated the difference between the average current and the current flowing during the period for which the gate was opened. The result was displayed as a voltage on a digital voltmeter, the voltage being proportional to the fluorescence signal.

In this work, fluorescence was monitored at heights of between 3 and ~30 mm above the burner surface. This was achieved by raising and lowering the burner by the motor drive unit.

The lenses in the optical system were arranged to focus the radiation from the flash lamp at points vertically above the centre of the burner, and to focus the fluorescence onto the entrance slit of the monochromator. An iris was used to cut down excitation of the outer regions of the flame and black card was arranged about the apparatus to minimise scattered light.

Extreme care was taken in the alignment of the apparatus. This was checked regularly, as a small deviation from ideal conditions would have drastically reduced the detected fluorescence.

All the flames used in this work were burned as close to blow off as possible to minimise heat loss to the burner. A shield of argon was used to prevent entrainment of air. The premixed gases were at room temperature initially and combustion took place at atmospheric pressure. The characteristics of the flames studied in this work were available from previous research carried out at Thornton Research Centre, and are

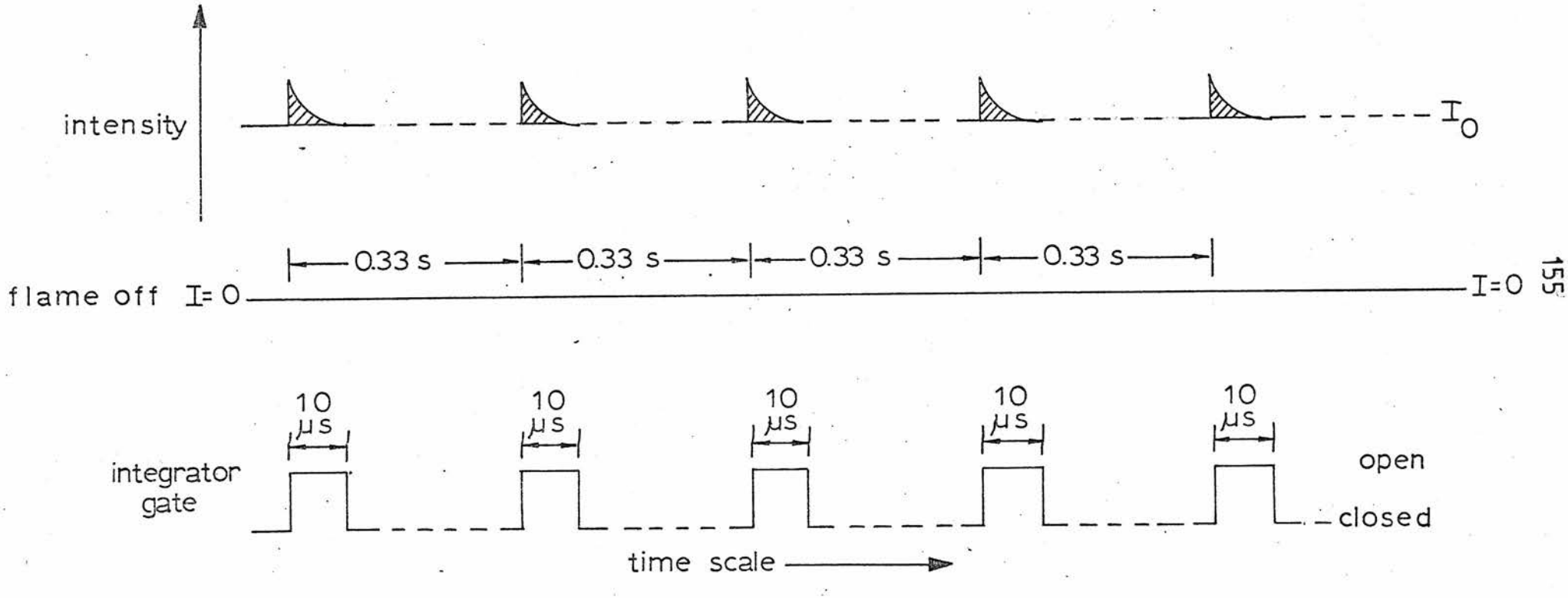

FIG.9.05 OPERATION OF GATED INTEGRATOR

I_0 corresponds to the background signal (thermal emission) produced by the flame. The shaded areas, corresponding to the fluorescence produced by each pulse of the flash lamp, are integrated by the device shown in fig. 9.04.

given in table 9.01. The flow rates of the gases, used directly from cylinders, were monitored on rotameters or capillary flow meters.

After a rough feasibility study, it was decided that OH resonance fluorescence would be more intense than that produced from CN, and so initially, the apparatus was set to monitor this signal. Later, attempts were made to monitor primarily CN radicals and then NH radicals. The wavelengths used to monitor each radical, OH, CN and NH corresponded to a maximum in the thermal emission from the flame, and also to a maximum in the flash lamp output when the appropriate gas mixture flowed through the lamp. The spectroscopic transitions involved and the gas mixtures used to monitor each radical are given in table 9.02.

RESULTS AND DISCUSSION

With maximum aperture of the iris and full slit height of the monochromator entrance slit (slit height = slit width as the monochromator was on its side), OH fluorescence could just be detected in the absence of an argon sheild round the flame. The signal was found to decrease if the argon shield was applied, suggesting that a large proportion of the OH signal was from OH at the periphery of the flame, formed by oxygen entrainment. Decreasing the iris aperture and slit height, so that only the centre of the flame was studied, decreased the observed fluorescence signal till it became of the order of the noise in the system.

No CN fluorescence was observed from any of the flames studied without the addition of NO to the flame. Nitric oxide was added by replacing the argon in the premixed gases by 1% NO in argon, thus maintaining a stable flame. Although the flow rate of 1% NO in argon was increased from zero to >31 $cm^3 s^{-1}$, the maximum fluorescence signal observed remained of the order of the noise in the system for all combinations of aperture and monochromator slit height.

Table 9.01

Flame Characteristics

Flame Number	Flame Temp /K	Velocity /cm s^{-1}	Burner Area /cm^2	Ratio of Premixed Gases C_2H_4: O_2 : Ar
SAR 3	2526	2.34×10^3	0.71	14.1:20.6:47.5
SAR 4	2401	1.22×10^3	0.71	14.1:20.6:60.0
SAR13	2525	1.17×10^3	0.71	7.2:16.7:80.0
†SAR20	2031	1.9×10^2	2.64	6.5:12.5:85.0

† not at equilibrium at the adiabatic flame temperature

Table 9.02

Spectroscopic Transitions and Flash Lamp Mixtures

Radical	Transition	λ/nm	Flash Lamp Mixture
OH	$A^2\Sigma \rightarrow X^2\Pi$	∿311	Ar bubbled through H_2O
CN	$B^2\Sigma \rightarrow X^2\Sigma$	∿388	Ar bubbled through MeCN
NH	$A^3\Pi \rightarrow X^3\Sigma$	∿336	Ar bubbled through a solution of NH_3 in H_2O

Attempts to observe NH fluorescence from flames with and without added NO were unsuccessful. Addition of NH_3 instead of NO could have increased the chances of observing NH by this technique.

Varying the flow rates and pressures of the gas mixtures in the flash lamp gave no marked change in the amount of fluorescence observed.

As a result of the work carried out with the pulsed resonance fluorescence apparatus, it was clear that too few fluorescence photons were being produced, and that the detection system was not sensitive enough to give a good signal to noise ratio. The reasons for this are well worth considering and give rise to a solution to the problem.

It is likely that all of the following factors contribute to some degree to the lack of fluorescence.

1. The intensity of the incident exciting radiation was too low. It is possible that pulsing the flash lamp could reduce the overall light output in the bands of interest compared with a continuous lamp, assuming the same average power is supplied to each lamp. Increasing the flash energy gave erratic pulsing and could not therefore be used to give an increase in intensity.
2. Mismatch of rotational temperatures of the radicals emitting in the flash lamp and the radicals absorbing in the flame may have been poor. This would lead to a low concentration of excited radicals in the flame, and a corresponding loss of fluorescence intensity.
3. As the flames were at atmospheric pressure, strong collisional

quenching would occur. The processes involved in the excitation and de-excitation of radical X may be written as follows, assuming the absence of intramolecular radiationless processes.

$$X + h\nu \xrightarrow{I_{abs}} X^* \qquad (9.12)$$

$$X^* \xrightarrow{A} X + h\nu \qquad (9.13)$$

$$X^* + M \xrightarrow{k_q} X + M \qquad (9.14)$$

I_{abs} is the intensity of light absorbed and k_q is the rate constant for collisional quenching. The emitted light intensity I_{em} (fluorescence) is then given by the following expression, where A is the Einstein coefficient for spontaneous emission.

$$I_{em} = \frac{A\, I_{abs}}{A + k_q[M]} \qquad (9.15)$$

For collisions with molecules other than inert gases, k_q is large (approaching the collision limit) for many excited states, and so fluorescence would be expected to be low in the atmospheric flames studied. It is possible to study flames at pressures of less than one atmosphere but this is less convenient.

4. The pulse rate was rather slow and increasing it would have given a better signal to noise ratio, but this caused erratic firing of the lamp. Hence the flash rate was restricted to 3 pulses/s.

A solution to the problem is to use a dye laser to excite the radicals in the flame. This would give an increase of several orders of magnitude to the intensity of the fluorescence. Also, it may be tuned to match the flame temperature of the radicals under investigation, thus optimising the absorption and hence fluorescence. The above advantages, together with the increased pulse rate obtainable, should

enable resonance fluorescence studies to be made of radicals in atmospheric flames without recourse to reduced pressure systems. It should also be possible to determine the rotational temperature of radicals in the flames.

Work with a dye laser system is now in progress at Thronton Research Centre and several radicals have been studied using this technique.

CHAPTER 10

CHAPTER 10

SUMMARY AND CONCLUSIONS

RESUME

The technique of resonance absorption spectroscopy and the use of a coaxial reaction vessel/flash lamp system, have led to the successful determination of new kinetic data for the reactions of CN radicals.

In particular, several new rate constants have been determined for the reactions of $CN(X^2\Sigma,v''=0)$ radicals, and suggestions have been put forward in an attempt to resolve the problem of conflicting literature values for previously measured rate constants.

By ensuring that the $CN(X^2\Sigma,v''=0)$ level was studied in the absence of higher vibrational levels, this work gives reliable rate constants for the reactions of $CN(X^2\Sigma,v''=0)$, in the absence of feeding by vibrational relaxation. In previous work, feeding may have been important, resulting in slower rate constants than obtained here.

The results of the new reactions studied in this work lend support to the proposal that CN radical reactions are analogous to the reactions of halogen atoms. Even the catalytic recombination of CN radicals by NO and CO shows the pseudo halogen nature of the CN radical. Both NO and CO catalysed recombination of CN have been explained by a mechanism analogous to that observed for catalysed halogen atom recombinations[113].

The measured rate constants were reasonable for such processes, and a small negative activation energy (a characteristic of such reactions) of -10 ± 4 kJ mol^{-1} was estimated for the NO catalysed

recombination. This activation energy was calculated from the rate constants of $(5.0\pm3.3)\times10^{-13}$ cm^3 $molecule^{-1}$ s^{-1} at 687 K given by Boden and Thrush[16], and $(5.28\pm0.27)\times10^{-12}$ cm^3 $molecule^{-1}$ s^{-1} at 295 K given in this work.

The reaction of CN with OCS was extremely fast ($k > 5\times10^{-11}$ cm^3 $molecule^{-1}$ s^{-1}) and was thought to form SCN. Spectroscopic evidence for this reaction product has recently been obtained by Addison et al.[151], who also produced evidence to support the above rate constant from a comparison of kinetic data for the CN + OCS and CN + C_2H_6 reactions.

CN radicals were also observed to undergo a hydrogen atom exchange reaction with hydrogen chloride, forming the molecule HCN, which may itself be regarded as a pseudo hydrogen halide.

$$CN + HCl \longrightarrow HCN + Cl \qquad (6.04)$$

$$\text{c.f.} \quad F + HCl \longrightarrow HF + Cl \qquad (6.06)$$

The study of the formation of cyanogen by the reaction of CN with HCN was of particular interest, as it led to the determination of the heat of formation of CN radicals ($\Delta H^\circ_{f_{295}}$ (CN) = 418 kJ mol^{-1}). In the light of more recent experimental values, this result supports the need for a revision of the value quoted in the JANAF tables[111].

The study of the effect of vibrational excitation, on the efficiency of the reaction of $CN(X^2\Sigma)$ radicals with molecular hydrogen, yielded an upper limit of $k_{v''=1}/k_{v''=0} = 1.7$. The rate constant, $k_{v''=1}$, for the removal of $CN(X^2\Sigma, v''=1)$ contains contributions from both reaction with H_2 and relaxation by H_2 (V→R). It was not possible to assess the relative contributions of each from the present data.

The work carried out at Thornton Research Centre was useful in determining the limitations of the resonance fluorescence technique used to study CN radicals in flames. This work indicated that a more intense source of exciting radiation was essential, and in fact a dye laser system was later chosen and is now in operation at Thornton Research Centre.

FUTURE EXPERIMENTS AND IMPROVEMENTS

Before the rate constants determined in this work can be used in flame modelling calculations, it is essential that extensive temperature dependence work is carried out to obtain the activation energies. This may be accomplished by using a modified form of the apparatus shown in fig.2.04, described by Smith and Zellner[150], designed for temperatures below ~300 K. For studies at much higher temperatures (2000-3000 K), it would be necessary to study CN radicals in flames or in shock tube experiments.

For further experiments on vibrationally excited $CN(X^2\Sigma)$ radicals, it would be advantageous to develop the apparatus so that faster decays could be monitored at shorter delay times. This would allow the study of higher vibrational levels (v">1). In addition, it would be possible to sort out the controversy over the effect of vibrational excitation on the reaction of CN with O_2, for which conflicting reports exist[17,21].

APPENDICES

APPENDIX I

MATERIALS

The gases used in this work may be divided into four categories as follows:-

1. gas to fill the flash lamp
2. diluent gases
3. gases used as precursors of CN radicals
4. reactant gases.

Whenever possible, the gases were condensed and thoroughly degassed, followed by vacuum distillation.

This operation was repeated at least three times, and the 'middle cut' fraction retained in each case.

In many cases, slow vacuum distillation through traps at higher temperatures was also carried out. Ideally, the trap temperature should be such that the vapour pressure of the gas to be purified is about 130 Nm^{-2} (1 Torr). This was not always practicable however. Where this type of distillation was carried out (at least 3 times), the temperatures of the slush baths used to cool the traps are given for each gas, and again the 'middle cut' fraction was retained.

1. Flash Lamp Gas

Kr : B.O.C. X-grade (>99.99% pure), supplied in a 'break-seal' bulb and used as received.

2. Diluent Gases

He : B.O.C. A-grade (>99.998% pure), passed through 2 liquid nitrogen traps (77 K) to remove condensable materials.

He : B.O.C. X-grade (>99.995% pure), used directly from cylinder.

He : B.O.C. A-grade (<1 vpm O_2, <1 vpm N_2, <5 vpm H_2O certified purity), passed through 2 traps at 77 K.

3. CN Precursors

CH_3CN : B.D.H. spectroscopic grade (>99% pure), thoroughly degassed, used only in a trial experiment.

C_2N_2 : Matheson Co. Inc. technical grade (>98.5% pure). This was used for the bulk of the experiments, although a sample prepared by the inorganic research department was used initially. The gas was purified by at least 3 distillations through a trap at 178 K (Toluene slush), followed by repeated condensing onto dry KOH pellets to remove further impurities. One criterion for the purity was a slow rate of removal of CN radicals in cyanogen/helium mixtures.

4. Reactant Gases

O_2 : B.O.C. commercial grade (>99.9% pure), dried by slow passage through a trap at 195 K (acetone/CO_2 bath).

NO : Air Products Ltd. C.P. grade (>99% pure), distilled 3 times through a trap at liquid oxygen temperature (90 K).

CO : Matheson Co. Inc. technical grade (>99% pure), passed through 2 traps at 77 K to remove condensable materials.

CO_2 : solid (distillers), thoroughly degassed and purified by 5 distillations through a trap at 143 K (n-Pentane slush) to remove condensable materials.

N_2O : B.O.C. medical grade (>99% pure), vacuum distilled 4 times, retaining 'middle cut' fraction.

OCS : supplied by inorganic research department, purified by distillation through a trap at 143 K (n-Pentane slush).

H_2 : B.O.C. commercial grade (>99.9% pure), dried by passage through 2 traps at 77 K.

CH_4 : Matheson Co. Inc. C.P. grade (>99.0% pure), thoroughly degassed by a series of freeze-thaw cycles.

C_2H_6 : Matheson Co. Inc. C.P. grade (>99.0% pure), thoroughly degassed by a series of freeze-thaw cycles.

H_2O : double distilled, thoroughly degassed.

D_2O : B.O.C. Prochem (>99.0% pure), thoroughly degassed.

HCl : supplied by inorganic research department, purified by distillation through a trap at 143 K (n-Pentane slush).

DCl : supplied by inorganic research department (> 91% DCl, by IR), purified by distillation through a trap at 143 K (n-Pentane slush).

HCN : supplied by inorganic research department, purified by vacuum distillation from liquid nitrogen temperature (77 K).

Prior to the experiments with D_2O and DCl, the vacuum line was thoroughly deuterated with D_2O. This procedure took about 3 days.

I would like to thank the inorganic research department of this university for supplying samples of the gases mentioned above. In particular, I would like to thank William Duncan for the samples of cyanogen used in the initial experiments.

APPENDIX II

II.A BAND HEAD WAVELENGHTS

Table II.01 gives the wavelengths of the band heads of the CN violet system, which are shown in fig. 3.01. As the emission from the CN lamp contains a contribution from the N_2 second positive system, the wavelengths of the relevant band heads are also given below. The values quoted, both for CN and N_2, are those given by Pearse and Gaydon[76].

Table II.01

Band Head Wavelengths

Species	Transition	v',v"	λ/nm
CN	$B^2\Sigma \rightarrow X^2\Sigma$	0,0	388.34
		1,1	387.14
		2,2	386.19
		3,3	385.47
		4,4	385.09
N_2	$C^3\Pi \rightarrow B^3\Pi$	0,3	405.94
		1,4	399.84
		2,5	394.30
		3,6	389.46
		4,7	385.79
		0,2	380.49
		1,3	375.54

II.B DENSITOMETER TRACE OF THE CN(0,0) BAND

A densitometer trace of the CN(0,0) band emitted by the CN resonance lamp is given in fig. II.01 and corresponds to the relevant section of the photograph in fig. 3.01. The lines observed are in fact unresolved doublets and have been numbered by their m values using the wavenumbers given by Herzberg[1]. The line at the band origin does not arise from the CN radical but is due to some other species present in the discharge lamp.

II.C DERIVATION OF EQUATION 3.12

For the method of Ladenburg and Reiche, it is convenient to use the following empirical expression[89] for the frequency distribution of emitted radiation for a resonance lamp for which the emitting layer thickness and gas pressure are not accurately known.

$$E_\nu = C \exp -(\omega/\alpha)^2 \qquad \text{(II.01)}$$

where $\omega = 2\sqrt{\ln 2}\ (\nu-\nu_o)/\Delta\nu_a$ and $\Delta\nu_a$ is the Doppler width of the absorption line.

The absorption coefficient, k_ν, for small absorptions at the centre of a line ($k_o l \sim 3$) is given by Mitchell and Zemansky[89] as

$$k_\nu = k_o \exp(-\omega^2) \qquad \text{(II.02)}$$

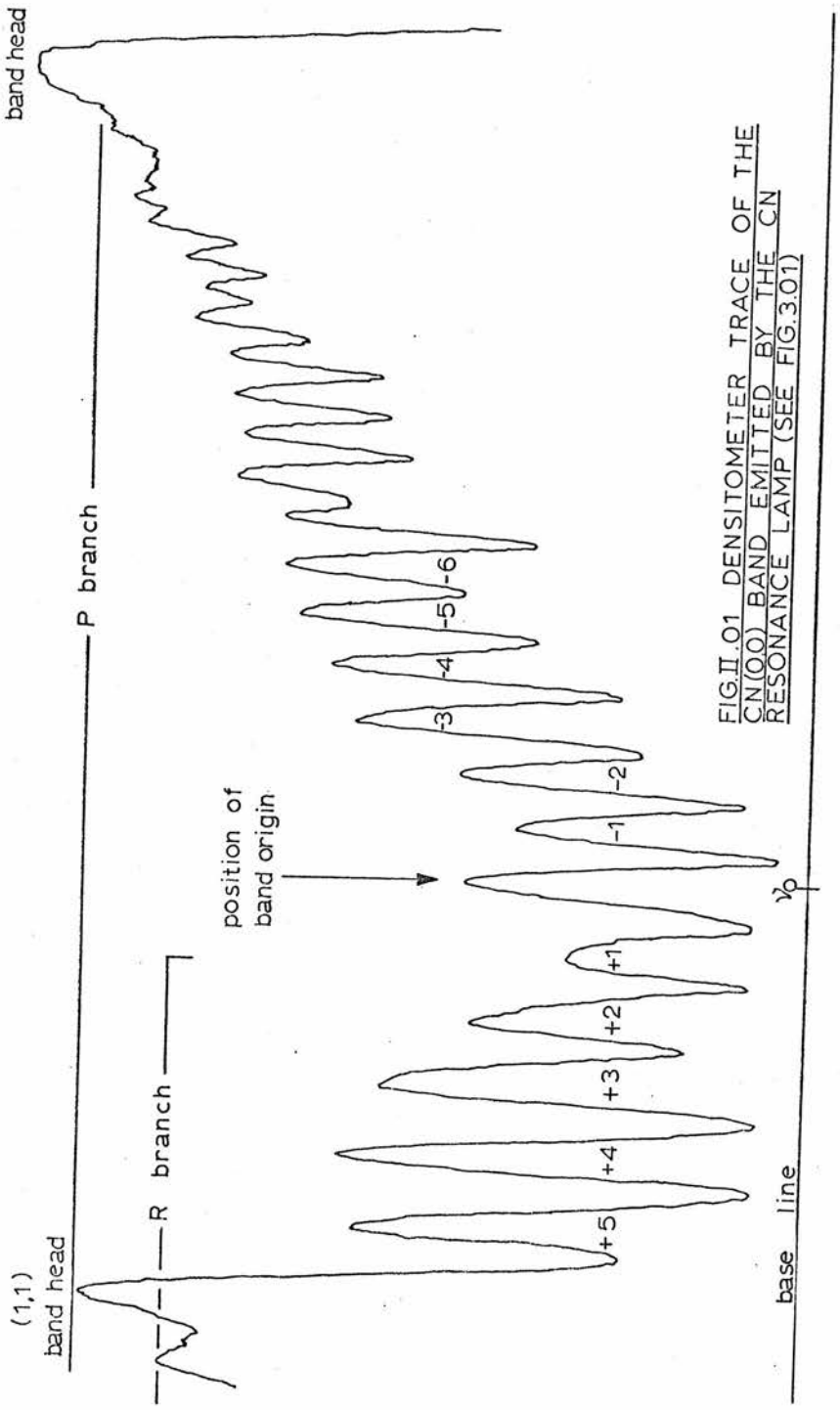

FIG.II.01 DENSITOMETER TRACE OF THE CN(00) BAND EMITTED BY THE CN RESONANCE LAMP (SEE FIG.3.01)

The fractional absorption is then given by the following expression.

$$A_\alpha = \frac{\int_{-\infty}^{\infty} e^{-(\omega/\alpha)^2} \left(1-e^{-k_o l e^{-\omega^2}}\right) d\omega}{\int_{-\infty}^{\infty} e^{-(\omega/\alpha)^2} d\omega} \qquad \text{(II.03)}$$

On integration, this simplifies to give the power series of equation 3.12. A table of A_α values for different combinations of $k_o l$ and α is given by Mitchell and Zemansky[89].

The fractional absorption A_α is also given by the following expression, which is related to experimental measurements.

$$A_\alpha = 1 - (I_t/I_o) \qquad \text{(II.04)}$$

where I_t and I_o are the transmitted and incident intensities.

Oscillator Strength

Knowing the oscillator strength, f, of a resonance line is equivalent to knowing the radiative lifetime, τ, of the upper electronic state[89], and they are related by the following expression

$$f\tau = 1.51\ (g_2/g_1)\lambda^2 \qquad \text{(II.05)}$$

where g_2 and g_1 are the statistical weights of the upper and lower electronic states respectively, and λ is the wavelength of the radiation.

II.D CALCULATION OF ABSOLUTE CN CONCENTRATION

For this calculation, the fractional absorption by CN ($X^2\Sigma, v''=0, K''=10$) was assumed to be equivalent to the fractional

absorption observed for a monochromator setting of 388.1 nm, i.e. A_α=0.89 from table 4.01. This corresponds to the initial CN concentration produced from the photolysis of 26.7 Nm^{-2} of cyanogen diluted to 1.33×10^4 Nm^{-2} using helium, at a flash energy of 125 J.

Taking the translational temperatures of the radicals in the resonance lamp and reaction vessel to be 1200 and 300 K respectively, a value of α=2 is obtained.

Using equations 3.12 and 3.13, together with the table of A_α values given by Mitchell and Zemansky[89], $k_{0,K}{}^1$ should be greater than 4.5 for α=2. The terms given in table II.02 were used to evaluate $k_{0,K}$ and hence N from relationship $k_{0,K}{}^1 > 4.5$. This yielded a lower limit of $N > 4.8 \times 10^{13}$ molecule cm^{-3}.

Table II.02

	Term	Value
	λ	388.11 nm
	$q_{0,0}$	0.90861
	S_K	9.975
	τ	60.8 ns
	Q_R	108.3
	Q_V	0.1987
†	$\Delta\nu_a$	5.893×10^{10} s^{-1}
	$K''(K''+1)/Q_R$	1.0157
	$\exp(-K''(K''+1)/Q_R)$	0.3621
	l	39.4 cm
	α	2.00
	A_α	0.89

† $\Delta\nu_a = 2(2RT\ln 2/M)^{\frac{1}{2}}\nu_o/c$

APPENDIX III

CALCULATION OF DIFFUSION COEFFICIENT

The following values given by Hirschfelder, Curtiss and Bird[96] were used in equations 4.06 and 4.07 to calculate the diffusion coefficient for CN radicals in a large excess of helium.

Table III.01

Parameters used in Equations 4.06 and 4.07

Gas	ε/k (K)	σ (Å)	M (a.m.u.)
He	10.22	2.576	4.00
CN ($\equiv N_2$)	91.5	3.681	26.0

From the above values, ε_{12}/k and σ_{12} were evaluated from the following expressions.

$$\varepsilon_{12}/k = (\varepsilon_1\varepsilon_2)^{\frac{1}{2}}/k \qquad \text{(III.01)}$$

$$\sigma_{12} = 0.5\,(\sigma_1 + \sigma_2) \qquad \text{(III.02)}$$

The reduced temperature is defined as $T_{12}^* = kT/\varepsilon_{12}$ and is used to find the value of Ω from tables of integrals, where

$$\Omega = \Omega_{1,2}^{(1,1)*}(T_{12}^*) \qquad \text{(III.03)}$$

in the notation of Hirschfelder, Curtiss and Bird[96].

As the reaction vessel length l is large (39.4 cm) and the radius r is 1 cm, equation 4.06 approximates to

$$\beta = 5.82\,D \qquad \text{(III.04)}$$

When the values given in table III.02 are substituted in equation 4.07, a value of D = 0.691 cm^2 s^{-1} is obtained corresponding to $\beta = 4.02$ s^{-1} for a total pressure of 1 atm.

Table III.02

Values used in Equation 4.07

Term	Value
T (K)	295
ε_{12}/k (K)	30.58
T_{12}^*	9.647
Ω	0.7471
σ_{12} (Å)	3.129
$(M_1+M_2)/2M_1M_2$	0.1442
p (atm)	1.000

APPENDIX IV

VIBRATIONAL RELAXATION

IV.A FUNDAMENTAL TRANSITIONS OF C_2N_2

The following transitions given by Herzberg[103] are for the ground electronic state of C_2N_2, ($X^1\Sigma_g^+$).

Table IV.01

Fundamental Transitions of C_2N_2

Mode		Wavenumber ν/cm^{-1}
ν_1	symmetric stretch	2329.9
ν_2	symmetric stretch	854.2
ν_3		2157.8
ν_4	bend	507
ν_5		233.1

The CN vibrational energies, calculated from the following equation are given in table IV.02

$$\varepsilon_v = (v+\tfrac{1}{2})\omega_e - (v+\tfrac{1}{2})^2\omega_e x_e \qquad \text{(IV.01)}$$

The values of ω_e = 2068.705 cm^{-1} and $\omega_e X_e$ = 13.144 cm^{-1}, given by Herzberg[1], were used in the calculations.

Table IV.02

Energy Levels of $CN(X^2\Sigma, v'')$

v''	ε_v/cm^{-1}	$\Delta\varepsilon_v/cm^{-1}$ $(\varepsilon_v - \varepsilon_{v-1})$
0	1031.07	
		2042.4
1	3073.48	
		2016.1
2	5089.61	
		1989.8
3	7079.45	
		1963.6
4	9043.01	
		1937.3
5	10980.27	
		1911.0
6	12891.25	
		1884.7
7	14775.94	
		1858.4
8	16634.34	
		1832.1
9	18466.45	
		1805.8
10	20272.28	

IV.B VIBRATIONAL RELAXATION CALCULATIONS

Vibrational relaxation (V→T) of a diatomic molecule by an inert gas atom may be considered as a collinear collision of atom A with diatomic oscillator B-C[100]. Two limits exist for this collision process, namely the spectator limit and the adiabatic limit. The spectator limit, where B aquires a velocity relative to C, occurs at high impact velocity when the duration of the collision, t_c, is less than the period of vibration, t_v. At temperatures around 300 K, t_c is usually greater than t_v and the

situation corresponds to the low velocity adiabatic limit.

In this work, therefore, energy transfer occurs at the adiabatic limit and is relatively inefficient[100] compared to the high velocity limit.

Exact calculations of the probability of V→T transfer are impossible for most systems, as accurate A---BC potentials are not yet known. However, Millikan and White[104] and Lifshitz[105] have obtained good agreement, to within ±50% of the experimental values, for their empirical calculations of $k_{1\rightarrow 0}$, the bimolecular rate constant for relaxation of v"=1 to v"=0.

The equation used is given below where P is the total pressure (atm), τ_v is the collisional lifetime of level v (s), T is the absolute temperature (K) and μ is the reduced mass of the colliding species (a.m.u.).

$$P\tau_v = \exp\left[A(T^{-0.33} - 0.015\ \mu^{0.25}) - 18.42\right] \qquad \text{(IV.02)}$$

This equation was used in this work to calculate $P\tau_v$ values for relaxation (V→T) of CN radicals by He atoms where A is given by the following expression

$$A = 1.16\times10^{-3}\ \theta^{1.33}\ \mu^{0.5} \qquad \text{(IV.03)}$$

This introduces the characteristic temperature, θ, of the diatomic oscillator which may be calculated from the relevant spectroscopic constants.

$$\theta = 1.48\ (\omega_e - 2\ \omega_e X_e) \qquad \text{(IV.04)}$$

It should be emphasised that the above equations apply for V→T transfer processes only and are not applicable to near resonant V→V processes.

The calculations of Millikan and White were for vibrational relaxation of the ground electronic states of CO, O_2 and N_2 by argon and helium, i.e. singlet and triplet states. The rationale behind the applicability of equation IV.02 to these molecules was that the repulsive exponential potential of the A + BC interaction did not differ much from one system to another. To assess a more general applicability to doublet states, the value of $k_{1\rightarrow 0}$ for $NO(A^2\Pi)$ was calculated for comparison with experimental data.

The data used to calculate the $k_{1\rightarrow 0}$ values for $CN(X^2\Sigma)$ and $NO(A^2\Pi)$ are given in table IV.03 The spectroscopic constants were those given by Herzberg[1].

The value of $k_{1\rightarrow 0} = 2.6 \times 10^{-17}$ cm^3 molecule^{-1}s^{-1}, calculated for NO(v"=1) in helium at 245 K, is within ± 50% of the experimental value of 3.8×10^{-17} cm^3 molecule^{-1}s^{-1} obtained by Stephenson[107] for the same temperature. This suggests that equation IV.02 is valid for V → T relaxation of doublet states, as well as singlet and triplet states.

The value of $k_{1\rightarrow 0} = 2.0 \times 10^{-17}$ cm^3 molecule^{-1}s^{-1}, calculated for the vibrational relaxation of CN (v"=1) by helium at 295 K, should therefore be a reasonable approximation.

Table IV.03

Data for Vibrational Relaxation Calculations

	T/K	ω_e/cm^{-1}	$\omega_e X_e/cm^{-1}$	θ/cm^{-1}	μ /a.m.u.	A	$P\tau/10^{-3}$ atm s	$k/10^{-17}$ cm^3 $molecule^{-1}$ s^{-1}
NO	245	1904.03	13.97	2777	3.529	82.8	1.30	2.6
CN	295	2068.705	13.144	3023	3.467	91.9	1.97	2.0

APPENDIX V

THE STUDY OF $CN(X^2\Sigma, v=1)$: CALCULATION OF R_0

For a helium/cyanogen mixture, 500:1, at a total pressure of 1.33×10^4 Nm^{-2}, the ratio of the optical density (O.D.) for the (0,0)R branch at 386.8 nm to the O.D. for the (0,0)P branch at 388.1 nm, at time t=0, was found to be 0.57 ± 0.02. This determination was carried out using the quartz reaction vessel, for delay times when the concentration of $CN(X^2\Sigma, v'' \geqslant 1)$ was zero.

For the Spectrosil reaction vessel, the optical densities at time t=0 are given in table 8.01 for the absorption of the (0,0)P branch at 388.1 nm, and for the absorption due to the overlap of the (0,0)R and (1,1)P branches at 386.8 nm.

To obtain a value for R_0, it is necessary to calculate the relative contributions of CN(v"=0) and CN(v"=1) to the O.D. measured at 386.8 nm. The O.D. at 386.8 nm due to absorption by CN(v"=0) may be calculated from the O.D. of the absorption by CN(v"=0) at 388.1 nm, using the ratio of 0.57 ± 0.02 given above for the quartz vessel (from the relative absorption coefficients calculated by Schmatjko,[95] averaged over the slit width of the monochromator, this ratio was found to be 0.44 ± 0.01[†]).

Hence for the data in the first row of table 8.01, the calculated O.D. at 386.8 nm due to CN(v"=0) is 81.5x0.57 = 46.5. The O.D. at 386.8 nm due to CN(v"=1) is therefore 54.6 - 46.5 = 8.1.

The ratio of the populations of the v"=1 to the v"=0 levels, at time t=0, is then obtained from the following expression,

$$\frac{\text{O.D. at 386.8 nm due to v"=1}}{\text{O.D. at 386.8 nm due to v"=0}} = B \times R_0 = B \times \frac{P(v''=1)}{P(v''=0)}$$

where B is the ratio of the absorption coefficient for CN(v"=1) at 386.8 nm to that of CN(v"=0) at 386.8 nm. According to the relative absorption coefficients calculated by Schmatjko,[95] B has a value of 1.9 ± 0.05.

[†] Use of this value would result in a larger value of R_0.

Rearranging the above equation, and substituting the values obtained from the data in the first row of table 8.01, the value of R_0 is obtained as follows.

$$R_0 = \frac{1}{B} \times \frac{\text{O.D. at 386.8 nm due to v''=1}}{\text{O.D. at 386.8 nm due to v''=0}}$$

$$R_0 = \frac{1}{1.9} \times \frac{8.1}{46.5} \simeq 0.09$$

Taking into account the uncertainty in the ratio given in the first paragraph (0.57 ± 0.02), R_0 lies in the range 0.07 to 0.11. The two remaining values of R_0 in table 8.01 were calculated in the same way.

REFERENCES

REFERENCES

1. G. Herzberg, 'Spectra of Diatomic Molecules', Vol. I of 'Molecular Spectra and Molecular Structure', Van Nostrand Reinhold, New York (1950) 2nd. edn.
2. Ya.B. Zeldovich, P.Ya. Sadovnikov and D.A. Kamenetskii, 'Oxidation of Nitrogen in Combustion'. (transl. by M. Shelef) Academy of Sciences of USSR, Institute of Chemical Physics, Moscow-Leningrad (1947).
3. J.P. Appleton and J.B. Heywood, Fourteenth Symposium (International) on Combustion, The Combustion Institute (1973) p.777.
4. P.A. Leighton, 'Photochemistry of Air Pollution', Academic Press, New York (1961).
5. P.J. Crutzen, Canad. J. Chem. 52 (1974) 1569.
6. H.I. Schiff, Canad. J. Chem. 52 (1974) 1536.
7. R.J. Cicerone, R.S. Stolarski and S. Walters, Science 185 (1974) 1165.
8. D.R. Bates and M. Nicolet, J. Geophys. Res. 55 (1950) 301.
9. A.U. Khan, J.N. Pitts Jr. and E.B. Smith, Environ. Sci. Tech. 1 (1967) 656.
10. J.P. Simons, 'Photochemistry and Spectroscopy', Wiley, London (1971).
11. J.U. White, J. Chem. Phys. 8 (1940) 79, 459.
12. C. Haggart and C.A. Winkler, Canad. J. Chem. 37 (1959) 1791, 38 (1960) 329.
13. D.E. Paul and F.W. Dalby, J. Chem. Phys. 37 (1962) 592.
14. N. Basco, Proc. Roy. Soc. A283 (1965) 302.
15. N. Basco, J.E. Nicholas, R.G.W. Norrish and W.H.J. Vickers, Proc. Roy. Soc. A272 (1963) 147.

15a. R.J. Cody, M.J. Sabetz-Dzvonik and W.M. Jackson, J. Chem. Phys. 66 (1977) 2145.

16. J.C. Boden and B.A. Thrush, Proc. Roy. Soc. A305 (1968) 107.

17. G.E. Bullock and R. Cooper, Trans. Faraday Soc. 67 (1971) 3258.

18. G.E. Bullock and R. Cooper, J.C.S. Faraday I, 68 (1972) 2175.

19. G.E. Bullock and R. Cooper, J.C.S. Faraday I, 68 (1972) 2185.

20. G.E. Bullock, R. Cooper, S. Gordon and W.A. Mulac, J. Phys. Chem. 76 (1972) 1931.

21. H. Schacke, K.J. Schmatjko and J. Wolfrum, Ber. Bunsengesellschaft phys. Chem. 77 (1973) 248.

22. H. Schacke, K.J. Schmatjko and J. Wolfrum, Arch. Procesow Spalania 5 (1974) 363.

23. E.A. Albers, K. Hoyermann, H. Schacke, K.J. Schmatjko, H.Gg. Wagner and J. Wolfrum, Fifteenth Symposium (International) on Combustion, The Combustion Institute (1975) p.765.

24. M.R. Dunn, C.G. Freeman, M.J. McEwan and L.F. Phillips, J. Phys. Chem. 75 (1971) 2662.

25. T. Morrow and W.D. McGrath, Trans. Faraday Soc. 62 (1966) 642.

26. K.J. Schmatjko and J. Wolfrum, Ber. Bunsengesellschaft. phys. Chem. 79 (1975) 696.

27. H. Hartel and M. Polanyi, Z. phys. Chem. (Leipzig) B11 (1930) 97.

28. T. Iwai, D.W. Pratt and H.P. Broida, J. Chem. Phys. 49 (1968) 919.

29. N.C. Robertson and R.N. Pease, J. Amer. Chem. Soc. 64 (1942) 1880.

30. C.A. Goy, D.H. Shaw and H.O. Pritchard, J. Phys. Chem. 69 (1965) 1504.

31. G.C. Fettis and J.H. Knox, Progr. Reaction Kinetics 2 (1964) 1.

32. N. Basco and R.G.W. Norrish, Proc. Roy. Soc. A283 (1965) 291.

33. R.G.W. Norrish and F.F.P. Smith, Trans. Faraday Soc. 24 (1928) 620.

34. J.P. Galvin and H.O. Pritchard, J. Phys. Chem. 68 (1964) 1035.

35. R. Dickinson, G.W. Kirby, J.G. Sweeny and J.K. Tyler, J.C.S. Chem. Comm. (1973) p.241.

36. E.A. Dorko and L. Buelow, J. Chem. Phys. 62 (1975) 1869.

37. P.M. Rentzepis and T.M. Sugden, Nature 202 (1964) 448.

38. T.L. Cottrell and A.J. Matheson, Trans. Faraday Soc. 58 (1962) 2336.

39. S. Arrhenius, Z. phys. Chem. (Leipzig) 4 (1889) 96.

40. M. Polanyi, 'Atomic Reactions', Williams and Norgate, London (1932).

41. J.H. Parker and G.C. Pimental, J. Chem. Phys. 51 (1969) 91.

42. J.C. Polanyi and K.B. Woodall, J. Chem. Phys. 57 (1972) 1574.

43. M.J. Berry, J. Chem. Phys. 59 (1973) 6229.

44. J.H. Parker and G.C. Pimental, J. Chem. Phys. 55 (1971) 857.

45. S.H. Bauer, D.M. Lederman, E.L. Resler Jr. and E.R. Fisher, Internat. J. Chem. Kinetics 5 (1973) 93.

46. S.B. Jaffe and J.B. Anderson, J. Chem. Phys. 49 (1968) 2859.

47. T.J. Odiorne, P.R. Brooks and J.V.V. Kasper, J. Chem. Phys. 55 (1971) 1980.

48. L.B. Sims, L.R. Dosser and P.S. Wilson, Chem. Phys. Letters 32 (1975) 150.

49. M.J. Kurylo, W. Braun, A. Kaldor, S.M. Freund and R.P. Wayne, J. Photochem. 3 (1974/75) 71.

50. R.J. Gordon and M.C. Lin, Chem. Phys. Letters 22 (1973) 262.

51. A.E. Potter, R.N. Coltharp and S.D. Worley, J. Chem. Phys. 54 (1971) 922.

52. Z. Karny, B. Katz and A. Szoke, Chem. Phys. Letters 35 (1975) 100.

53. K.D. Bayes, Canad. J. Chem. 39 (1961) 1074.

54. D.W. Setser and B.A. Thrush, Nature 200 (1963) 864.

55. I.M. Campbell and B.A. Thrush, Proc. Chem. Soc. (1964) p.410.

56. I.M. Campbell and B.A. Thrush, Ann. Reports 62 (1965) 17.

57. D.W. Setser and B.A. Thrush, Proc. Roy. Soc. A288 (1965) 256, 275.

58. I.M. Campbell and B.A. Thrush, Proc. Roy. Soc. A296 (1967) 201.

59. J.C. Boden and B.A. Thrush, Proc. Roy. Soc. A305 (1968) 93.

60. R.L. Brown and H.P. Broida, J. Chem. Phys. 41 (1964) 2053.

61. T. Iwai, M.I. Savadatti and H.P. Broida, J. Chem. Phys. 47 (1967) 3861.

62. T. Iwai, D.W. Pratt and H.P. Broida, J. Chem. Phys. 49 (1968) 919.

63. G.M. Provencher and D.J. McKenney, Chem. Phys. Letters 10 (1971) 365.

64. G.M. Provencher and D.J. McKenney, Canad. J. Chem. 50 (1972) 2527.

65. W.M. Jackson, J. Chem. Phys. 59 (1973) 960.

66. C.K. Luk and R. Bersohn, J. Chem. Phys. 58 (1973) 2153.

67. G.A. West and M.J. Berry, J. Chem. Phys. 61 (1974) 4700.

68. G.A. Chamberlain and J.P. Simons, J.C.S. Faraday II, 71 (1975) 2043.

69. R. Bersohn, in 'Molecular Energy Transfer', Editors R.D. Levine and J. Jortner, John Wiley and Sons, New York (1976) p.154.

70. C.A. Brau and J.J. Ewing, J. Chem. Phys. 63 (1975) 4640, App. Phys. Letters 27 (1975) 435.

71. B.S. Ault and L. Andrews, J. Chem. Phys. 64 (1976) 3075.

72. C. Morley and I.W.M. Smith, J.C.S. Faraday II, 68 (1972) 1016.

73. G. Porter, Proc. Roy. Soc. A200 (1950) 284.

74. G. Porter and M.A. West, 'Investigation of Rates and Mechanisms of Reactions', 3rd edition, part 2, Editor G.G. Hammes, Vol. VI, Wiley-Interscience (1974) p.367.

75. C.R. Boxall and J.P. Simons, Proc. Roy. Soc. A328 (1972) 515.

76. R.W.B. Pearse and A.G. Gaydon, 'The Identification of Molecular Spectra', Chapman and Hall, London (1963), 3rd edn. with supplement.

77. M.I.T. Wavelength Tables, John Wiley and Sons, New York (1939).

78. J.I. Morrow, International Laboratory (Nov./Dec. 1971) p.21.

79. R.H. Strain, Ph.D. Thesis, University of Edinburgh (1977).

80. D.D. Davies and H. Okabe, J. Chem. Phys. 49 (1968) 5526.

81. S.W. Benson, Bond Energies Resources Paper
The Advisory Council on College Chemistry (1965).

82. F.A. Jenkins, Phys. Rev. 31 (1928) 539.

83. M.W. Feast, Proc. Phys. Soc. A62 (1949) 121.

84. K.M. Evenson and H.P. Broida, J. Chem. Phys. 44 (1966) 1637.

85. E.M. Bulewicz, P.J. Padley and R.E. Smith, Fourteenth Symposium (International) on Combustion, The Combustion Institute (1973) p.329.

86. R.J. Cody, M.J. Sabetz-Dzvonik and W.M. Jackson, J. Chem. Phys. 66 (1977) 2145.

87. I. Tokue, T. Urisu and K.Kuchitsu, J. Photochem. 3 (1974/75) 273.

88. W. Braun and T. Carrington, J. Quant. Spectrosc. Radiat. Transfer 9 (1969) 1133.

89. A.C.G. Mitchell and M.W. Zemansky 'Resonance Radiation and Excited Atoms', Cambridge University Press (1934).

90. R.W. Nicholls, J. Res. Nat. Bur. Stand. A68 (1964) 75.

91. R.G. Bennett and F.W. Dalby, J. Chem. Phys. 36 (1962) 399.

92. R. Engleman Jr., J. Photochem. 1 (1972/73) 317.

93. W.M. Jackson and R.J. Cody, J. Chem. Phys. 61 (1974) 4183.

94. M.A. Pollack, Appl. Phys. Letters 9 (1966) 230.

95. K.J. Schmatjko, private communication.

96. J.O. Hirschfelder, C.F. Curtiss, and R.B. Bird, 'Molecular Theory of Gases and Liquids', John Wiley and Sons, New York (1954).

97. C.B. Moore, Adv. Chem. Phys. 23 (1973) 41.

98. R.C. Amme, Adv. Chem. Phys. 28 (1975) 171.

99. A.B. Callear, 'Photochemistry and Reaction Kinetics' (Eds. P.G. Ashmore, F.S. Dainton and T.M. Sugden) Cambridge University Press (1967), chap. 7, p.133.

100. R.D. Levine and R.B. Bernstein, 'Molecular Reaction Dynamics', Oxford University Press (1974).

101. M.A.A. Clyne and H.W. Cruse, J.C.S. Faraday II, 68 (1972) 1377.

102. W.H. Wong and G. Burns, J. Chem. Phys. 58 (1973) 4459.

103. G. Herzberg, 'Electronic Spectra of Polyatomic Molecules', Vol. III of 'Molecular Spectra and Molecular Structure', Van Nostrand Reinhold, New York (1966).

104. R.C. Millikan and D.R. White, J. Chem. Phys. 39 (1963) 3209.

105. A. Lifshitz, J. Chem. Phys. 61 (1974) 2478.

106. L. Landau and E. Teller, Phys. Z. Sowjetunion 10 (1936) 34.

107. J.C. Stephenson, J. Chem. Phys. 60 (1974) 4289.

108. H. van den Bergh and J. Troe, Chem. Phys. Letters 31 (1975) 351.

109. T.R. Hogness and L. Ts'ai, J. Amer. Chem. Soc. 54 (1932) 123.

110. D.R. Safrany and W. Jaster, J. Phys. Chem. 72 (1968) 3305.

111. JANAF Thermochemical Tables, NSRDS-NBS 37, Nat. Bur. Stds. (1971) 2nd edn.

112. H. Okabe, J. Chem. Phys. 53 (1970) 3507.

113. T.C. Clark, M.A.A. Clyne and D.H. Stedman, Trans. Faraday Soc. 62 (1966) 3354.

114. C.T. Ratcliffe, J.M. Shreeve and K.J. Wynne, Inorg. Synth. 11 (1968) 194.

115. D.E. Milligan, M.E. Jacox, A.M. Bass, J.J. Comeford and D.E. Mann, J. Chem. Phys. 42 (1965) 3187.

116. M.E. Jacox and D.E. Milligan, J. Chem. Phys. 43 (1965) 866.

117. W.G. Burns and F.S. Dainton, Trans. Faraday Soc. 48 (1952) 39.

118. P.G. Ashmore and M.S. Spencer, Trans. Faraday Soc. 55 (1959) 1868.

119. B.G. Gowenlock, C.A.F. Johnson, C.M. Keary and J. Pfab, J.C.S. Perkin II, (1975) p.351.

120. J.G. Calvert and J.N. Pitts Jr., 'Photochemistry', John Wiley and Sons, New York (1966).

121. G. Black, R.L. Sharpless, T.G. Slanger and D.C. Lorents, J.Chem. Phys. 62 (1975) 4274.

122. R.J. Donovan and D. Husain, Chem. Rev. 70 (1970) 489.

123. P.M. Scott, K.F. Preston, R.J. Andersen and L.M. Quick, Canad. J. Chem. 49 (1971) 1808.

124. R. Simonaitis, R.I. Greenberg and J. Heicklen, Internat. J. Chem. Kinetics 4 (1972) 497.

125. J.A. Ghormley, R.L. Ellsworth and C.J. Hochanadel, J. Phys. Chem. 77 (1973) 1341.

126. K.L. Kompa and J. Wanner, Chem. Phys. Letters 12 (1972) 560.

127. K. Bergmann and C.B. Moore, J. Chem. Phys. 63 (1975) 643.

128. T. Fueno, K. Tabayashi and O. Kajimoto, J. Phys. Chem. 77 (1973) 575.

129. R.W. Nicholls, J. Res. Nat. Bur. Stand. A68 (1964) 75.

130. C.T. Bowman, Progr. Energy Combustion Sci. 1 (1975) 33.

131. A.G. Gaydon and H.G. Wolfhard, 'Flames, Their Structure, Radiation and Temperature', Chapman and Hall, London (1960).

132. C.P. Feminore, 'Chemistry in Premixed Flames', in The International Encyclopaedia of Physical Chemistry and Chemical Physics, Topic 19: Gas Kinetics, Vol. 5, Ed. A.F. Trotmann-Dickenson (1964).

133. R.M. Fristrom and A.A. Westenberg, 'Flame Structure', McGraw-Hill, New York (1965).

134. A.G. Gaydon, 'The Spectroscopy of Flames', Chapman and Hall, London (1974) 2nd edn.

135. B. Lewis and G. von Elbe, 'Combustion, Flames and Explosions of Gases', Academic Press, New York (1961) 2nd edn.

136. D.R. Jenkins and T.M. Sugden, Shell Research Ltd., Thornton Research Centre Report No. TRCP.1364 (1967).

137. G. Damkohler and R. Edse, Z. Electrochem. 49 (1943) 178.

138. C.P. Ferminore, Thirteenth Symposium (International) on Combustion, The Combustion Institute (1971) p.373.

139. C. Morley, Combust. Flame 27 (1976) 189.

140. A.N. Hayhurst and H.G. McLean, Nature 251 (1974) 303.

141. C.P. Feminore, Combust. Flame 19 (1972) 289.

142. B.S. Haynes, Combust. Flame 28 (1977) 113.

143. M.P. Nadler, V.K. Wang and W.E. Kaskan, J. Phys. Chem. 74 (1970) 917.

144. R.P. Wayne, 'Photochemistry', Butterworth and Co. Ltd., London (1970) p.103.

145. W. Braun and M. Lenzi, Discuss. Faraday Soc. 44 (1967) 252.

146. L. Brewer and J.B. Tellinghuisen, J. Chem. Phys. 54 (1971) 5133.

147. R.H. Strain, J. McLean and R.J. Donovan, Chem. Phys. Letters 20 (1973) 504.

148. A. Schultz, H.W. Cruse and R.N. Zare, J. Chem. Phys. 57 (1972) 1354.

149. R.N. Zare and P.J. Dagdigian, Science 185 (1974) 739.

150. I.W.M. Smith and R. Zellner, J.C.S. Faraday II, 69 (1973) 1617.

151. M.C. Addison, A.J. Leitch, C. Fotakis and R.J. Donovan, to be published.

152. R.D. Sharma and C.W. Kern, J. Chem. Phys. 55 (1971) 1171.

LECTURES ATTENDED

The following is a list of the post-graduate lectures attended during the period of research:-

quantum optics

molecular scattering

Hückel and Möbius systems

high speed liquid chromatography

vibrational spectroscopy

oil products research

chemistry of the atmosphere.

In addition a selection of seminars, run by the department and by the kinetics and molecular beams groups, was attended, as well as a course in computing.